1959

High temperature allotropy of the rare-earth elements

Joseph John Hanak
Iowa State University

HIGH TEMPERATURE ALLOTROPY OF THE RARE-EARTH ELEMENTS

by

Joseph John Hanak

A Dissertation Submitted to the
Graduate Faculty in Partial Fulfillment of
The Requirements for the Degree of
DOCTOR OF PHILOSOPHY

Major Subject: Physical Chemistry

Approved:

Signature was redacted for privacy.

In Charge of Major Work

Signature was redacted for privacy.

Head of Major Department

Signature was redacted for privacy.

Dean of Graduate College

Iowa State University
Of Science and Technology
Ames, Iowa

1959

TABLE OF CONTENTS

INTRODUCTION

The rare earths have long been recognized for their unique behavior, which prompted the early scientists to do painstaking research to determine the nature of these substances. In recent years, the development of convenient methods for separating the pure compounds and for preparing the pure metals has imparted a new impetus to this effort.

Much of the research concerned with the pure rare-earth metals has been directed to an explanation of metallic bonding. At this time there is no theory of metallic bonding which is completely satisfactory for explaining the properties of these metals. A better understanding of these metals can be achieved by studying and correlating their individual physical properties. The physical properties of a substance are related to the interactions of the atoms with the electrons, the relationship being more obvious with some properties than with others. Crystal structure is a particularly sensitive property in reflecting the bonding characteristics of a substance. It gives rise directly to such properties as atomic volume, density, atomic radii, and bond distances, and is directly related to most of the properties of a substance, as can be shown vividly in cases where an isotropy exists.

Because of the lack of information, it has often been thought that the rare earths are very similar in their

physical properties. Actually, remarkable differences occur in these metals, as exemplified by the existence of five different crystal structures within the series at room temperature. At different temperatures and pressures other solid phase modifications are known and still others are suspected.

Early studies of the physical properties on samples of questionable purity presented a very complicated picture of the high temperature allotropy of these metals. Recent investigations on pure metals helped to resolve this complexity somewhat, in that they gave a clearer definition of the conditions under which the solid phase transformations of some of these metals take place. Nevertheless, the crystal structures of the high temperature solid phase modifications remained unknown because of the lack of appropriate X-ray techniques.

Since the information concerning the high temperature allotropy is desirable and since the pure rare-earth metals are now available, it has been decided to develop appropriate X-ray techniques and by their use to study in detail the structure of the known high temperature solid phase modifications. It has also been decided to investigate the possibility of existence of other crystalline modifications by these X-ray techniques and by electrical resistivity measurements. Since the crystallographic method offers a means of accurate measurement of the lattice dimensions, the

determination of the expansion characteristics has also been undertaken.

HISTORICAL

Literature Survey of the Rare-Earth Allotropy

A considerable amount of information has appeared in the literature concerning the allotropy of the rare-earth elements. Much of the earlier information has been obtained with metals of questionable purity; hence, these data often are at variance with the more recent data. A notable exception to this is the work of Klemm and Bommer (1) who have undertaken the task of characterizing almost all of the rare-earth elements. In the recent years methods of preparing pure rare-earth metals have been developed and, consequently, the data now appearing on various physical constants are more consistent and reliable. In this literature review an attempt has been made to correlate the data pertaining to the allotropy of the rare earths at high temperatures with special emphasis on the more recent data.

Lanthanum

At room temperature, lanthanum has been reported to exhibit a hexagonal closest packed (hcp) structure by McLennan and McKay (2) and by others (3, 4, 5, 6, 7), a face centered cubic (fcc) structure by Klemm and Bommer (1) and by others (8, 9), or a mixture of both by James et al. (10) and by Ziegler et al. (7). According to Zintl and Neumayr (4) and others (6, 7, 11) annealing of lanthanum at 350°C tends to

stabilize the fcc structure at room temperature. Upon closer examination of the X-ray patterns of the hcp allotrope of lanthanum, Spedding et al. (12) found that the lattice constant c_o was twice that found by others. This meant that in lanthanum, planes are present in a stacking sequence ABAC... instead of ABAB.... These authors also reported the lattice constants of 99.8 per cent lanthanum as a_o = 3.770 Å and c_o = 12.159 Å. The value of the lattice constant of the fcc phase reported by various investigators (1, 4, 6, 7, 9, 11) varies between 5.296 and 5.305 Å.

The study of various properties of lanthanum gave evidence for the existence of allotropic transformations in the metal at higher temperatures. Jaeger et al. (13) studied the specific heat and the electrical resistance of lanthanum as a function of temperature using 98.8 per cent lanthanum with one per cent iron impurity. They found anomalies occurring in the specific heat at 548°C, 655°C, and 709°C and in the electrical resistivity at 421°C-436°C, 560°C, and 709°C-715°C, from which they concluded that the metal exhibited four reversible "states" and that at any temperature a mixture of two or more phases was present. Recent electrical resistivity measurements reported by Spedding et al. (14) indicated a solid state transformation appearing as a 10 per cent discontinuous increase in resistivity at 860°C-868°C; a small hysteresis loop observed at lower temperatures indicated a transformation between 230°C and 340°C.

Further evidence for the existence of the high temperature transformation was obtained from phase diagram studies. Vogel and Heumann (15) in reporting the lanthanum-magnesium phase diagram indicated a transformation in lanthanum at 830°C and the melting point at 915°C. Massenhausen (16) investigated the lanthanum-sodium phase diagram and reported a transformation at 812°C and the melting point at 863°C for a "slightly" contaminated lanthanum. Vogel and Klose (17) studied the cerium-lanthanum phase diagram and for a 97 per cent lanthanum sample they reported the melting point at 865°C with transformations at 775°C and at 300°C-350°C, the lower transformation presumably being the hcp-fcc transformation.

Bridgman (18) reported a transformation in lanthanum occurring at a pressure of 23,400 kg./cm.^{2} at room temperature, and appearing as a 0.26 per cent change in volume. A similar change in volume was reported by Trombe and Foex (19) who performed dilatometric studies on 99.2 per cent lanthanum and observed the transformation with a hysteresis loop between 150°C on cooling and 350°C on heating. Dilatometric results reported by Barson *et al.* (20) indicate a transformation between 310°C on heating and 230°C on cooling, accompanied by a 0.3 per cent decrease in volume. At 800°C their sample became very soft and began to collapse.

Spedding and Daane (21) reported the results of thermal analyses performed on 200-300-gram samples cast in tantalum

crucibles. For lanthanum they found the melting point to be at 920°C and a transformation at 868°C.

Recent results obtained with pure samples, therefore, indicate that two solid phase transformations occur in lanthanum above room temperature. One of these is the transformation occurring near 300°C over a temperature range of about 100°. This transformation is rather sluggish and is generally thought to involve the hcp and fcc phases because they are found together even at room temperature. The other transformation occurs near the melting point, and is essentially isothermal. The structure of the high temperature phase is not known.

Since it would be difficult to determine the exact transformation temperatures and the melting points by the X-ray technique used in the present study, it was decided to use the data reported by Spedding and Daane (21) as given above. These data were selected because the early data on these properties indicate that impurities tend to lower the second transformation temperature and the melting point. The data of Spedding and Daane not only show the highest values, but also are consistent with other recent results.

Cerium

The structure of cerium at room temperature was found to be fcc by Quill (3) and by others (1, 5, 12, 22) for samples as pure as 99.9 per cent, whereas for samples containing as

much as 10 per cent impurities, the fcc phase was found to coexist with the hcp phase by Hull (23) and by Ziegler (6). The latter reported that annealing at 350°C of a sample containing some of the hcp phase stabilized the fcc phase at room temperature. Thermal cycling of a 99.9 per cent pure sample down to about 4°K produced some hcp phase which persisted at room temperature, as shown by James et al. (10). Spedding et al. (12) reported the lattice constant for the fcc phase at room temperature to be 5.1612 Å, which they determined by using a 99.9 per cent cerium specimen and a focussing back-reflection camera.

Trombe (24) reported a large hysteresis loop between 100°K and 170°K in the magnetic susceptibility of cerium containing 0.1 per cent silicon and 0.01 per cent iron. La Blanchetais (25) showed that this effect was not due to the presence of ferromagnetic material in the sample, since the results were reproduced with a sample containing only 0.005 per cent iron.

Phenomena indicating a drastic change in the structure of cerium in this temperature range were also reported by Trombe and Foex (19, 26) who observed a 10 per cent contraction in volume of a cerium sample at 109°K on cooling, and the reverse phenomenon at 175°K on heating. The volume contraction was suppressed by thermal cycling. Similar phenomena occurring in the electrical resistivity were reported by Foex (27) and James et al. (10), in the Hall effect, by

Kevane et al. (28) and in the atomic heat, by Parkinson et al. (29). Bridgman (18, 30) reported a similar transformation in cerium when it was subjected to a pressure of 12,430 atmospheres. His latest results indicate an over-all contraction in volume of 16.55 per cent at 15,000 atmospheres.

Trombe and Foex attributed these low temperature phenomena to the existence of three phases, namely, γ, the fcc phase, appearing at ambient and higher temperatures, β, the hcp phase, appearing at lower temperatures, and α, the condensed phase, appearing at low temperatures. They also pointed out that the γ form gives rise to the α form on rapid cooling, whereas the β form cannot undergo such a transformation. The β form can be obtained by slow cooling of the γ form, or by thermal cycling at low temperatures.

Schuch and Sturdivant (31) investigated the condensed form at low temperatures with X rays at the suggestion of L. Pauling and found that the α form was also fcc with a lattice constant of 4.82 $\mathring{A}$; this corresponds to a decrease of 16.5 per cent in volume for the contracted form. Pauling reasoned that the $\gamma - \alpha$ transformation is due to the transfer of one 4f electron into the 5d orbital.

Lawson and Tang (32) performed an X-ray study of cerium under a pressure of 15,000 atmospheres at ordinary temperature and observed the α form, which was 16.5 per cent smaller by volume than the γ form.

McHargue et al. (33) reported their studies of the

allotropic modifications of cerium metal in the temperature region 77°K to 455°K. They reported the fcc to hcp transformation at 263 ± 5°K and the reverse transformation at 363 ± 5°K. They also reported the hexagonal form with the c-axis doubled, as in lanthanum, the lattice constants being a_o = 3.68 Å and c_o = 11.92 Å. According to the same authors, the transformation of the γ form to the α form starts at 123 ± 5°K in previously transformed samples heated 20° to 30° above 210°K and then cooled, and at 103 ± 3°K in samples cooled from room temperature or higher. The reverse transformation begins at 170 ± 5°K and it is completed at 200 ± 5°K. McHargue (34) reported, contrary to Trombe's observations, that both the β and γ forms give rise to the α form near 4°K. In the same paper the author noted that working of the metal inhibits the formation of the hcp phase.

As for the high temperature allotropy of cerium, Jaeger et al. (13) reported two transformations for a sample containing one per cent iron, one being at 393°C and the other at 440°C. Thermal anomalies were also observed around 630°C by Vogel and Heumann (15), at 640°C, 710°C, and 740°C by Loriers (35), at 703°C by Ahmann (36), at 720°C by Vogel and Klose (17), and 754°C by Spedding and Daane (21).

Gaume-Mahn and Cohen (37) investigated the cerium-magnesium system dilatometrically and reported a γ - δ transformation taking place at 500°C for a 98.5 per cent cerium alloy.

Barson et al. (20) made dilatometric measurements on 99.3 per cent cerium in the temperature range 0°C to 716°C and did not observe any discontinuities in the expansion curve, except that at the highest temperature their sample became soft and started to collapse.

Spedding et al. (14) reported an increase of 8.5 per cent in the electrical resistivity at 726°C-733°C.

A magnetic anomaly was observed by Gaume-Mahn (38) between 667°C and 708°C. This anomaly appeared as an eight per cent decrease in the susceptibility on warming. Bates et al. (39) studied the magnetic susceptibility of cerium between room temperature and 780°C and obtained a continuous curve in the entire temperature region. If there were a discontinuity in the magnetic susceptibility at the high temperature transformation, it was less than one per cent.

McKeown (40) determined the enthalpy of cerium in the temperature range 0°C to 1100°C. He observed a transformation in the vicinity of 730°C accompanied by a heat of transformation of 700 calories per mole. For the heat of fusion at 804°C he reported a value of 1238 calories per mole.

Much variation is found in the values of the melting point of cerium reported in the literature. Recent determinations of the melting point with specimens of reasonable purity yielded the values 793 ± 5°C, 804°C, and 815°C, as reported by Ahmann (36), Spedding and Daane (21) and Loriers (35), respectively.

From the preceding survey of the allotropy of cerium it can be concluded that cerium exhibits at least four stable allotropes at different temperatures. The first three allotropes, namely, the collapsed fcc phase, the hcp phase, and the normal fcc phase are often found together at low temperatures, although their respective regions of stability have been defined. The relative amounts of each phase found at any temperature depend on the thermal and mechanical history of the sample.

Above room temperature usually the normal fcc structure is observed, except when the sample has been cooled previously much below room temperature; in the latter case the hcp phase is observed. One high temperature transformation occurs, which is apparently isothermal, and for which the value of 730°C reported by Spedding et al. (14), was adopted because this value is consistent with other recent data obtained with pure samples. The melting point reported by Spedding and Daane (21) to be 804°C has been adopted in the present study because it is also consistent with other recent data and because the method of determining it seems preferable.

Praseodymium

The structure of praseodymium at room temperature was found to be hcp by Rossi (5, 41). Klemm and Bommer (1) examined their reduction mixture of praseodymium and potassium chloride and found praseodymium to be fcc with the lattice

constant of 5.162 Å. Later, however, they performed X-ray studies on a 98-99 per cent sample of praseodymium and observed the hcp structure which could not be transformed to the fcc form by annealing below 425°C (42). They observed irregularities in the line intensities along with some extra lines, which could be accounted for by doubling the value of the c_o-axis. James et al. (10) observed a mixture of both phases in a sample about 99.9 per cent pure. Spedding et al. (12), on the other hand, observed only the hcp modification in praseodymium with a specimen of comparable purity. Noting the similarity between the diffraction pattern of praseodymium and neodymium, they were able to substantiate the existence of the double c_o-axis in praseodymium, suspected by Klemm and Bommer, and to determine the lattice constants to be a_o = 3.6725 Å and c_o = 11.8354 Å.

There seems to be no evidence of a solid phase transformation in praseodymium at low temperatures, with the possible exceptions of a slight dip in the atomic heat at about 98°K reported by Parkinson et al. (29) and a slight anomalous decrease in the coefficient of expansion, reported by Barson (43).

The existence of a high temperature transformation in praseodymium was established by several investigators. Spedding and Daane (21) reported two thermal arrests, one at 798°C, due to a solid phase transformation and another at 935°C, due to the melting of the metal. The electrical

resistivity measurements reported by Spedding et al. (14) showed a sharp increase in the resistivity of 5.7 per cent at 789°C-795°C, corresponding to the solid phase transformation. Dilatometric data of Barson et al. (20) indicate a discontinuous increase in volume of 0.1 per cent at 790°C-793°C. The existence of the transformation was also verified by the enthalpy measurements of Spedding et al. (40) who observed the transformation in the vicinity of 798°C and reported the heat of transformation to be 722 calories per mole. The heat of fusion of praseodymium was found by Berg (44) to be 1652 calories per mole at 935°C.

The studies performed on pure praseodymium samples indicate that at high temperature a solid phase transformation occurs which is apparently isothermal. The values of the transformation temperature and of the melting point adopted for the present study are 798°C and 935°C reported by Spedding et al. (21). The structure of the high temperature phase has not been reported.

Neodymium

The structure of neodymium at room temperature was found to be hcp by Quill (3) and by Klemm and Bommer (1). However, the latter found in the diffraction patterns additional lines which could be accounted for by doubling the c_o-axis. Ellinger (45) verified conclusively the structure suspected by Klemm and Bommer; he determined the structure by powder

methods, using a specimen of neodymium containing 0.03 per cent calcium as its major impurity and less than 30 ppm carbon. The space group was given as $P6_3/mmc$ with four atoms of the unit cell at the positions (0, 0, 0), (0, 0, 1/2), (1/3, 2/3, 1/4), and (2/3, 1/3, 3/4), and the lattice constants were reported as a_o = 3.655 Å and c_o = 11.796 Å. He also found this structure to be stable to at least 680°C by high temperature X-ray methods. Behrendt et al. (46) verified this structure by investigating a single crystal of neodymium by X-ray methods. Spedding et al. (12) redetermined the lattice constants using a focussing back-reflection camera and obtained the results shown in Table 1. (See page 21b.)

The data on electrical resistivity reported by James et al. (10) for the temperature range 20°K to 320°K consist of a smooth curve and, therefore, do not give evidence of a phase transformation at the low temperatures.

Jaeger et al. (13) reported anomalies occurring in the electrical resistivity, atomic heat, and coefficient of expansion near 540°C and near 700°C, which they ascribed, without proof, to hcp-fcc and fcc-δ transformations, respectively. Trombe and Foex (47) noted an anomaly at 600°C to 650°C in their dilatometric data and associated it with the hcp-fcc transformation supposed by Jaeger and his co-workers. Ahmann (36) reported the melting point of neodymium as 820°C for a sample containing one per cent of magnesium and 0.5 per cent calcium; he did not find any transformations below this

temperature. Bates et al. (48) did not note any indications of a phase transformation in their magnetic susceptibility investigation of this element in the region 18°C to 727°C. Thermal analysis reported by Spedding and Daane (21) revealed a solid transformation at 868°C and a melting point at 1024°C. In the same report the authors mentioned that X-ray studies at high temperatures gave evidence that between 800°C and 900°C neodymium transformed from hcp to what seemed to be fcc structure; however, no lattice constants were given. A striking evidence for the existence of a high temperature transformation in neodymium was obtained by Spedding et al. (14) in the form of a sharp increase of 6.4 per cent in the electrical resistivity at 861°C-864°C. The transformation was also confirmed by the dilatometric results reported by Barson et al. (20) who noted a 0.1 per cent increase in the volume of the metal at 867 ± 2°C. The data on the enthalpy of neodymium reported by McKeown (40) reveal clearly that the phase transformation and the melting point occur near 862°C and 1024°C, respectively, the heats of transformation and of fusion being 713 and 1705 calories per mole, respectively.

Recent studies on pure samples of neodymium, therefore, indicate one transformation occurring at high temperature. The high temperature structure is thought to be fcc, although a positive identification has not been reported. Perhaps the best values of the transformation temperature and the melting

point, from the standpoint of the sample purity and the method of determination of these constants, seem to be 868°C and 1024°C as reported by Spedding et al. (21).

Europium

Klemm and Bommer (1) determined the structure of europium at room temperature using for their specimen a reduction mixture consisting of potassium chloride and europium. They found the metal to be body centered cubic (bcc) and reported the lattice constant to be a_o = 4.582 Å. Spedding et al. (12) also reported the same structure for 98-99 per cent europium with a lattice constant of 4.606 Å. Barrett (49) showed that the bcc structure persists throughout the temperature range 5°K to 300°K with the lattice constant at 5°K, 78°K, and 300°K being 4.551 Å, 4.551 Å, and 4.577 Å, respectively. Spedding et al. (50) determined the lattice constant to be 4.5820 ± 0.0004 Å for a sample containing less than 0.1 per cent ytterbium and 0.05 per cent samarium as its major metallic impurities and having a residual resistivity close to zero as found by Curry (51). The same authors (50) also reported the melting point to be 826°C and their thermal analysis did not reveal any other anomalies below that temperature. Trombe (52) reported the melting point of europium to be between 1100°C and 1200°C; however, the properties which he reported for his specimen definitely indicate that his specimen was not europium metal.

Europium is ferromagnetic at low temperatures and it has a magnetic transformation (Curie point) near 90°K as reported by Klemm and Bommer (1) and by others (51, 53).

Ytterbium

Klemm and Bommer (1) reported the structure of ytterbium to be fcc at room temperature with a lattice constant of 5.479 Å. Spedding et al. (12) confirmed this structure and found the lattice constant for 99.9 per cent ytterbium to be 5.8462 Å.

The melting point of ytterbium was determined by means of a thermal analysis by Spedding and Daane (21) to be at 824°C; another thermal arrest at 798°C preceded the melting of the metal.

Bridgman (18) studied the electrical resistivity of the metal as a function of the pressure and found at 50,000 kg/cm^2 a maximum in this property, some thirteen times its normal value. Above 60,000 kg/cm^2 the resistivity dropped suddenly to a smaller value than the normal one and remained relatively constant with further increases in the pressure.

Dilatometric measurements were performed by Barson et al. (20) who observed a small discontinuous decrease in volume on cooling, indicative of a phase transformation.

Curry (51) investigated the electrical resistivity of ytterbium in the temperature range 1.3°K to 900°K and observed a discontinuity and a change of slope of the curve at

about 327°C. A second small discontinuity was observed at about 177°C but it was attributed to an annealing process. Residual resistivity of 2×10^{-6} ohm-cm was observed for the sample, indicating the presence of impurities.

Berg (44) found a discontinuous increase of 30 calories per mole in the enthalpy of ytterbium at 280°C. He observed another discontinuity in the solid phase region at 765°C in the form of an increase of 425 calories per mole. He found the melting of the metal to be accompanied by an increase of 1800 calories per mole in the enthalpy.

Scandium, yttrium, gadolinium, terbium, dysprosium, holmium, erbium, thulium, and lutetium

All the elements under this heading have the same crystal structure at room temperature, namely, the hcp structure, similar to the structure of magnesium.

The structure of scandium was determined by Meisel (54) and by Bommer (8). The former used a specimen of 94-98 per cent purity and found in the same sample a fcc phase with a lattice constant $a_o = 4.532$ Å, in addition to the hcp phase. Later investigators (55) indicated that the fcc structure may be due to scandium nitride.

The structure of yttrium was determined by Quill (3, 56) and verified by Bommer (8); the structure of erbium was reported by Monkman (57) and later by Klemm and Bommer (1); the structure of holmium was first reported by Bommer (8). The

structures of the remaining elements, namely, gadolinium, terbium, dysprosium, and thulium were determined by Klemm and Bommer (1).

Spedding et al. (12) redetermined the lattice constants of all the metals in this group and obtained lattice constants which are given in Table 1. Included in this table are the lattice constants obtained by them for the light rare earths, as well as the lattice constants of europium and samarium determined by others (50,58). All of the metals appearing in Table 1, with the exception of cerium, praseodymium, neodymium, and gadolinium, were prepared for the X-ray investigation by distilling the metals in a high vacuum furnace.

The information regarding the allotropy of these elements at different temperatures is meager. As for scandium, there is no concrete evidence for the existence of a fcc allotrope, discounting the report of Meisel.

Spedding et al. (59) distilled a considerable quantity of the metal and determined the melting point to be 1538 $\pm$ 5°C.

From the phase diagram studies a considerable amount of evidence has accumulated regarding the existence of a high temperature solid phase transformation in yttrium. Eash (60) reported a region of complete solid solubility of the high temperature (bcc) form of thorium with yttrium. He was able to show by high temperature X-ray methods that the alloys containing 50 weight per cent (and possibly 80 weight per cent) yttrium remained bcc above 1400°C. He also showed a

Table 1. Lattice constants of Sc, Y, and the rare-earth metals by Spedding, Daane, and Herrmann (12)

Element	Crystal structure	Lattice constants (Å) a_o	c_o
Sc	hcp	3.3090	5.2733
Y	hcp	3.6474	5.7306
La	hcp	3.770	12.159
Ce	fcc	5.1612	-
Pr	hcp	3.6725	11.8354
Nd	hcp	3.6579	11.7992
Sm[a]	rhom.-hcp	3.621	26.25
Eu[b]	bcc	4.5820	-
Gd	hcp	3.6360	5.7826
Tb	hcp	3.6010	5.6936
Dy	hcp	3.5903	5.6475
Ho	hcp	3.5773	5.6158
Er	hcp	3.5588	5.5874
Tm	hcp	3.5375	5.5546
Yb	fcc	5.4862	-
Lu	hcp	3.5031	5.5509

[a]Values reported by Daane *et al.* (58).

[b]Value determined by Spedding *et al.* (50).

discontinuous decrease in the electrical resistivity of yttrium at 1495°C. The extrapolation of the $\alpha - \beta$ solvus of the yttrium-rich alloys to pure yttrium also indicated a transformation at this temperature. Valletta (61) observed a region of complete solid solubility of yttrium and the phase of lanthanum at high temperatures. By extrapolating the solvus of the yttrium-rich alloys he determined the transformation in yttrium to be between 1470°C to 1490°C. He also showed a continuum in the solid solubility of the γ phase of gadolinium with yttrium at high temperatures. Gibson (62) successfully quenched a magnesium-90 per cent yttrium alloy from a one phase region above a eutectoid that exists at this composition at 778°C. The solid solution, which in the phase diagram extends to pure yttrium, was retained and was identified as bcc with a lattice constant of 3.90 Å. The data on electrical resistivity obtained by Fischer and Fullhart (66) in the temperature range 20°C to 1000°C combined with those of Eash (60) in the range 800°C to 1495°C show continuity and do not give any indication of an additional transformation in yttrium.

The reported values of the melting point of yttrium range between 1475°C and 1550°C, depending on the method of preparation. Habermann et al. (64) recently reported the melting point of a distilled specimen of yttrium as 1509±5°C, which is believed to be the most reliable value so far.

The heavy rare earths, beginning with europium and excluding ytterbium and lutetium, undergo magnetic transformations at low temperatures, and, consequently, they also exhibit interesting phenomena in other properties. In the case of gadolinium, the dilatometric results of Trombe and Foex (65) showed a bend in the expansion curve at about 16°C, which is the Curie point of gadolinium. Below this temperature the coefficient of expansion of the metal was nearly zero, whereas above this temperature the coefficient of expansion was about 8×10^{-6} $(^{\circ}C)^{-1}$. There was also a small hysteresis loop in the expansion curve between 100°C and 250°C. The anomaly in the dilatometric results at the Curie point was verified by Barson et al. (20), who showed a minimum in the expansion curve at the Curie point. This indicates that for a small temperature range below the Curie point the coefficient of expansion of the metal assumes a negative value. Bannister et al. (66) investigated the behavior of the metal at low temperatures by X-ray methods and showed that gadolinium retains its hcp structure to at least 105°K. From this temperature to the Curie point they observed a negative coefficient of expansion for the c_o-axis, and a positive coefficient of expansion for the a_o-axis, the resulting coefficient of expansion being about 1×10^{-6} $(^{\circ}C)^{-1}$.

A similar minimum in the expansion curve was observed in the case of terbium by Barson et al. (20) near the temperature of 230°K which is in the vicinity of two magnetic

transformations at 220°K and 228°K, reported both by Jennings et al. (67) and by Thoburn et al. (68).

Dysprosium exhibits two magnetic transformations at low temperatures, one being the Néel point at 176°K and the other the Curie point at 92°K as shown by Trombe (69) and Elliot et al. (70). Trombe and Foex (65) showed that above the Néel point dysprosium has a normal coefficient of expansion, but below it, the metal has a very small coefficient of expansion. There is a minimum in the expansion curve at the Néel point. Bannister et al. (66) made a crystallographic study of dysprosium at low temperatures and showed that the metal retains its hcp structure down to at least 38°K. Below the Néel point they observed a negative coefficient of expansion for the c_o-axis and a positive coefficient of expansion for the a_o-axis, the resulting value of the macroscopic coefficient of expansion being almost zero.

Holmium also exhibits magnetic transformations at low temperatures; however, neither crystallographic nor expansion data are available for this region.

The Curie point and the Néel point of erbium are about 20°K and 78°K, respectively, as reported by Elliot et al. (71). A dilatometric study of the metal by Barson (43) in the range from 100°K to room temperature did not disclose any anomalies and yielded a normal coefficient of expansion. The X-ray results reported by Bannister et al. (66) indicate that erbium retains its hcp structure down to at least 43°K and

exhibits below the Néel point a negative coefficient of expansion of the c_o-axis and a positive one for the a_o-axis, the value of the macroscopic expansion being almost zero. Above the Néel point the coefficient of expansion was given as $10 \times 10^{-6}\ (^{o}C)^{-1}$.

Thulium exhibits a magnetic transformation at low temperatures, its Néel point being near 52°K as shown by Rhodes et al. (72) and by others (51, 73). Neither the expansion data nor the crystallographic data are available for this element in this temperature region.

Very little investigation has been done regarding the allotropy of the trivalent heavy rare earths at high temperatures. Barson et al. (20) undertook the dilatometric investigation of gadolinium, terbium, dysprosium, and erbium up to about 950°C and observed a slight anomaly in the expansion curve of terbium between 700°C and 850°C and of dysprosium between 650°C and 900°C.

Spedding and Daane (74) reported two distinct thermal arrests in the thermal analysis of gadolinium; one at 1264°C and the other at 1322°C, representing a transformation in the solid phase and the melting point, respectively.

Terbium was reported to exhibit a similar behavior at high temperatures by Spedding et al. (75) who listed the transformation temperature as 1310°C. Perhaps the most reliable value of the melting point was obtained by Habermann et al. (64) who used a distilled sample of terbium and determined

the melting point to be 1356 ± 5°C.

Curry (51) measured the electrical resistivity of lutetium from 1.3°K to 444°C and obtained a smooth curve throughout the region except below 5°K, where a decrease in this property occurred, probably because a sufficient amount of tantalum was present in the sample to render it superconducting.

The remaining additional information regarding the high temperature allotropy of the trivalent heavy rare earths is that on the melting points. The latest values, which are probably most reliable, because they were obtained with distilled materials, are 1407 ± 5°C for dysprosium, 1497 ± 15°C for erbium, 1545 ± 15°C for thulium, and 1652 ± 10°C for lutetium. These values were determined by Habermann et al. (64).

Literature Survey of High Temperature X-Ray Methods

Introduction

Pure solid substances exist in one or more forms or allotropes, crystalline or amorphous. At fixed conditions of temperature and pressure it is often possible to obtain the same substance in various allotropic modifications, although usually only one of these forms is thermodynamically stable. The existence of the unstable or metastable phases is then ascribed to unfavorable kinetic processes for the phase transformation. The three modifications of carbon serve as an

example of such a situation. When either the temperature or pressure is varied, another phase may become thermodynamically favored and a transformation into this phase will occur if the kinetics for such a process are favorable. The properties of a substance as functions of temperature or pressure are generally different for various allotropes and this fact renders the detection of phase changes feasible by the measurement of these properties. The actual identification of a phase can be done by microscopic observations, by solubility determinations with a substance of a known structure, or it can be done most effectively by X-ray diffraction studies. X-ray studies have been performed successfully both at high temperatures and at high pressures although both techniques present several experimental problems. One of the problems at high temperatures is the controlled heating of the sample. Heating is generally accomplished by means of a resistance furnace placed around the specimen, by direct heating of the specimen by passing current through it, or by depositing the specimen on a heated wire. The problem of heating becomes considerable at very high temperatures where power consumption may become very large, and where the heating element may become susceptible to oxidation.

The measurement of temperature is perhaps the most difficult task, and it is approached in several ways. In one of these techniques, a standard substance is mixed in with the specimen and the temperature is determined from the lattice

constant of this standard substance. This technique can be used only when there is no chemical reaction or solution taking place between the two substances. Thermocouples in contact with, or in the vicinity of, the samples are often used to determine the temperature. This technique has a special merit when the thermal gradients in the furnace are small. The temperature can also be determined by calibrating a thermocouple imbedded in the furnace, by calibrating the power input against the temperature of the specimen as determined from the lattice spacings of some standard substance, or from the transformation temperatures of several calibrating substances. For a metallic sample, the resistivity of the specimen can be used as an indication of the temperature if black body conditions prevail; in the absence of black body conditions the temperature can still be determined from the current through the sample if both the emissivity and the electrical resistivity are known as functions of temperature. Finally, the temperature can be measured by means of an optical pyrometer, but again, black body conditions must prevail.

Other details that pose problems in the high temperature X-ray diffraction techniques are those of the environment of the sample. A given sample may require an oxidizing, reducing, or an inert atmosphere when it is being heated. Whenever an environment other than air is needed, the sample must be enclosed in a container and the problem of selecting proper window material transparent to X-rays arises. An additional

problem is encountered with volatile samples, where the specimen must be kept in containers capable of containing gas at a pressure of several atmospheres.

The rare-earth metals pose a special problem at high temperatures because they react readily with all but the inert gases. Even the gases adsorbed on the walls of the furnace parts create a problem, because the rare-earth metals, being the most reactive substances in the furnace, act as getters for the gases which are liberated as the furnace is heated. Since the rare-earth metals react at high temperatures with solid materials transparent to X rays, devising a suitable container for the rare-earth metal specimen becomes a problem also.

High temperature X-ray cameras

The preceding introduction perhaps explains why so many various high temperature cameras have been described and built by various investigators. The type of a high temperature X-ray diffraction device most flexible in its usefulness is the diffractometer. In addition to affording the determination of various phases and expansion characteristics of a given substance, the diffractometer enables one to detect isothermal transformations with speed and accuracy, to determine Debye temperatures, to observe annealing effects, and to study phase transformation kinetics or the kinetics of a chemical reaction. Several devices of this type have been

built and they resemble, in general, the unit described by Chiotti (76) which has a furnace consisting of a tantalum foil, and can contain either powdered or bulk specimens in a vacuum at temperatures as high as 1650°C. This unit can be attached to a Norelco diffractometer and it is capable of recording Bragg angles as high as 160° of 2θ. A similar unit capable of recording the entire Bragg spectrum was described by Spreadborough and Christian (77), and a high temperature diffractometer attachment for use with vacuum or with controlled atmospheres was reported by Kennedy and Calvert (78). Several other diffractometer furnaces appear in the literature (79, 80, 81, 82). One difficulty associated with the diffractometer units is that they require samples of rather large size, and, hence, a rather large furnace requiring a high power input (several hundred watts). The operation of these cameras above 1650°C becomes impractical because of the large power loss incurred by their furnaces.

High temperature cameras of the Debye-Scherrer type have become relatively popular. Excellent cameras of this type have been described by Hume-Rothery and Reynolds (83) and by Goldschmidt and Cunningham (84, 85). The former used their camera to determine the lattice constants of silver up to 950°C; these data provide a means for the calibration of high temperature cameras with an accuracy of $\pm$ 1°C. The latter built a 19 cm diameter camera with many desirable features. Buerger *et al.* (86) described a Debye-Scherrer type camera

with a small furnace operating in air and attaining a temperature of 600°C, while requiring only 32 watts at this temperature. A commercial camera of this design was built by Otto von der Heyde*. It has an interchangeable film holder so that either 114.6 mm or 57.3 mm film can be used, and films can be changed without interrupting the heating of the sample. This camera, with modifications which will be described later, was used in the present investigation. Another Debye-Scherrer camera with a provision for containing gases under pressure up to 20 atmospheres was built by Basinski and Christian (87). They used this camera with success in the determination of the γ and δ phases of manganese and the expansion characteristics of these phases up to 1245°C. Debye-Scherrer cameras capable of operating above the melting point of platinum have been built with a tubular carbon heater, capable of attaining temperatures up to 1800°C when using resistance heating, as reported by Matuyama (88) and 3000°C when using high frequency induction heating, as reported by Edwards et al. (89). A similar camera using a tantalum foil heater was reported by Austin, Richard, and Schwartz (90) to be capable of attaining 2000°C. A Debye-Scherrer camera especially suited for the investigation of ceramic materials was reported by Kubo and Akabori (91) who used a 0.2 mm thick platinum wire as a sample support, heater, and thermometer.

---

*Note: The manufacturer's address is: Otto von der Heyde, Box 1168, Maynard, Mass.

The sample was pasted onto the wire which was heated by the passage of current through it, and the temperature was determined from the lattice constants of platinum with an accuracy of $\pm$ 5°C at 1000°C. An ingenious Debye-Scherrer camera was built by Aruja et al. (92) who utilized the hot junction of a thermocouple for supporting their sample, for heating it, and for recording its temperature. The heating was effected by applying rapid pulses of electric current to the thermocouple. An appropriate switching mechanism made it possible to measure the temperature of the hot junction, and, thus, the temperature of the sample. The maximum temperature attainable with thermocouples employing platinum-rhodium alloys was 1850°C.

For accurate determination of coefficients of expansion of substances at high temperatures, a back-reflection focussing camera of the type described by Gordon (93) can be used. He determined the lattice constants of beryllium up to 1000°C with such an accuracy that the resulting mean coefficients of expansion constituted a smooth curve. These results were made possible through the appearance of sharp lines even at high Bragg angles. Such a behavior is desirable; unfortunately, it is not displayed by all solid substances.

APPARATUS AND METHODS

High Temperature X-Ray Equipment

It was implied in the literature survey that in high temperature X-ray studies, the physical and chemical properties of a sample determine the type of camera to be used. Since the rare-earth metals are very reactive, the emphasis is placed on maintaining high vacua or very pure inert atmospheres for long periods of time. To achieve this requirement the following experimental conditions are helpful:

1. A container of small dimensions for the sample and its atmospheric surrounding in order to minimize de-gassing.

2. A closed system (i. e., static vacua or permanent inert atmospheres). The assumption here is that after initial gettering of the residual reactive gases, the atmosphere (or vacuum) remains essentially free of such gases.

3. A furnace with small heat capacity to permit rapid attainment of thermal equilibrium.

4. A camera with a small diameter to permit short exposure times.

5. A camera capable of operating at temperatures as high as the melting point of the samples.

Previous brief attempts made at the Ames Laboratory to obtain diffraction patterns of the rare-earth metals above 700°C showed that a camera in which the furnace is included

in the vacuum system is unsuitable, because the furnace components de-gas appreciably thereby causing prohibitive contamination of the surface of the specimen. Since a camera having all the listed specifications was not available, it was decided to make appropriate modifications on an available Debye-Scherrer camera. This camera was a 57.3 mm diameter camera described by Buerger et al. (86) and commercially produced by Otto von der Heyde (see footnote on page 31). The collimator of this camera was substituted by one having a circular slit of only 0.018 inch in diameter and reaching to within 1/4 inch of the X-ray specimen. This change made it possible to expose samples to X rays for up to five hours without objectionable darkening of the film by scattered radiation, although, ordinarily, only 1 1/2-hour exposures for the rare earths were necessary.

Actually, three different methods were employed in obtaining the diffraction patterns of the rare-earth metals at high temperatures. In the first two methods, which were applicable in the temperature ranges of 20°C to 1000°C and 800°C to 2200°C, respectively, the available Debye-Scherrer high temperature was used. These two methods differed in the manner in which the samples were contained and heated. A detailed description of these two methods will follow shortly.

In the third method a high temperature diffractometer attachment described by Chiotti (76) was used to substantiate some observations made for ytterbium by the first method.

X-ray method for the temperature range 20°C to 1000°C

In this method an external resistance furnace was used to heat the sample which was contained in an evacuated or inert gas-filled silica capillary. The furnace which was supplied with the camera was designed by the manufacturer to operate in the temperature range of 20°C to 600°C; therefore, in order to operate at higher temperatures, it had to be modified as shown in Figure 1. The furnace consisted of two hollow ceramic cylinders which were machined out of Lavite and were subsequently fired at 1200°C for one day. The outer surface of the smaller cylinder was grooved in order that about 4 feet of 0.010-inch platinum-13 per cent rhodium wire could be wound on it uniformly. The smaller cylinder was made to fit inside the larger one and the ensemble was inserted into the original metal housing of the camera. A thermocouple consisting of 0.005-inch thick platinum, platinum-13 per cent rhodium wires was imbedded in the furnace at a point about 1/16 inch from the X-ray specimen. In the manufacturer's design the resistance wire, in form of a spiral, was placed loosely in the inner part of a similar small cylinder, so that it was exposed to the sample. Such a construction allowed large temperature gradients and made the calibration of the furnace subject to sporadic variations, since the shape of the heating element could easily be altered by accidental touching or bumping with the specimen or the specimen holder.

In order to protect the sample from atmospheric

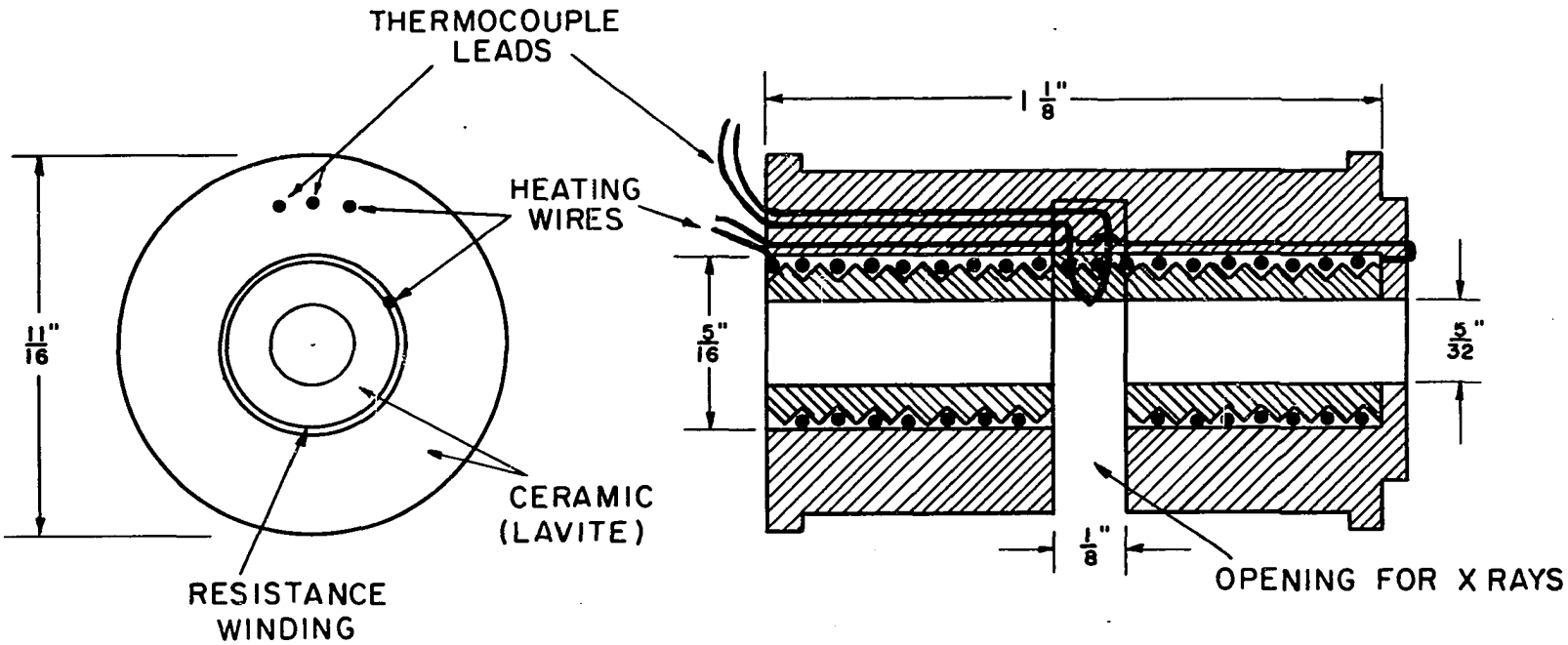

Figure 1. The design of a furnace used in the high temperature Debye-Scherrer X-ray camera

contamination, it was necessary to provide high vacua or purified inert atmospheres for its environment. This was accomplished by placing the sample in a silica capillary which was either evacuated or filled with an inert atmosphere prior to being sealed off. Since silica reacts with the rare earths at elevated temperatures, it was necessary to use wire samples which were kept from contact with the capillary by means of two tungsten spacers. The metal specimens were prepared by rolling a small piece of metal to a thickness of 0.007 inch, from which thin wires were cut by means of a sheet metal shear. The wires were first scraped with a hardened steel edge to make them approximately cylindrical and 0.1 to 0.2 mm thick, were then cut into 6 mm sections which weighed about 0.8 mg.

The tungsten spacers were made of sections of tungsten filament taken from a 200-watt Sylvania light bulb. The spacers were made by inserting a 0.010-inch conductor wire into the filament, welding the end of the filament shut by means of a Heliarc welder, and breaking off a 3 mm spacer with a knife. The spacers were subsequently de-gassed under vacuum at about 1000°C.

Silica capillaries 0.5 mm in diameter and 0.01 mm in wall thickness were obtained from Caine Sales, Chicago.

The samples were mounted in the capillaries as shown in Figure 2. Prior to being sealed off, the capillaries were attached to a vacuum system by means of Apiezon-W wax and were

Figure 2. A rare-earth sample mounted in an evacuated silica capillary. The spirals are the tungsten spacers. The photograph was taken after the sample was heated at 850°C for about one hour. Both pictures are magnified.

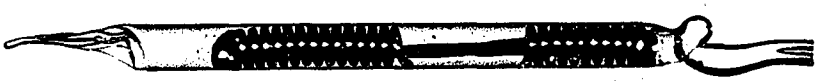

evacuated to a pressure of 5×10^{-7} mm Hg, while being heated at about 400°C. In the case of very volatile metals, the capillaries were filled with argon gas after being evacuated. For very reactive metals, namely, lanthanum, cerium, praseodymium, neodymium, and europium, mounting operations were carried out in a vacuum dry box filled with helium, while for the rest of the rare earths, including scandium and yttrium, such precautions were not necessary.

Initially, the X-ray furnace was heated by alternating current which was regulated by a Stabiline voltage stabilizer and controlled by two powerstats connected in series. The furnace required about 160 watts at 1000°C. The temperature of the sample was determined by means of a thermocouple already described, which was calibrated in terms of the temperature of the sample. The furnace voltage served as a rough check on the calibration of the thermocouple. The determination of temperature was felt to be somewhat unsatisfactory, since only one thermocouple was used and there was a possibility that changes in the calibration of the thermocouple would go undetected. It was, therefore, decided to use the power input as an additional means of temperature measurement; the power input could be determined accurately with a potentiometer if direct current were used. The change to the direct current was arranged by placing a full wave selenium rectifier at an appropriate point in the furnace circuit. The existence of two independent means of temperature measurement

made it unlikely that random changes in calibration would pass unnoticed, unless, of course, an identical change occurred in both calibrations.

The temperature calibration was done by taking diffraction patterns of 99.999 per cent silver at various temperatures and using the resulting lattice constants to obtain the temperature from the data reported by Hume-Rothery and Reynolds (83). As an additional calibration point, the transformation temperature of iron was used by observing the transformation of electrolytically prepared iron at 910°C. The average standard deviation of the lattice constants of silver was 0.002 Å, which corresponds to a temperature uncertainty of ± 20°C. The large standard deviation in the lattice constants of silver stems from the fact that only four to six lines were used to calculate the lattice constants and that a small camera was used. When the calibration points were plotted, the average deviation of the points from the curve drawn through them was ± 7°C.

X-ray method for the range 800°C to 2200°C

In order to take X-ray diffraction patterns of the high melting rare-earth metals, a specimen holder was made in which wire specimens could be heated up to their melting points by resistance heating of the specimen wire. Samples mounted in this specimen holder resembled a light-bulb as can be seen from the sketch of such an assembly in Figure 3 and from the

Figure 3. The design of an X-ray specimen holder in which thin wire specimens can be heated up to their melting points under a vacuum

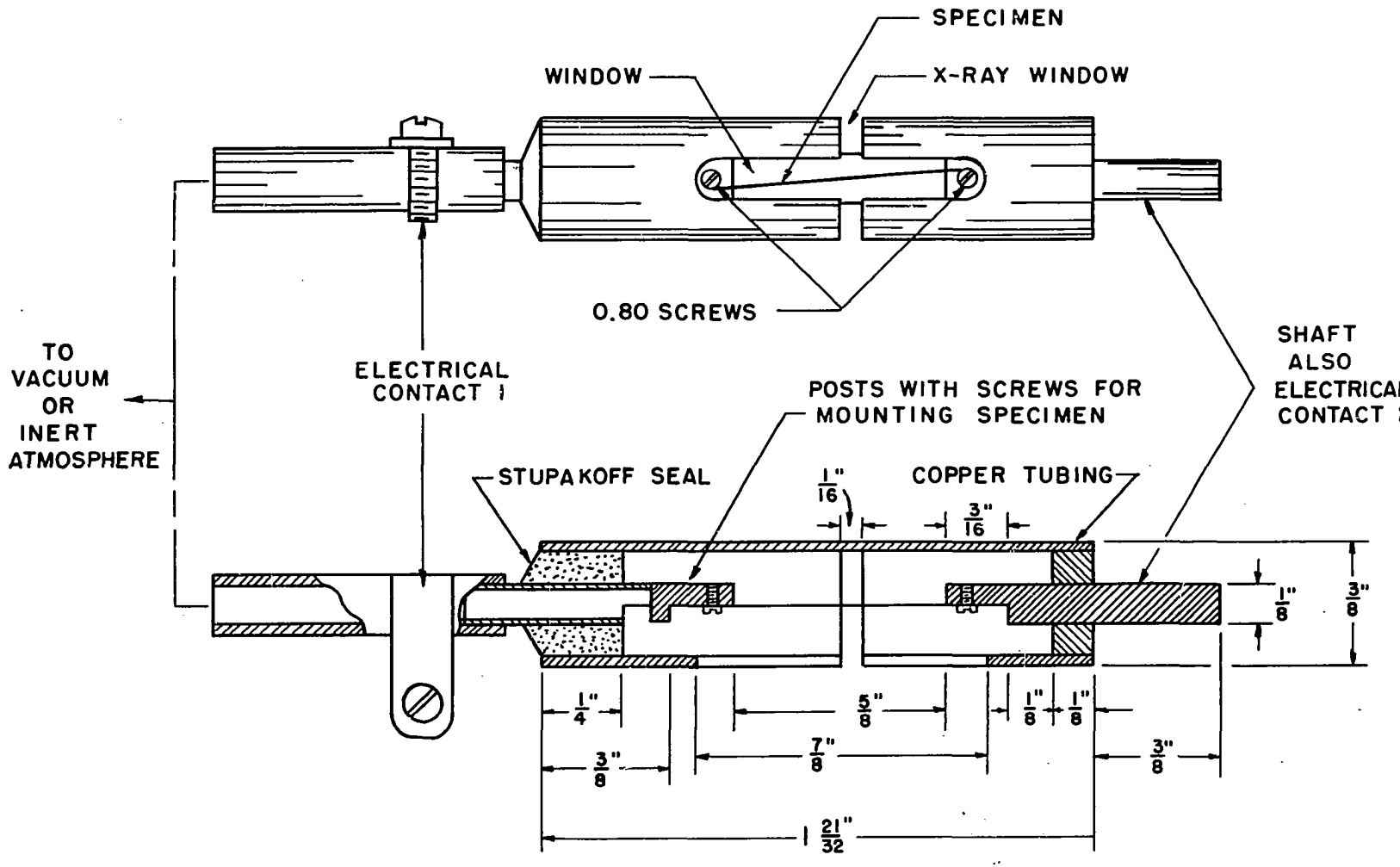
SPECIMEN
WINDOW
X-RAY WINDOW
0.80 SCREWS
TO VACUUM OR INERT ATMOSPHERE
ELECTRICAL CONTACT 1
SHAFT ALSO ELECTRICAL CONTACT 2
POSTS WITH SCREWS FOR MOUNTING SPECIMEN
STUPAKOFF SEAL
COPPER TUBING
1/16"
3/16"
1/8"
3/8"
1/4"
5/8"
1/8"
1/8"
3/8"
7/8"
3/8"
1 21/32"

SCALE : 2" = 1"

Figure 4. Top: Photograph of the X-ray specimen holder sketched in Figure 3. Both the wire specimen and a reflection of light from the Saran Wrap covering the window can be seen

Bottom: The location of the X-ray specimen holder in the Debye-Scherrer camera

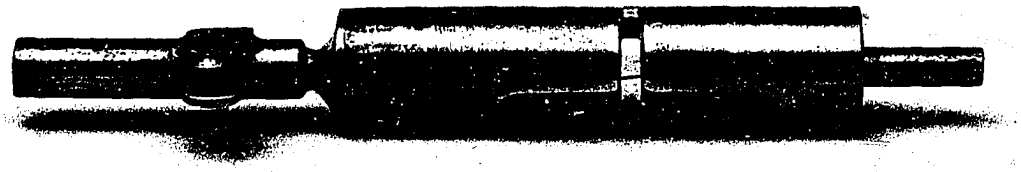

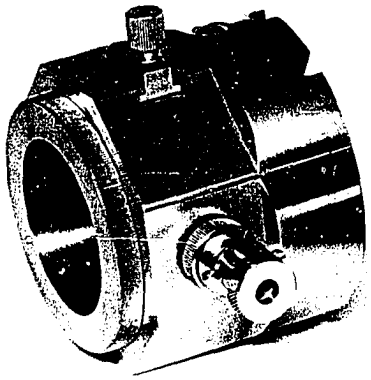

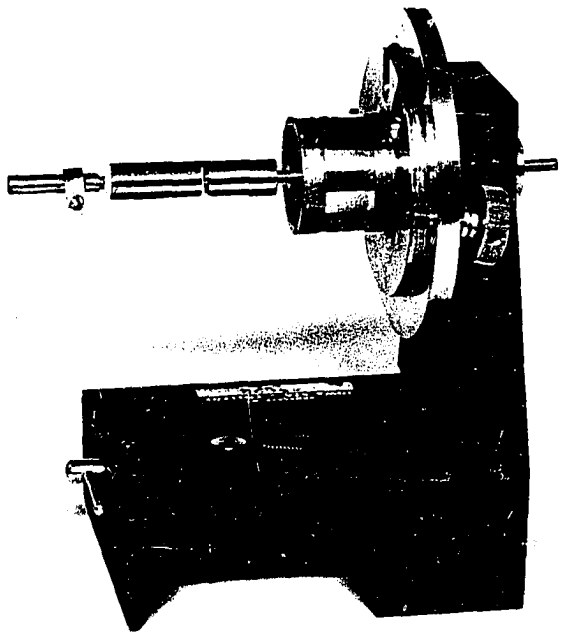

photograph in Figure 4. The specimen holder was made to fit inside the Debye-Scherrer camera described previously; the partially assembled camera is shown in the lower half of Figure 4.

The specimen holder consists of a copper tube inside which are two copper electrical conductors to which the wire specimens can be fastened by means of two set screws. One of these conductors is soldered to a Stupakoff seal, which serves both as an electric insulator and as a means to provide an exhaust for the gases within the specimen holder. The copper tube has two windows cut into it, one of which allows the incident and diffracted X rays to pass in and out of the sample holder, while the other window facilitates the installation and the removal of the wire specimen. After the specimen is mounted, the windows are covered with Saran Wrap*. This is done most effectively by spraying the outside of the copper tube (while the windows are covered with masking tape) with a transparent Krylon spray coating and covering the copper tube with Saran Wrap before the spray coating dries. The specimen holder is then placed inside a drying oven at 100°C for about two minutes, in order for the Saran Wrap to shrink and to adhere tightly to the copper tubing. Heavy rare-earth specimens mounted in this manner retained their metallic brightness after the short heating in air and their

*Note: Manufactured by The Dow Chemical Company, Midland, Michigan.

diffraction patterns did not reveal any impurity lines. Samples assembled in this manner can be evacuated through the hole in the Stupakoff seal. It may seem surprising that the Saran Wrap does not break under these conditions and that vacua as low as 1×10^{-6} mm Hg. can be achieved. In order to prevent even minute amounts of air from diffusing into the specimen holder, a helium atmosphere was provided around the outside of the specimen holder. This was accomplished by covering the openings in the camera casing with aluminum foil and creating a positive pressure of helium in the camera. The specimen holder was connected to a vacuum system by means of rubber tubing which was greased on the inside and outside with Apiezon-N grease to minimize the diffusion of air into the system. A sample assembled in this manner could not be rotated; therefore, a provision was made for oscillating the sample by replacing the motor belt with a "four bar mechanism".

The heated portion of the specimen wire was about 5/8 inch long and about 0.005 inch thick. As long as the thickness of the wire did not exceed this value, it was not necessary to cool the specimen holder, since the amount of heat dissipated was small.

The temperature of the sample was measured approximately by means of an optical pyrometer. Accurate temperature measurements could be made if the metal specimen had a known crystalline transformation accompanied by a discontinuity in electrical resistivity. To utilize the transformation of the

metals for the purpose of temperature calibration, the circuit shown in Figure 5 was used. The sample was heated by direct current supplied by a large 6-volt lead storage battery which was connected in series with the specimen and two rheostats. One of these rheostats was a 10-ohm manual rheostat and the other was a 1.6-ohm rheostat which consisted of a four-foot length of Nichrome wire 0.040 inch in thickness stretched out in a vertical glass tube to which was connected a reservoir of mercury. By changing the height of mercury in the glass tube one could vary the resistance of the rheostat and, hence, the voltage applied to the sample. The resistance of this rheostat could be varied in a continuous fashion by varying the flow of mercury either into or out of the glass tube by means of gravity. A fraction of the voltage across the sample was recorded by means of a Bristol recording potentiometer, while the rest of this voltage was bucked out with an auxiliary potentiometer. Such an arrangement allowed for greater sensitivity in the measurement of the voltage and, hence, in the detection of discontinuities in the resistivity of the sample at the transformations.

This X-ray technique was tested by making two 30-minute exposures of a tungsten sample 0.003 inch in diameter at 1880°C and 2190°C, as measured with an optical pyrometer. Satisfactory patterns were obtained, in that all possible reflections appeared, although at the higher temperature the lines were very spotted, indicating an extensive

Figure 5. A circuit for variable heating of an X-ray specimen and for continuous recording of its voltage

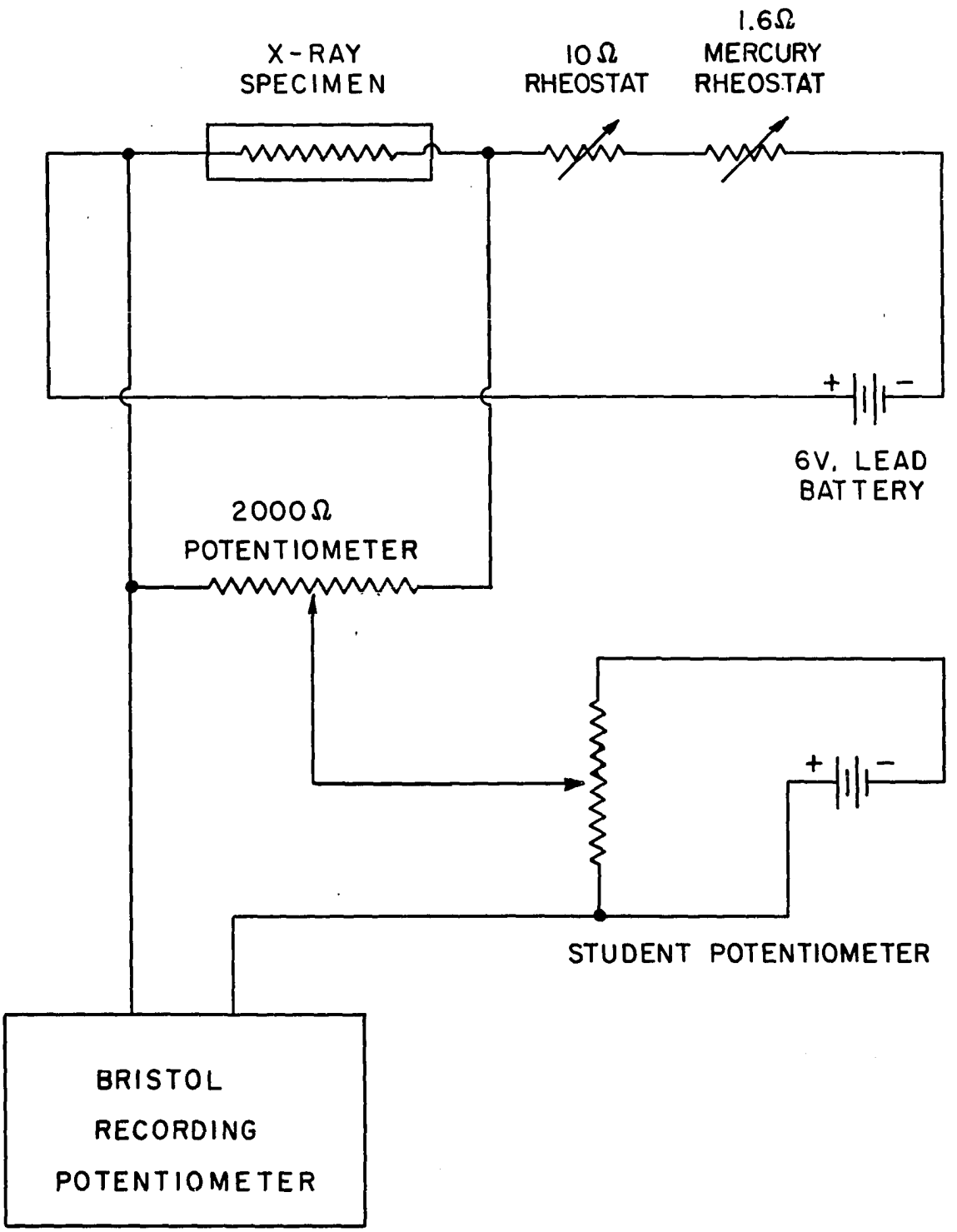
X-RAY
SPECIMEN
10Ω
RHEOSTAT
1.6Ω
MERCURY
RHEOSTAT
+
−
6V. LEAD
BATTERY
2000Ω
POTENTIOMETER
+
−
STUDENT POTENTIOMETER
BRISTOL
RECORDING
POTENTIOMETER

recrystallization of the specimen. The metal retained its bcc structure through the entire temperature range; the lattice constants as a function of temperature appear in Figure 6. The mean coefficient of expansion at 2035°C calculated from the two lattice constants, was 12 x 10^{-6} $(°C)^{-1}$.

Determination of crystalline transformations by means of electrical resistivity

In order to establish the existence of crystalline transformations in some of the heavy rare-earth metals, the method of measuring electrical resistivity as a function of temperature was used. The technique and apparatus employed in the present investigation was that described by Chiotti (95). This method involved the use of massive samples about three inches long and 0.3 inches thick, which were heated either in vacuum or in an inert atmosphere by passing alternating current through them. The temperature was measured by means of an optical pyrometer focussed on a tiny sight hole drilled in the metal, or by means of a thermocouple with a junction wrapped in a tantalum foil and then spot-welded to the specimen; the latter was used only with erbium metal. The voltage drop across the specimen was measured by an alternating current potentiometric technique.

Mathematical methods

Cohen's least-squares method (96) was used to calculate the lattice constants of both cubic and hexagonal lattices.

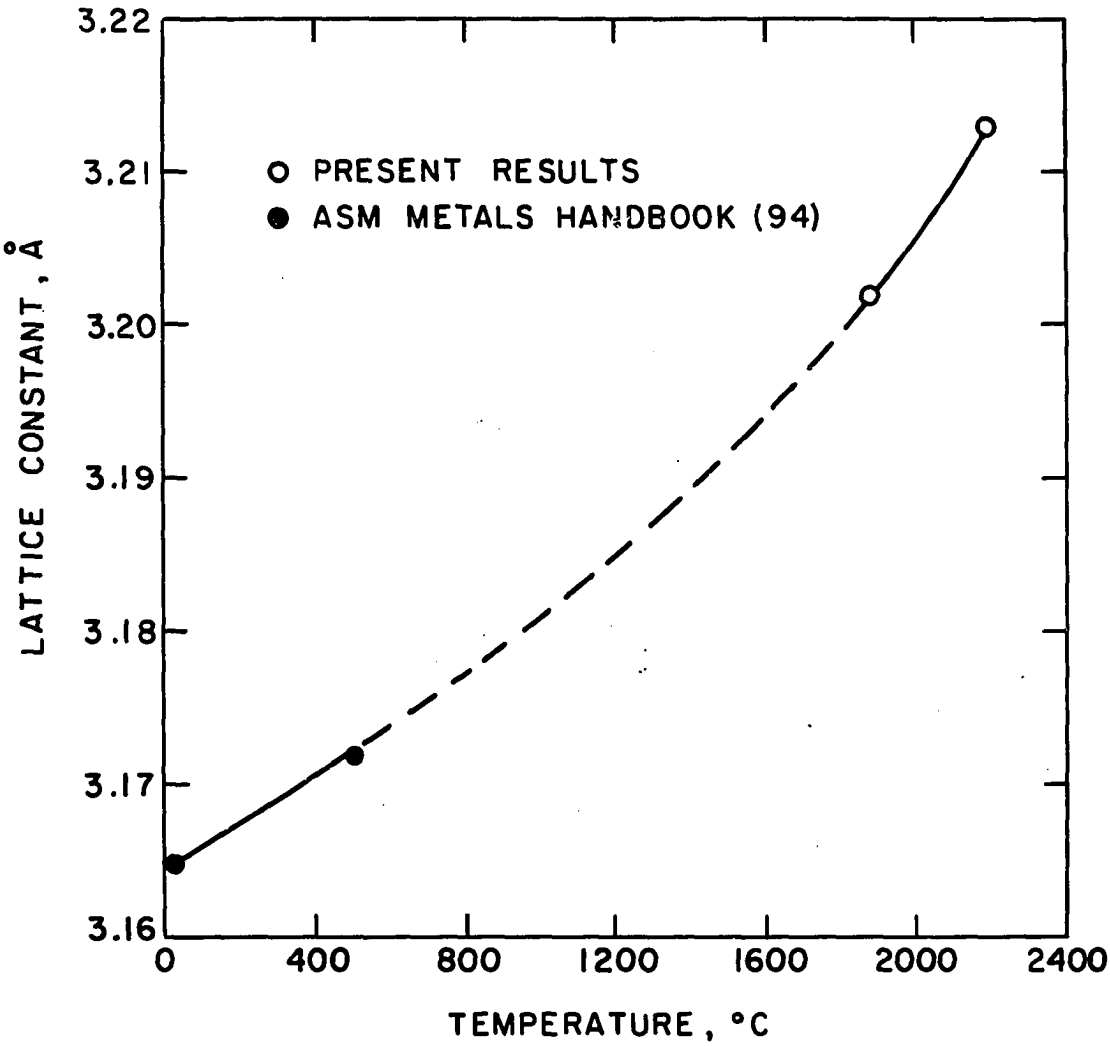

Figure 6. Lattice constant of tungsten versus temperature

For X-ray diffraction patterns where reflections of good quality were available in the region $\theta > 60^{\circ}$, where θ is the Bragg angle, the Bradley and Jay function (97) was used in the least-squares analysis, whereas for patterns having only lower angle reflections, the Nelson and Riley function (98) was used. The calculations were done by means of an IBM-650 computer. In the case of the cubic lattice it was feasible to determine the Miller indices by visual inspection and, therefore, a program was written which utilized only the Bragg angles and the Miller indices as the input data. In the case of the hexagonal lattice, indexing of the diffraction patterns is more involved and time consuming; therefore, a program was written which would first index the pattern and then perform the calculation of the lattice constants by the least-squares method. The input data required for this program were the Bragg angles and the approximate lattice constants a and c. If the approximate lattice constants were not known, they could be easily determined manually from the first few lines of the pattern for which the Miller indices are usually known. From these lattice constants all allowed reflections were calculated in terms of $\sin^2\theta$. The calculated reflections were then compared to the observed reflections. If the two values were within a certain limit of each other, the set of Miller indices for that particular calculated reflection was assigned to the observed reflection. This limit was expressed as

$$\delta = (\sin^2\theta_{observed} - \sin^2\theta_{calculated})$$

and its value was set at $\pm$ 0.002. In the case where several sets of Miller indices could be assigned to a given observed reflection, the best set of indices was selected by computing an average δ from those reflections which had only one set of indices and then comparing the individual deviations to it.

Since the lattice constants obtained from the individual reflections at lower Bragg angles tend to have lower values than at the high angles, it was necessary to make a slight correction for each $\sin^2\theta_{calculated}$ before comparing it to $\sin^2\theta_{observed}$. This correction was made by adding to each $\sin^2\theta_{calculated}$ the value of $\Delta\sin^2\theta$ which was readily obtained from the calculated reflections as shown below:

$$\Delta\sin^2\theta = D(\cos^2\theta_{calculated}) = D\ (1 - \sin^2\theta_{calculated}).^*$$

The constant D was assigned a value of 0.002, which was determined empirically. This expression for the correction

---

*Note: Selecting $D(\cos^2\theta)$ for the correction term amounts to assuming that the total systematic error in d-spacings can be expressed as

$$\frac{\Delta d}{d} \propto \cot^2\theta.$$

This assumption was substantiated by plotting lattice constants obtained from individual reflections versus $\cot^2\theta$. A nearly linear relation was obtained in the range $\theta > 40^\circ$.

yields values that are similar to those obtained from the expression derived from the Bradley and Jay function (97) in the range $\theta > 60^{\circ}$ and from the expression derived from the Nelson and Riley function (98) in the range $\theta > 30^{\circ}C$.

In order to obtain a relation between the lattice constants and temperature, the data were fitted by the least-squares method to empirical equations of the type

$$r = A + Bt + Ct^2 + Dt^3$$

where r is the lattice constant, t, the temperature in $^{\circ}C$, and A, B, C, and D are the coefficients of t^n. Approximate values of the coefficients of expansion were obtained from such equations by differentiation followed by division by the value of the lattice constant at room temperature.

Quantities related to the lattice constants, such as atomic volumes, densities, and axial ratios were calculated from the lattice constants and subsequently fitted to similar equations. In some cases the lattice constants and the related data were fitted to a linear equation relating them to temperature.

An estimate of accuracy in the lattice constants was obtained by using the method described by Jette and Foote (99) which was modified in the present work for the ease in programming and for decreasing the time of calculation. In the normal method, a set of $\Delta \sin^2\theta$ is obtained from individual reflections by back calculation after the lattice

constants have been obtained. The quantity $\sum(\Delta \sin^2\theta)^2$ is then used in determining the standard deviation. The method used in the present work employed the total systematic error in $\sin^2\theta$, namely, $\sum(\Delta \sin^2\theta)^2$ computed on the basis of the assumption that the total systematic error can be expressed in terms of the Bradley and Jay (97) or the Nelson and Riley (98) functions.

There is a qualitative connection between the two methods, namely, that the errors increase with decreasing Bragg angles. Actual comparison of the errors obtained by the two different methods revealed that the errors obtained here were about twice as large as the errors computed by the normal method. The errors computed by the modified method were useful in indicating abnormally large errors made in the reading of the diffraction patterns. It is not known how accurately small random errors are indicated by this method.

An excellent indication of the accuracy of the lattice constants was obtained by plotting the lattice constants as a function of temperature and noting the deviations between these points and the calculated curve drawn through them. It was found, incidentally, that points lying substantially far from such curve showed a large deviation calculated by the modified method.

SOURCE AND QUALITY OF MATERIALS

Source of Scandium, Yttrium, and the Rare-Earth Elements

The metals for the X-ray and electrical resistivity specimens were prepared at the Ames Laboratory. Scandium, yttrium, and the rare-earth elements, excepting samarium, europium, and ytterbium, were prepared by metallothermic reduction of the corresponding trifluorides with calcium, as described by Spedding and Daane (21). Some of the high-melting metals, namely, dysprosium, holmium, erbium, and thulium were subsequently distilled to reduce the amounts of impurities, especially tantalum. The X-ray and the resistivity specimens for a given metal were made from the same batch, except in the case of holmium and erbium. The metal used for the electrical resistivity studies of erbium was not distilled after the preparation by the usual method.

Samarium, europium, and ytterbium were prepared by distilling these metals from a mixture of the corresponding oxides and lanthanum turnings, as described by Daane et al. (100) and by Spedding et al. (50).

Chemical Analysis of Materials

The chemical analyses of the metallic samples appear in Table 2; the list and explanation of the symbols and of the

Table 2. Analyses of metals, per cent

Impurity	Sc	Y	La	Ce	Pr	Nd	Eu	Gd
Y								
La				⩽.02	⩽.005		—	⩽.05
Ce			⩽.03		<.1			
Pr			⩽.04	⩽.02		T		
Nd			⩽.05	⩽.02	<.1			
Sm						⩽.06	.045	⩽.05
Eu							<.01	⩽.01
Gd		.0002					<.01	
Tb								⩽.02
Dy		.008						
Ho								
Er								
Tm								
Yb							<.1	
Lu								
Al	W		FT					
Ca	<.02	.1	<.03	<.03	.05	<.05	W	<.04
Cr	<.06	.006						
Cu		.006	FT					
Fe	<.1	.02	<.006	<.006	.006	.006		<.005
Mg	<.02	.06	<.01	.01	.01	<.01	VW	<.02
Ni		.06	FT					
Si			<.025	.1	<.025	<.025		<.03
Ta		.4	<.1	<.1	.1	.1	—	<.1
Zn	FT						—	
C		.016	.006	.001		.009		.023
H		.013		.012	.001	.004		
N		.008	.015	.005	.013	.004		.013
O		.048			.08	.19		
Br_2 insoluble		1.47						

Table 2. (Continued)

Impurity	Tb	Dy	Ho[a]	Ho[b]	Er[a]	Er[b]	Tm	Yb	Lu
Y						≪.001			.05
La	≪.005							<.01	
Ce									
Pr									
Nd									
Sm									
Eu									
Gd	≪.01								
Tb		≪.1	—						
Dy	≪.02		≪.04			≪.005			
Ho		≪.02			≪.008	≪.008			
Er		≪.02	<.02				<.02	<.01	
Tm			<.01		≪.002	≪.002		<.01	
Yb						.03	≪.001		≪.005
Lu								<.01	
Al					—			VW	
Ca		<.05		.1	VW	<.05	.03	.03	<.05
Cr	VW		<.005					<.005	<.01
Cu	—		—	T		.1		VW	<.02
Fe				.05	—	.02	≪.03	<.01	
Mg							<.03	<.02	<.03
Ni		<.01		—					
Si	T	<.03		<.03		.2	<.03	<.02	<.03

[a]Metals used for high temperature X-ray diffraction study.

[b]Metals used for resistivity study.

Table 2. (Continued)

Impurity	Tb	Dy	Ho[a]	Ho[b]	Er[a]	Er[b]	Tm	Yb	Lu
Ta	VW	≲.1	—	.05			≲.01	<.03	M-S
Zn								—	FT
C	.007	.009		.007	.0075	.026		.005	.007
H									
N	.073	.002		.045	.009	.008		.008	.072
O									
Br_2 insoluble									

Table 3. Code for Table 2

Symbol or abbreviation[a]	Meaning
≪	element not detected at stated detection limit
—	element not detected
<	less than
S	strong (greater than 1 per cent)
M	moderate (.01 to 1 per cent)
W	weak
VW	very weak
T	trace
FT	faint trace

[a]The amounts of impurities decrease in the order, S - M - W - VW - T - FT.

abbreviations used therein are given in Table 3.

The analyses were performed on the original metal preparations from which the investigated specimens were made. This was done because the X-ray specimens were two small (about 0.8 mg) for chemical analysis and because it was desired to preserve the electrical resistivity specimens for further use.

The determination of metallic impurities was carried out by spectrographic methods. The analysis for hydrogen and

oxygen was performed by the vacuum-fusion method, which in the case of the rare earths is applicable only to the metals of relatively low volatility. The analysis for carbon was done by a method involving the burning of the metal in a stream of oxygen and collecting the resulting carbon dioxide in a solution of barium hydroxide. The amount of carbon is determined by the change of electrical conductivity of this solution.

RESULTS

X-Ray Crystallographic Results in the Temperature Range 20°C to 1000°C

Lanthanum

The X-ray diffraction patterns showed that below 288°C both the fcc and the hexagonal (double c_o-axis) structures coexist, whereas at 292°C lanthanum transforms entirely into the fcc phase. In the two-phase region, the lines in the diffraction patterns were broad and rather faint, except for those which were common to both the fcc and the hexagonal lattices. This phenomenon gave an indication of structural defects which are apparently caused by the failure of the atoms to occupy their equilibrium positions in the new structure in the process of the transformation from the fcc to the hexagonal phase. The relative amounts of both phases which were present varied sporadically from sample to sample. In some cases only the fcc phase was found even at room temperature, whereas in other cases, the hexagonal phase was predominant. The fcc phase seemed to be stabilized by atmospheric impurities below 292°C, since it was much more difficult to obtain the hexagonal phase with powdered samples possessing a large surface area than with samples made of wire possessing a much smaller surface area, hence being less susceptible to atmospheric contamination. Samples mounted in air had also a higher proportion of the fcc phase than those

mounted under an atmosphere of helium.

Annealing of the samples at 200°C for a week seemed to improve the hcp patterns slightly; however, when a sample was heated above 290°C and then cooled, the quality of the hcp pattern was extremely poor. For this reason, samples were not heated initially above 290°C when the hcp phase was to be investigated.

The lattice constants of hcp lanthanum, as a function of temperature, appear in Figure 7, where the filled circles represent the data reported by Spedding et al. (12) and where the present data (open circles) were fitted to an equation representing a straight line. The lattice constants of fcc lanthanum appear in Figure 8; they were fitted to a cubic equation. The fcc phase persisted up to the high temperature transformation; however, it was not possible to obtain accurate lattice constants above 600°C for the lack of back reflection lines.

Above 868°C lanthanum was found to be body centered cubic. The diffraction patterns obtained above this temperature showed both the metal pattern and impurity patterns. The metal pattern was easily discernible by its spottings, caused by extensive recrystallization of the sample, and by the absence of the back-reflection lines. The impurity patterns, on the other hand, consisted of an entire spectrum of full, unspotted lines, indicative of polycrystalline, well subdivided samples. The appearance of the impurity pattern

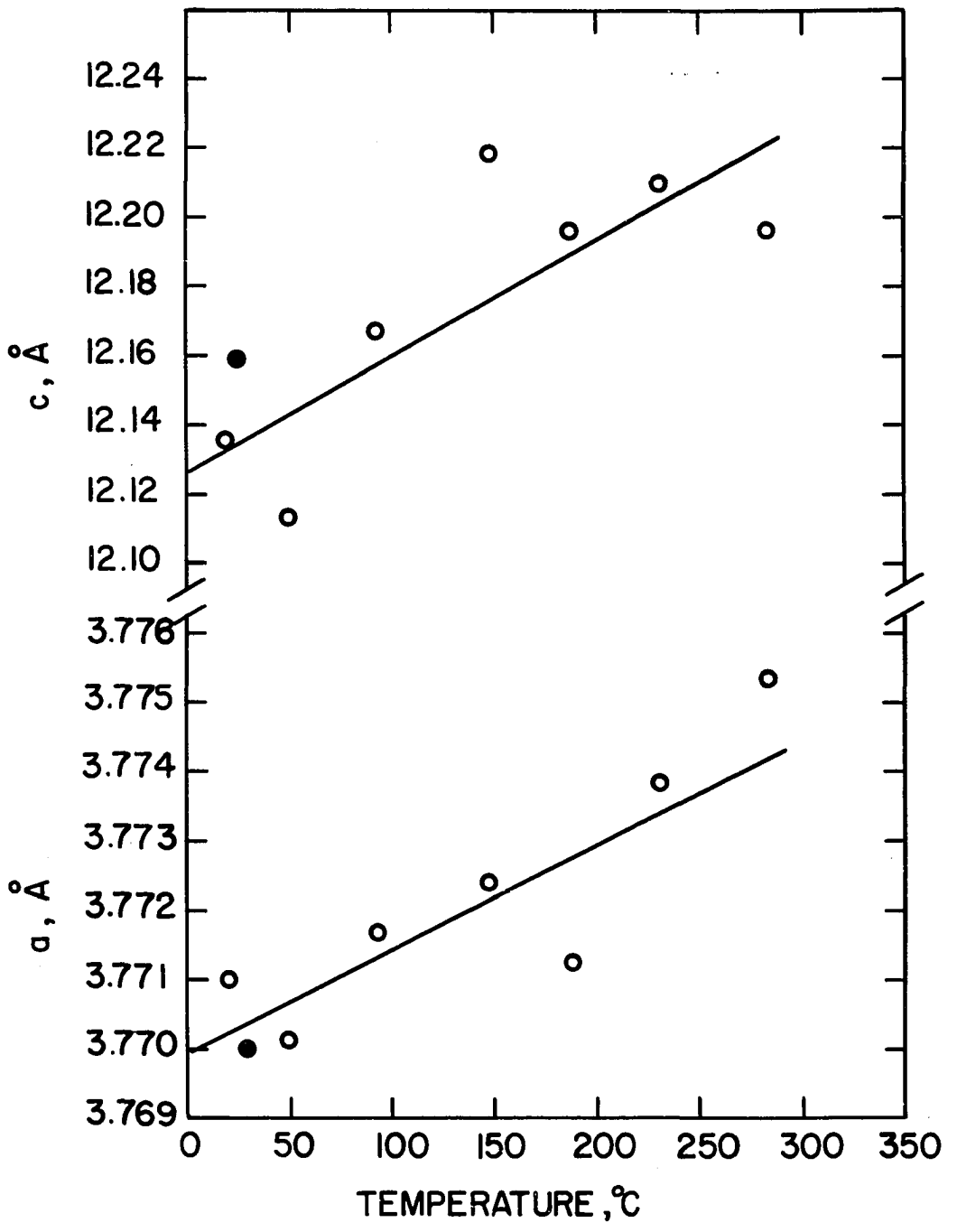

Figure 7. The lattice constants of hexagonal lanthanum versus temperature

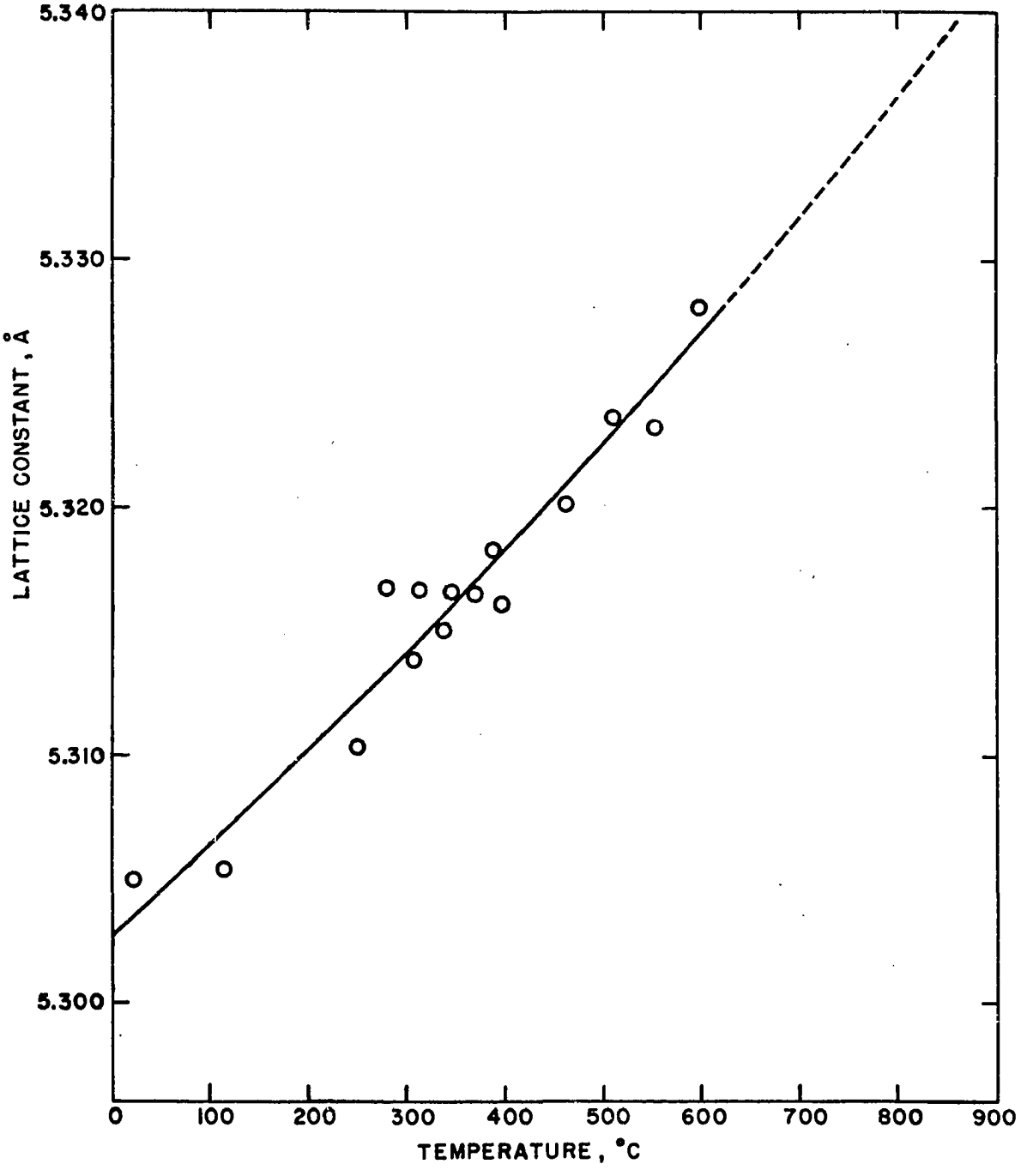

Figure 8. Lattice constant of fcc lanthanum versus temperature

usually began at 600 to 700°C and was more pronounced at higher temperatures and after a prolonged heating at these temperatures. The samples usually acquired a dark blue cast probably caused by impurities formed by residual gases assorbed on the silica walls or by gases slowly diffusing through the silica capillaries. It was found impossible by the present method to keep the sample from contact with these small amounts of gases.

In some cases patterns belonging to a fcc impurity appeared, the lattice constant of which is given in Table 4; in other cases, patterns of an impurity of an unknown structure appeared.

The transformation of lanthanum at this temperature was shown to be reversible by lowering the temperature of the specimens that displayed the bcc structure and obtaining the fcc structure just below the transformation temperature. During such transformations the impurity patterns remained unchanged.

Three patterns of two different samples showed the bcc structure for which the observed reflections are given in Table 5. The average of three lattice constants calculated individually from three different patterns taken at different temperatures was found to be 4.26 Å, the average temperature being 887°C.

A direct comparison of the three phases observed in lanthanum can be made on the basis of the atomic volume

Table 4. Fcc impurities of the rare-earth elements

Element	Temperature C°	Lattice constant of impurity, Å	$\frac{V_{metal}-V_{impurity}}{V_{metal}} \times 100$	Lattice constant of RN at 25°C[a] Å
La	870	5.29	2.8	5.30
Ce[b]	25	5.14	1.4	
Ce[c]	25	5.03	7.5	5.02[d]
Pr	832	5.18	1.6	
Nd	847	5.15	3.4	5.15
Eu	51	5.15	29.0	5.01
Gd	897	5.02	6.4	4.99
Tb	998	4.96	8.5	4.93
Dy	669	4.92	7.7	4.90
Ho	921	4.90	7.8	4.87
Yb	268	4.83	33.1	4.78
Lu	25	4.83	4.7	4.76
Y	25	4.88	12.0	

[a]Values reported by Klemm and Winklemann, (101).

[b]The lattice constants of this impurity as a function of temperature appear in Figure 13.

[c]This impurity is probably CeN. The lattice constants as a function of temperature appear in Figure 13.

[d]Value reported by Iandelli and Botti, (102).

Table 5. X-ray diffraction data for bcc lanthanum[a]

hkl	$\sin^2\theta_{obs.}$	Lattice constant Å
110	0.0661	4.240
200	0.1325	4.235
211	0.1976	4.248
220	0.2637	4.246
310	0.3282	4.255
222	0.3945	4.252
321	0.4604	4.251
	$a = 4.26 \pm 0.01$ Å	
	$t = 887^{\circ}C$ avg.	

[a]Data are a composite of three diffraction patterns taken at 878°C, 881°C, and 902°C.

calculated from the lattice constants. Such a comparison was made by plotting the atomic volume as a function of temperature as shown in Figure 9, which shows a 0.5 per cent decrease in volume of lanthanum as it transforms from the hexagonal to the fcc phase, and a 1.3 ± 0.4 per cent increase in volume as the metal transforms from the fcc to the bcc phase.

The change in volume for the transformation at 292°C is

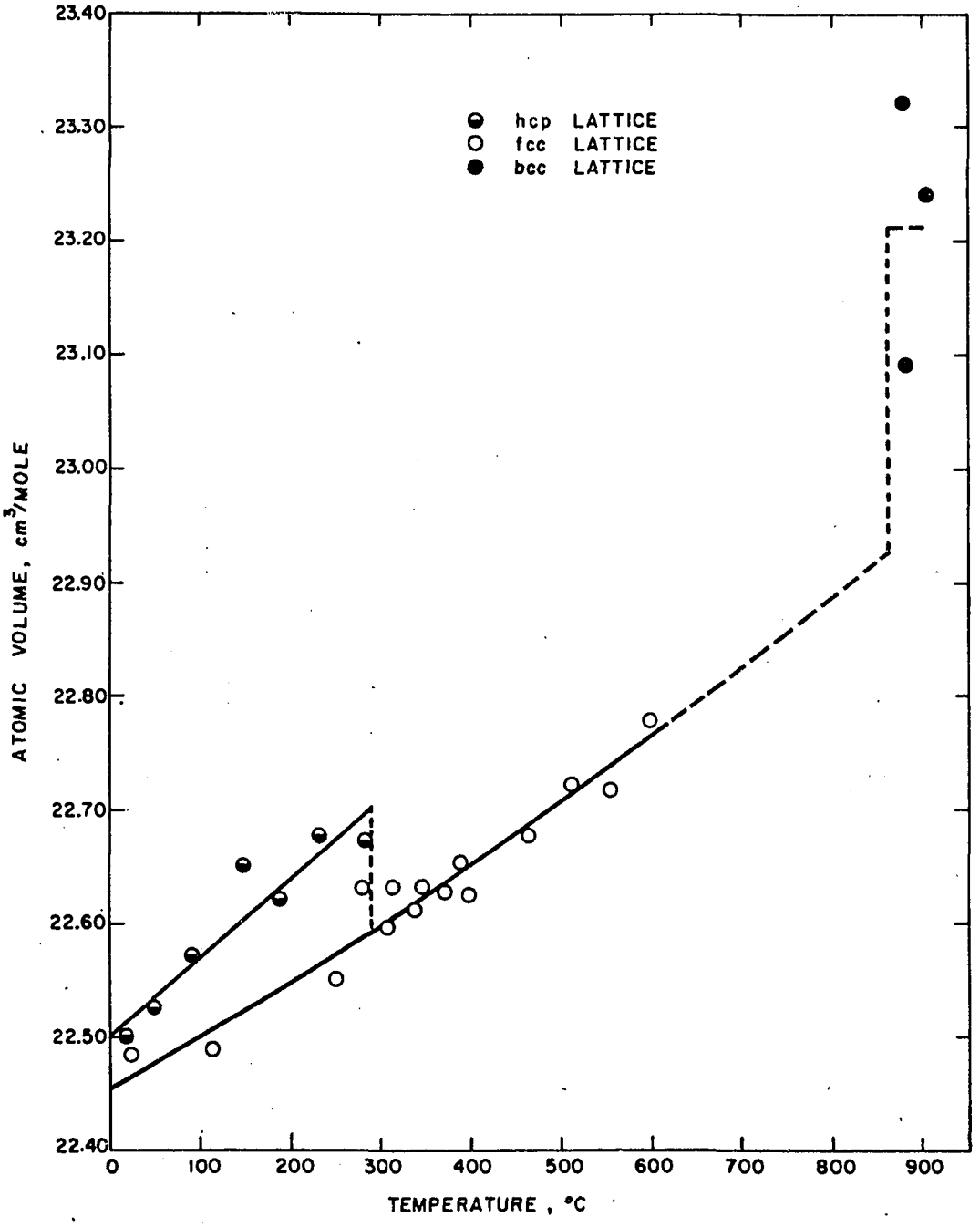

Figure 9. Atomic volume of lanthanum versus temperature

somewhat higher than the 0.3 per cent change observed dilatometrically by Barson, Legvold, and Spedding (20). This discrepancy is to be expected since they measured the volume change of the sample as such, in which the transformation was most likely incomplete, and, furthermore, where an anisotropy effect could be present. In the X-ray method the absolute difference in volume of the hexagonal lattice and the fcc lattice was measured without regard for the actual change in volume of the sample.

The coefficient of expansion of fcc lanthanum calculated from the empirical equation relating the lattice constants to temperature appears in Figure 10. The coefficients of expansion for the other two phases were not obtained because of the lack of sufficient accuracy of the lattice constants. A comparison of the coefficient of expansion obtained in the present investigation with that obtained by dilatometric studies appears in Table 6.

Cerium

In the case of cerium some of the best lattice constants of the light rare-earth series were obtained because reflections at very high angles were available. This situation persisted to about 600°C where the back reflections gradually faded out; however, it was still possible to obtain patterns of the metal which indicated that cerium retained its fcc structure to at least 740°C. In one instance the fcc pattern

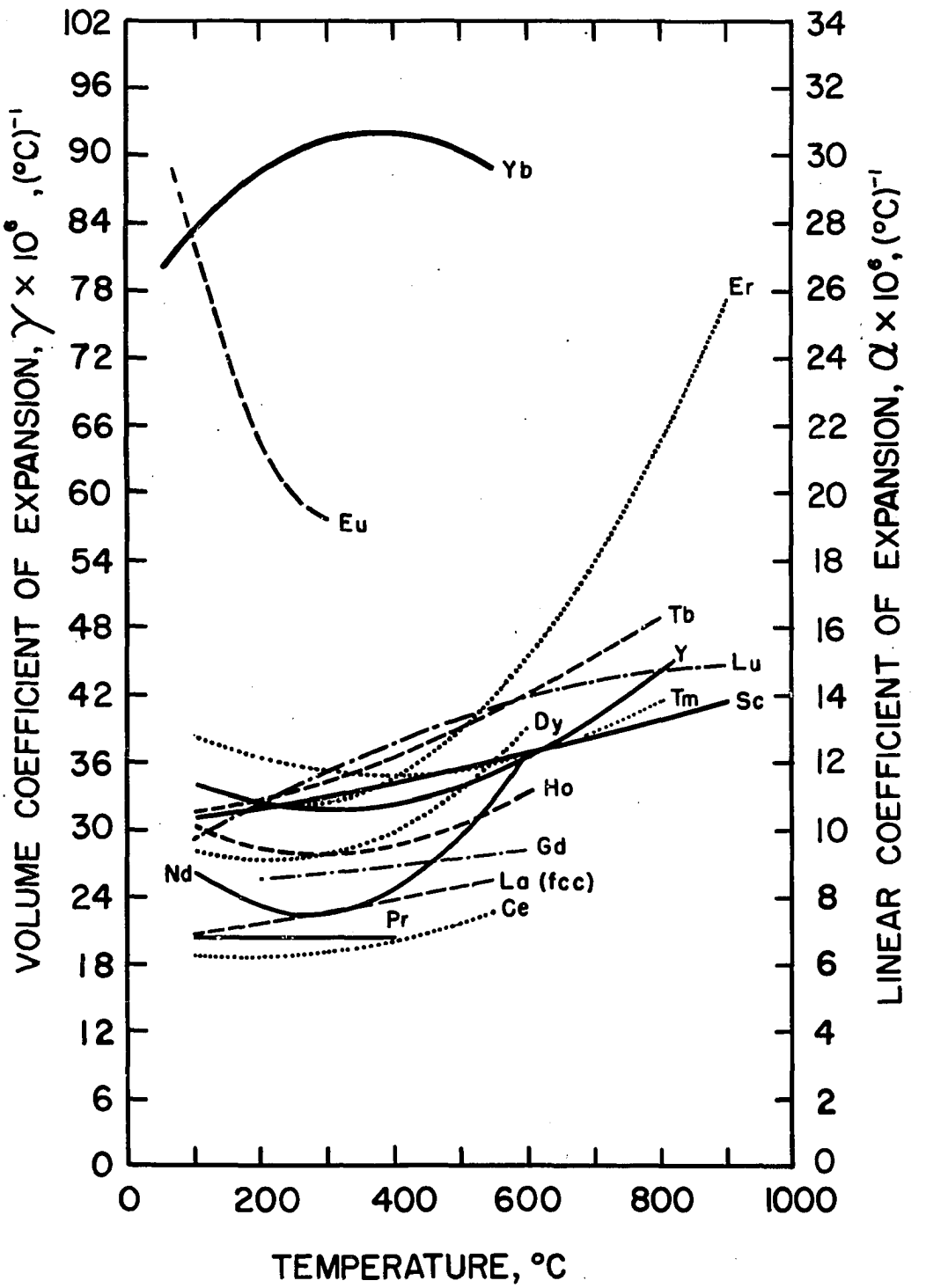

Figure 10. Thermal expansion coefficients of the rare-earth elements versus temperature

Table 6. Comparison of expansion coefficients of the rare earths obtained by two different methods

Element	Linear expansion coefficient, $\alpha \times 10^6$, $(^\circ C)^{-1}$					
	100°C[a]	100°C[b]	400°C[a]	400°C[b]	700°C[a]	700°C[b]
La			7.9	8.4		
Ce	6.2	6.8	6.7	6.6		
Pr	6.8	4.5	6.8	6.5		
Nd	8.7	6.6	8.3	8.1		
Gd			8.9	8.7		
Tb	10.5	8.2	12.1	10.6	15.1	13.6
Dy	9.4	9.7	9.9	11.1		
Er	11.3	9.8	11.6	10.7	17.9	14.3
Yb	27.8	27.0	30.6	31.0		
Y	11.4	9.5[c]	10.8	11.2[c]	13.3	13.0[c]

[a]Present results obtained by X-ray method.

[b]Dilatometric results by Barson, Legvold, and Spedding (20).

[c]Dilatometric results by Born (103).

of the metal was observed as high as 750°C, however, there was an admixture of faint bcc pattern also belonging to the metal. At 754°C the metal was completely converted to the bcc form. Once the fcc to bcc transformation took place, it

was possible to supercool the bcc form to at least 742°C. Upon lowering the temperature to 717°C the metal was completely converted to the fcc form.

The lattice constants of fcc cerium appear as a function of temperature in Figure 11. For the bcc cerium metal the pertinent crystallographic data are given in Table 7. For this phase the average of eight lattice constants computed individually from eight different patterns taken in the temperature range 742 to 779°C is 4.12 Å, the average temperature being 757°C. The comparison of the two phases on the basis of their atomic volumes appears in Figure 12, from which one can estimate the volume change for the fcc to bcc transformation to constitute an increase of 0.1 ± 0.7 per cent at 730°C.

As the cerium samples were kept at elevated tempera- for some time, a pattern of an impurity having a fcc structure gradually appeared and persisted unchanged through the metallic transformation in each direction. The characteristics of the impurity pattern were the same as those of the lanthanum impurities. The lattice constant of the cerium impurity at room temperature is 5.138 Å, hence, smaller than cerium by about 0.025 Å, and it remains smaller by the same margin throughout the entire temperature range investigated as shown in Figure 13.

In two instances when a slow leak developed in the silica capillary containing a cerium sample at about 700°C,

Table 7. X-ray diffraction data for bcc cerium[a]

hkl	$\sin^2\theta_{obs.}$	Lattice constant Å
110	0.0710	4.087
200	0.1414	4.100
211	0.2119	4.102
220	0.2810	4.114
310	0.3528	4.104
222	0.4249	4.097
321	0.4941	4.104
400	0.5642	4.111

$a = 4.11 \pm 0.01$ Å

$t_{avg.} = 768^{\circ}C$

[a]These data are a composite of three diffraction patterns taken at 761°C, 763°C, and 779°C.

another impurity with a fcc structure appeared having a lattice constant at room temperature of $a_o = 5.029$ Å. This impurity might be cerium nitride since its lattice constant is reported to be 5.02 Å (102). This impurity appeared to be brilliant purple in color when it was examined under a microscope. The lattice constants of this impurity as a function

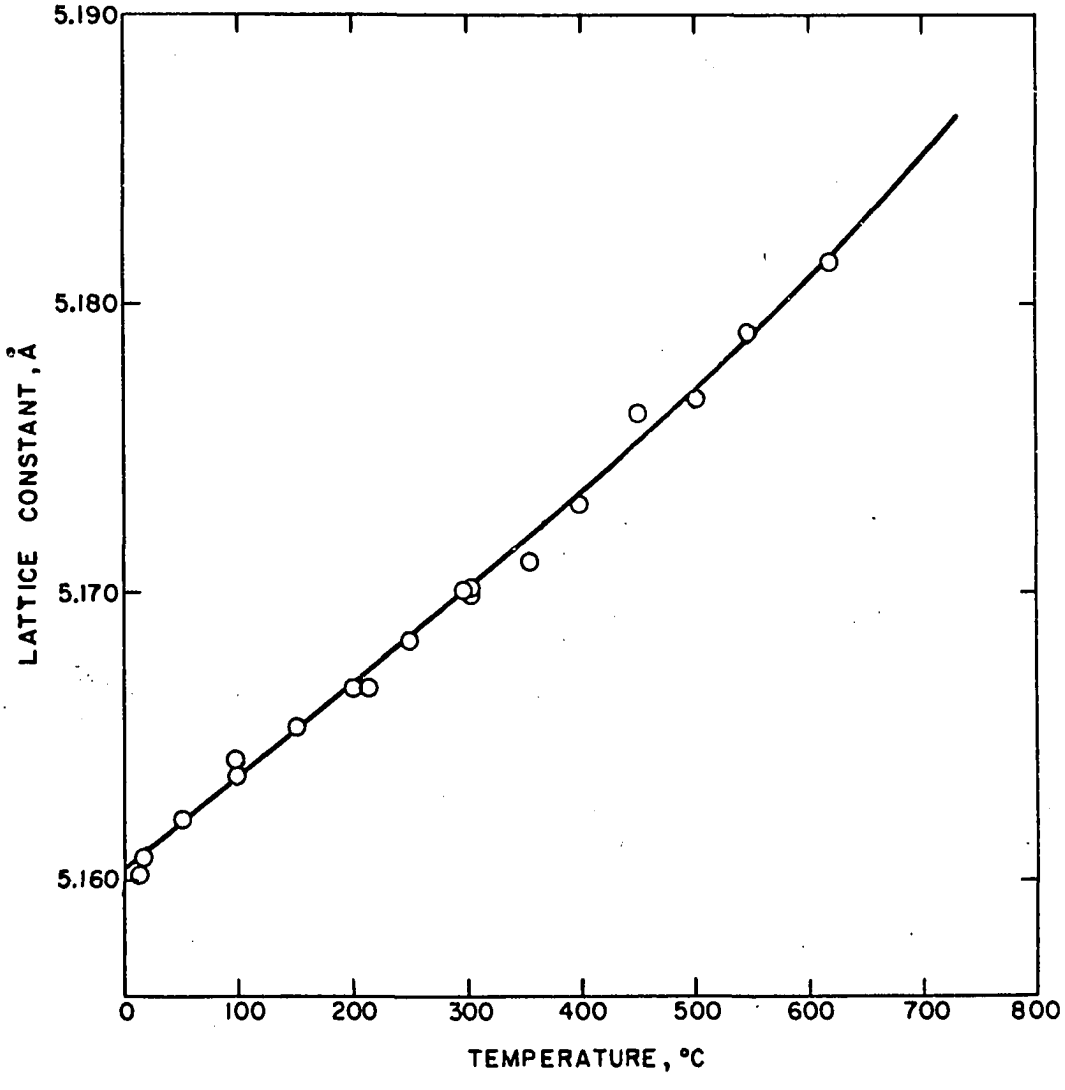

Figure 11. Lattice constant of cerium versus temperature

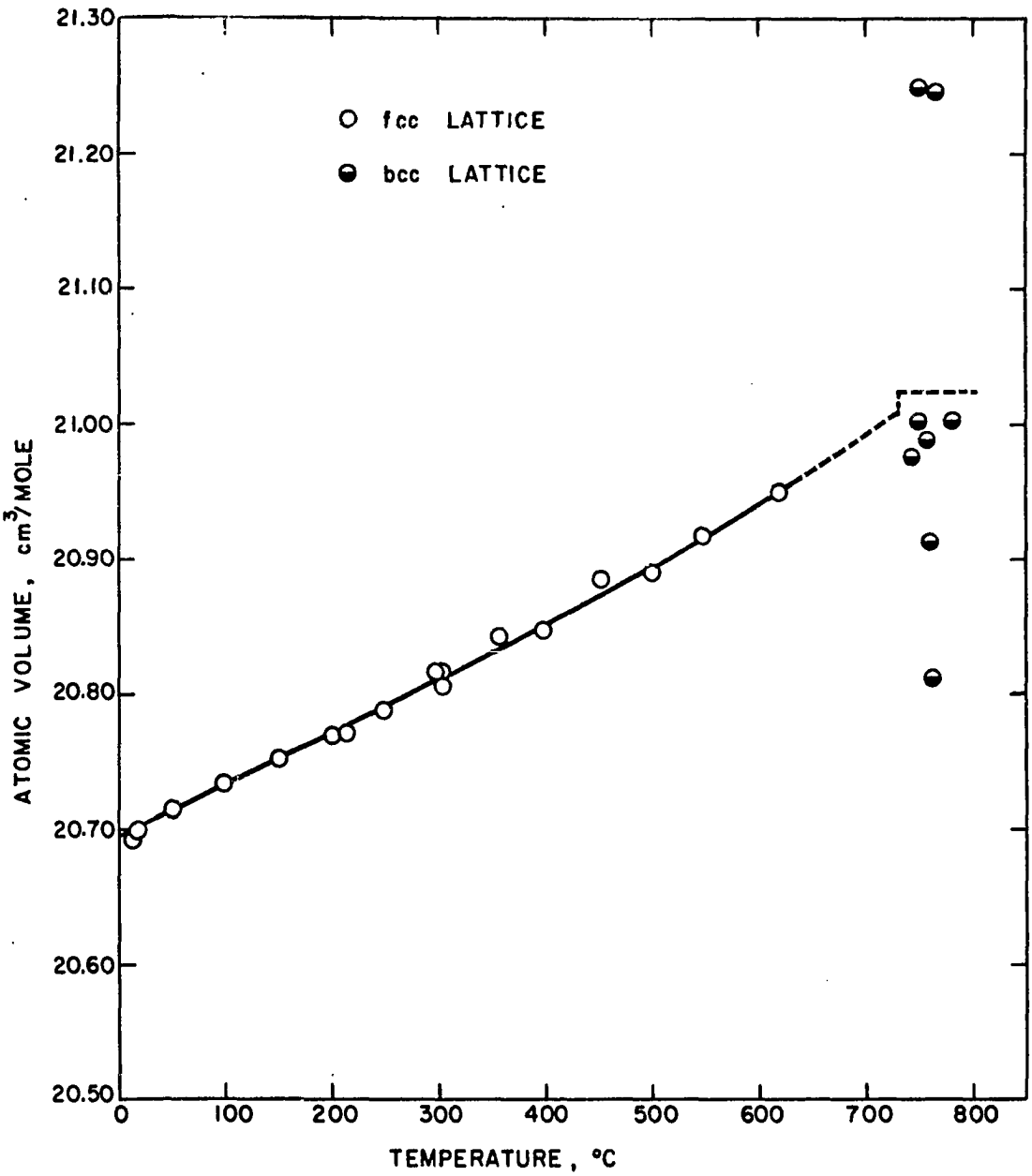

Figure 12. Atomic volume of cerium versus temperature

of temperature are also shown in Figure 13 so that a comparison can be made of cerium and the two impurities observed on the surface of the metal. The impurity just described displays an unusually high coefficient of expansion namely, about 40 x 10^{-6} $(^{o}C)^{-1}$, which is about six times as large as that of cerium metal or the cerium impurity mentioned previously.

The coefficient of expansion of fcc cerium calculated from an equation relating the lattice constant to temperature appears in Figure 10. It is also compared to values obtained dilatometrically in Table 6.

Praseodymium

The hexagonal structure of praseodymium was found to persist in the temperature range 20°C to 798°C. Due to the fading of the back-reflection lines at higher temperatures and a very high absorption coefficient for the Cu K radiation, it was impossible to obtain accurate lattice constants at temperatures higher than 450°C. Since the lattice constants were available for only a short range of temperature, they were related to temperature by means of a linear equation. The lattice constants for this metal appear in Figures 14 and 15.

Above 798°C, praseodymium transformed into a bcc phase. The average of six lattice constants computed individually from six different patterns taken in the temperature range

Figure 13. Lattice constants of cerium and its impurities *versus* temperature

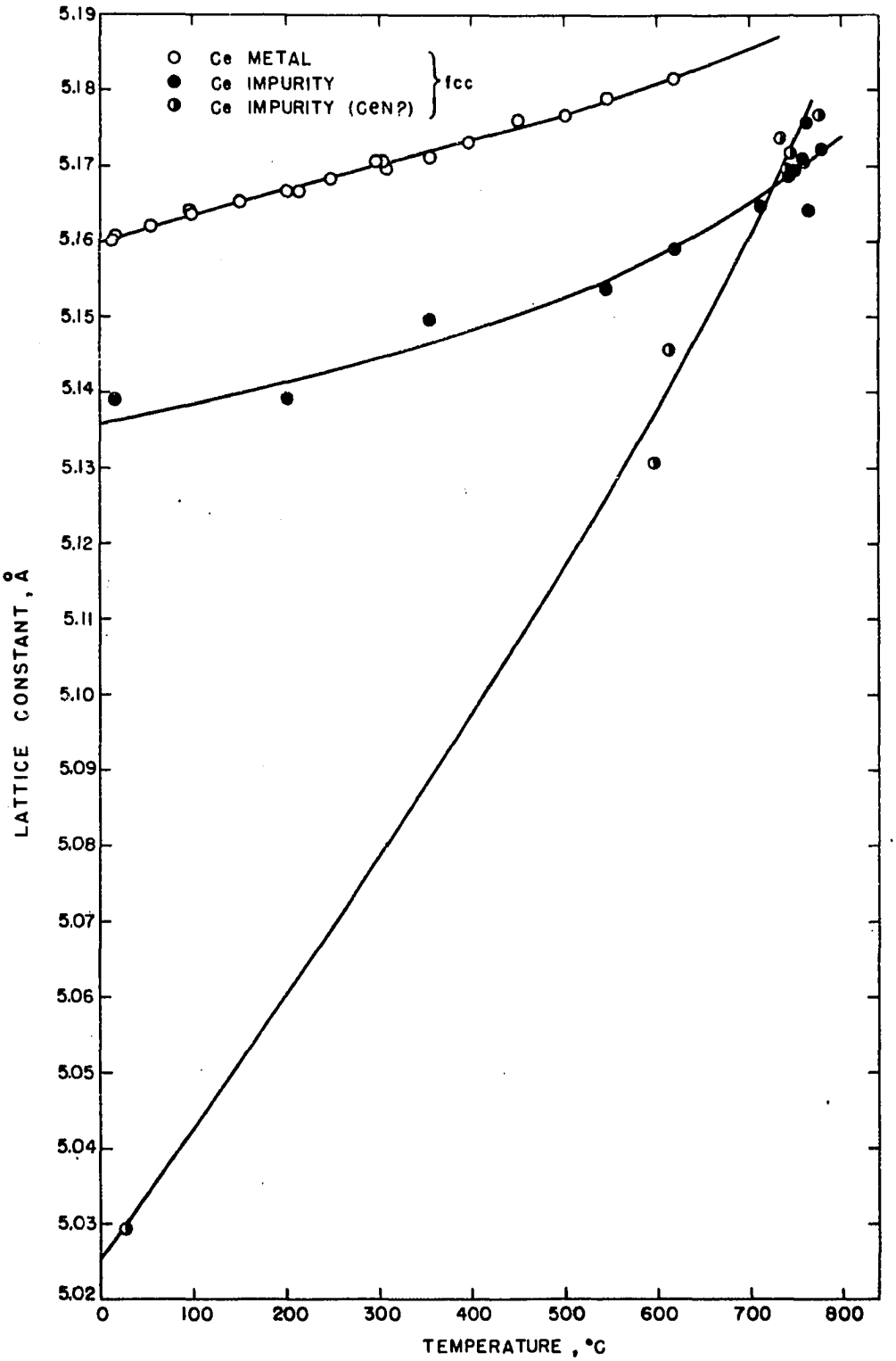
Ce METAL
Ce IMPURITY
Ce IMPURITY (CeN?)
fcc
LATTICE CONSTANT, Å
TEMPERATURE, °C
5.19
5.18
5.17
5.16
5.15
5.14
5.13
5.12
5.11
5.10
5.09
5.08
5.07
5.06
5.05
5.04
5.03
5.02
0
100
200
300
400
500
600
700
800

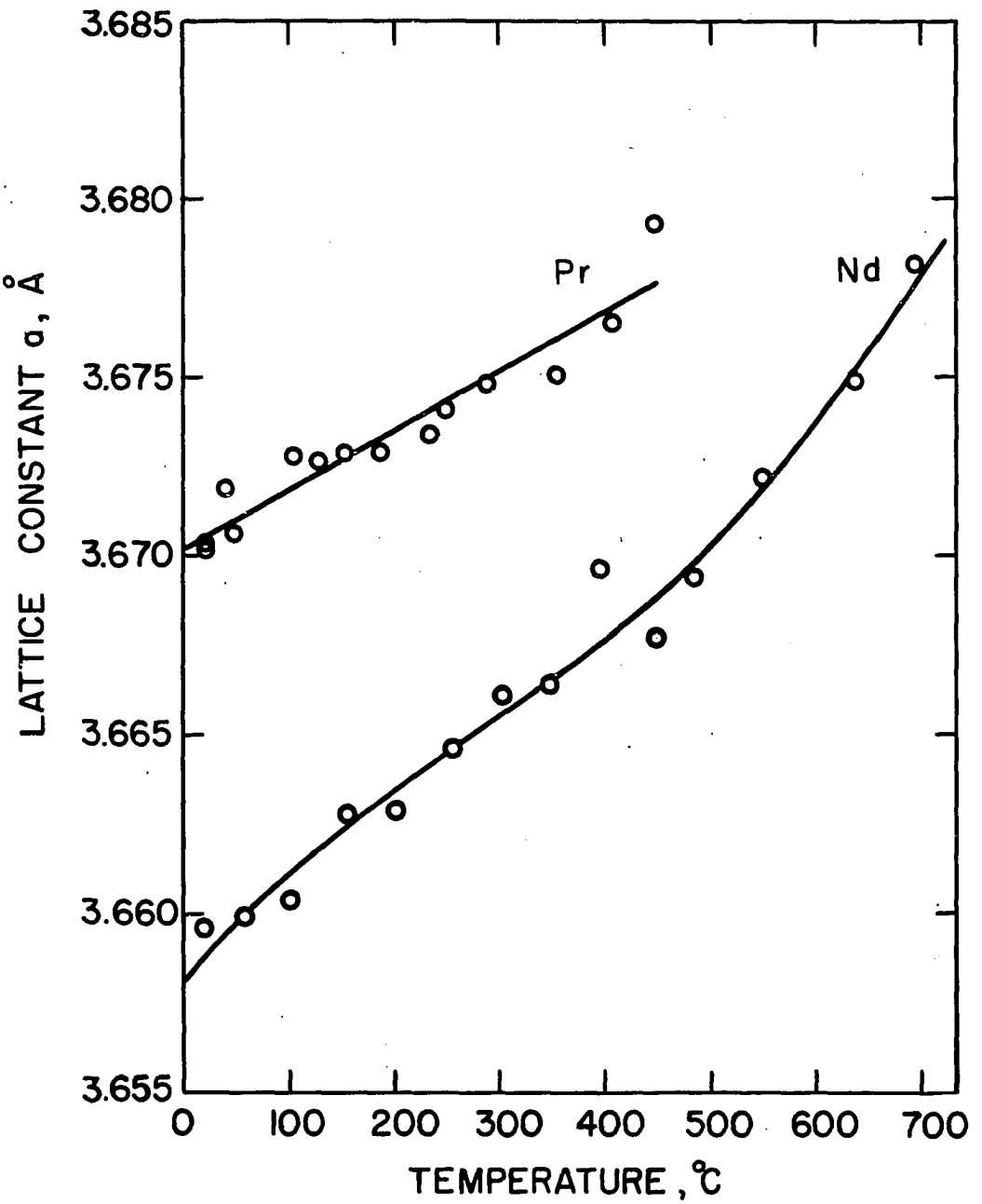

Figure 14. Lattice constants "a" of praseodymium and neodymium versus temperature

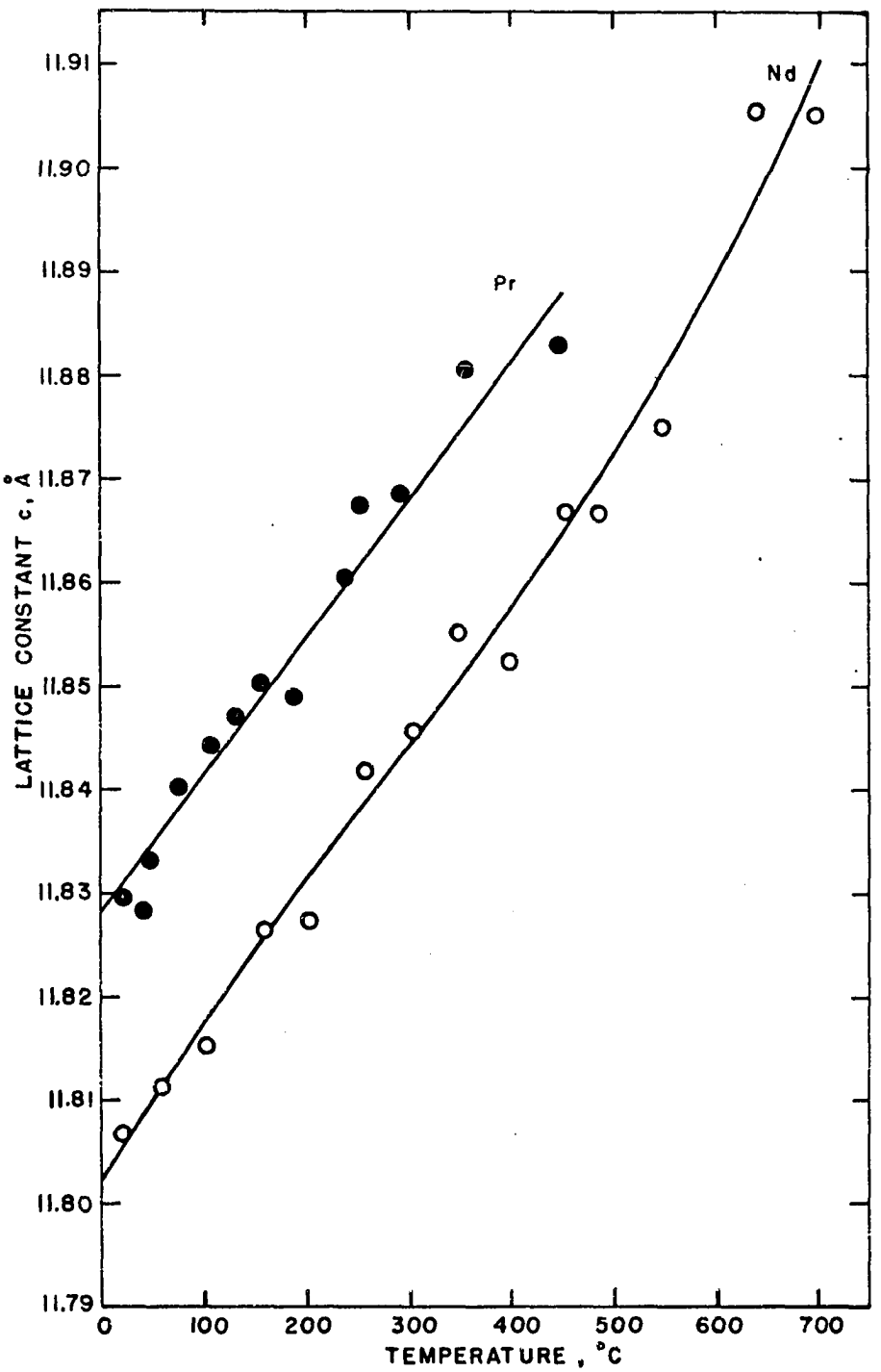

Figure 15. Lattice constants "c" of praseodymium and neodymium versus temperature

Table 8. X-ray diffraction data for bcc praseodymium[a]

hkl	$\sin^2\theta_{obs.}$ (Cu K_α)	$\sin^2\theta_{obs.}$ (Cu K_β)	Lattice constant Å
110		0.0576	4.104
110	0.0705		4.105
200		0.1147	4.110
200	0.1403		4.116
211		0.1715	4.118
211	0.2098		4.123
220		0.2286	4.118
220	0.2794		4.125
310	0.3482		4.131
222	---	---	---
321	0.4888		4.125
400	---	---	---
411, 330	---	---	---
420		0.5680	4.130
420	0.6963		4.131
	$a = 4.13 \pm 0.01$ Å		$t = 814^\circ C$

[a]These data are from one pattern taken at 814°C.

814°C to 832°C is 4.13 Å, the average temperature being 821° C. The observed reflections for this phase appear in Table 8. The transformation was shown to be reversible by the reappearance of the hexagonal phase when the temperature of the sample was lowered to 788°C.

The comparison of the atomic volumes of the two phases, as shown in Figure 16, indicates an increase in volume of 0.5 ± 0.7 per cent for the transformation of the hexagonal phase into the bcc phase.

Since the praseodymium data were fitted to a linear equation, only a constant average value of the coefficient of expansion could be calculated for each axis and for the volume. These values are plotted in Figures 17, 18 and 10, respectively, and the comparison with the dilatometric data appears in Table 6.

In the case of praseodymium, an impurity having a fcc structure was also observed when the surface of the metallic sample became slightly contaminated through prolonged heating. The lattice constant of the impurity appears in Table 4.

Neodymium

Neodymium was also found to retain its hexagonal structure up to the reported high temperature transformation at 868°C. As in the case of praseodymium, it was difficult to obtain patterns of good quality above 500°C which would permit the calculation of accurate lattice constants. By chance,

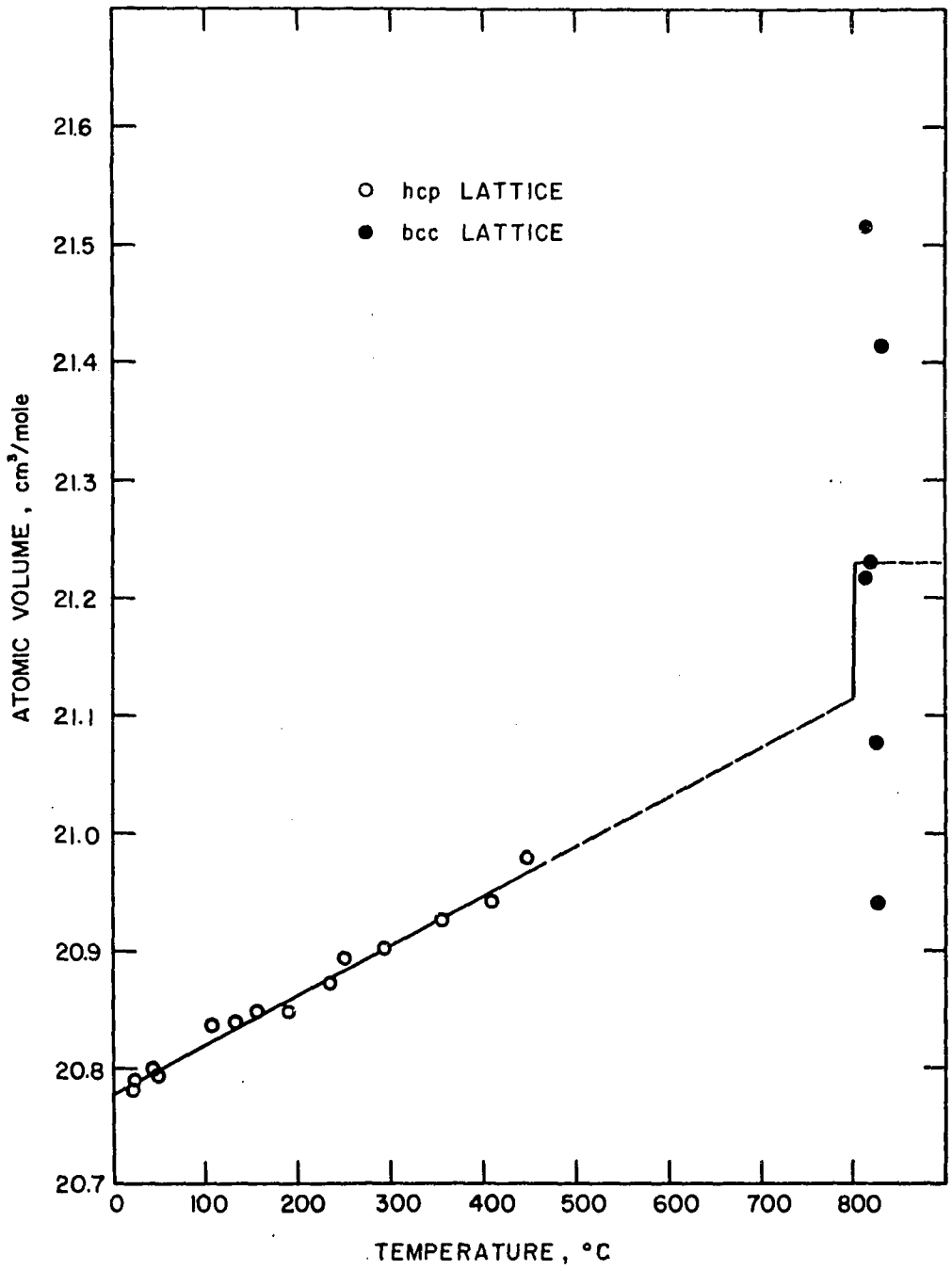

Figure 16. Atomic volume of praseodymium versus temperature

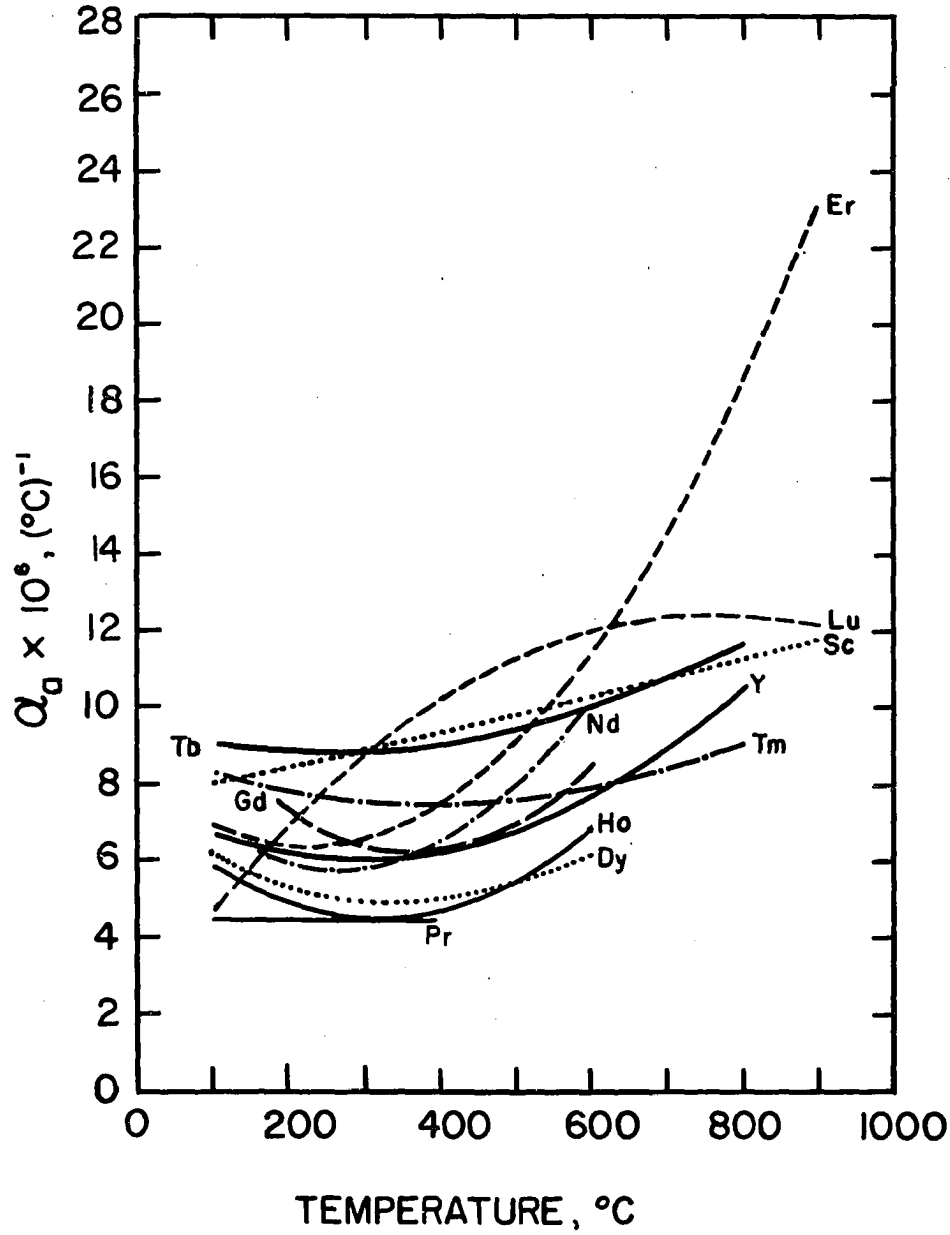

Figure 17. Thermal expansion coefficient of the a_o-axis of the hexagonal rare-earth elements versus temperature

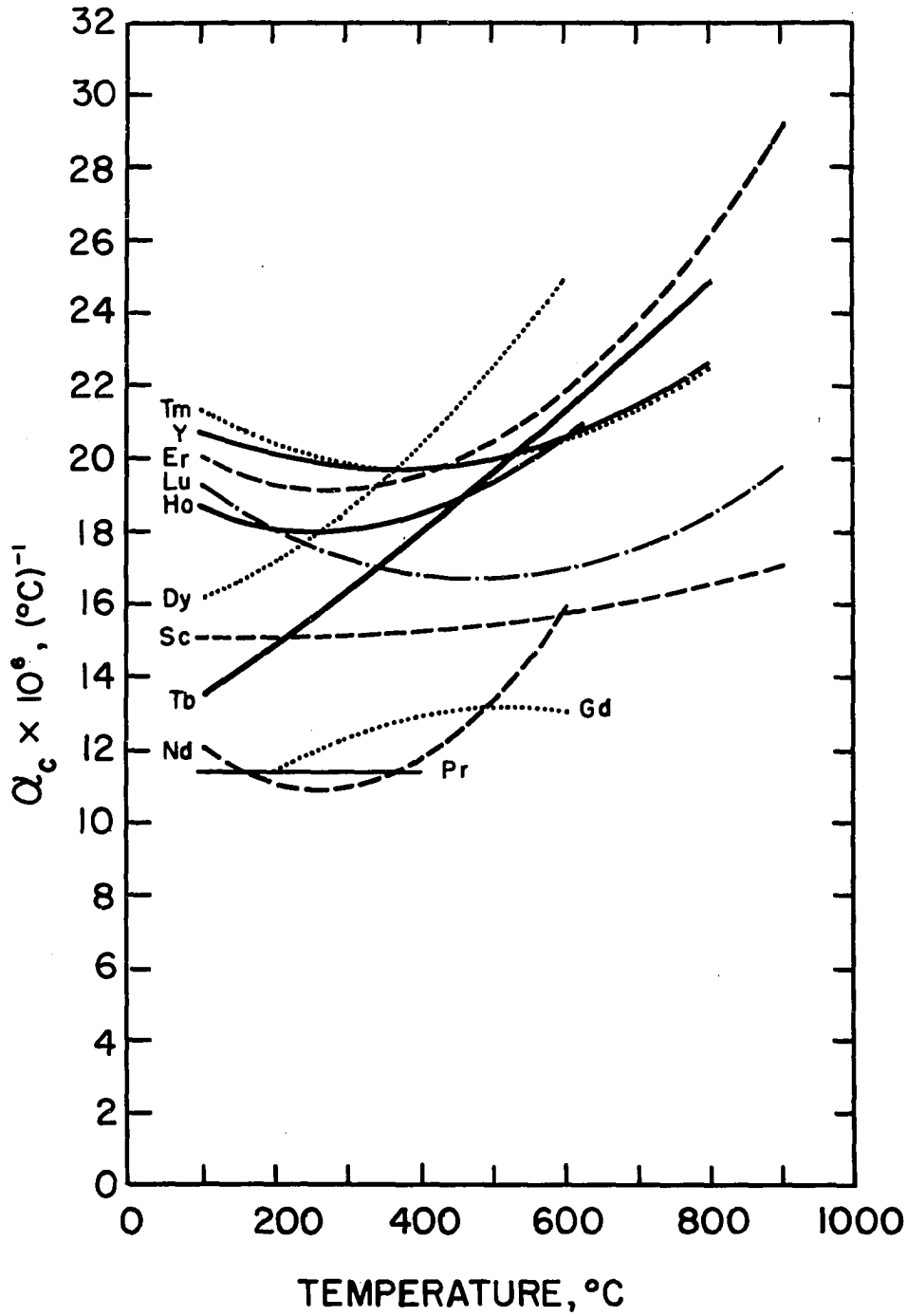

Figure 18. Thermal expansion coefficient of the c_o-axis of the hexagonal rare-earth elements versus temperature

however, one of the samples crystallized in such manner that a single crystal was formed in the spot where the X-ray beam was striking the sample. The crystal oriented itself in such a way that some of its intense reflections were visible even at high angles. It was possible, therefore, to obtain fairly accurate data for neodymium up to 700°C, as shown in Figures 14 and 15.

Above 868°C neodymium was found to possess a bcc phase. The average of four lattice constants computed individually from four different patterns taken in the temperature range of 850°C to 895°C is 4.13 Å, the average temperature being 883°C. In one instance the bcc phase was found at a temperature of 850°C, which is 18 degrees below the reported transformation temperature. It is possible that the lowering of the transformation temperature was due to the diffusion of the surface impurities into the metal. When the temperature of the same sample was lowered to 840°C, the hexagonal phase reappeared, indicating reversibility. The pertinent diffraction data for the bcc phase appear in Table 9.

The comparison of the two phases on the basis of the atomic volume appears in Figure 19, which gives an indication of a 0.1 ± 0.6 per cent increase in volume at 868°C for the hcp to bcc transformation.

The coefficients of expansion of hexagonal neodymium as a function of temperature, calculated from empirical equations relating the lattice constants and the atomic volume

Table 9. X-ray diffraction data for bcc neodymium[a]

hkl	$\sin^2\theta_{obs.}$	Lattice constant Å
110	0.0703	4.111
200	0.1406	4.112
211	0.2104	4.117
220	0.2802	4.119
310	0.3490	4.126
222	0.4194	4.124
321	0.4888	4.126
	$a = 4.13 \pm 0.01$ Å	
	$t_{avg.} = 880^{\circ}C$	

[a]These data are a composite of three diffraction patterns taken at 850°C, 895°C, and 895°C.

to temperature, appear in Figures 17, 18, and 10, respectively, and a comparison of the linear coefficient of expansion with the dilatometric data appears in Table 6.

An impurity having a fcc structure was observed in this case also, and it is similar to the impurities observed with the preceding rare-earth metals as can be seen in Table 4.

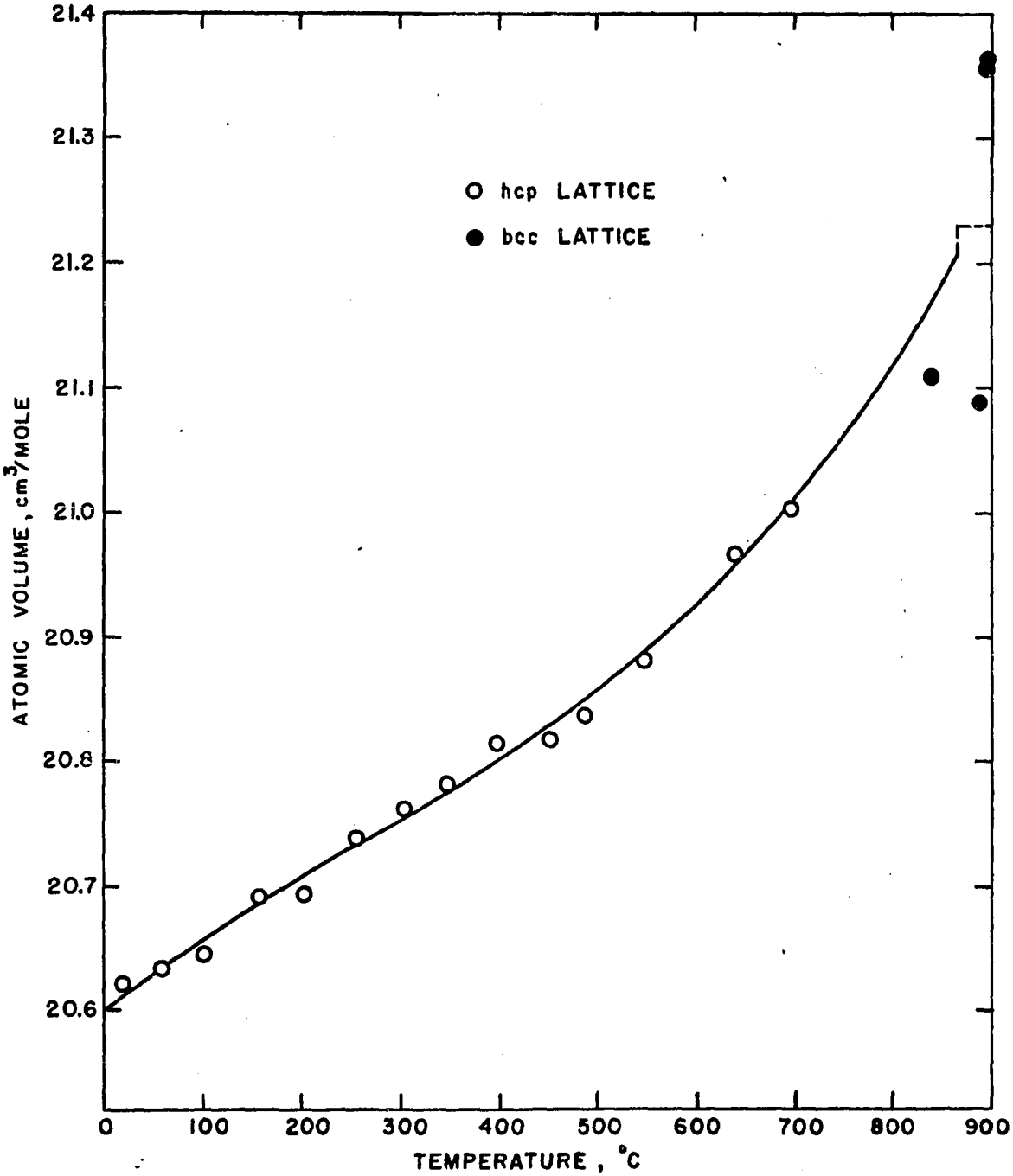

Figure 19. Atomic volume of neodymium versus temperature

Samarium

Samarium is a fairly volatile metal even at temperatures as low as 500°C. Although the X-ray specimens were mounted under an atmosphere of argon, the evaporation was so rapid that the inner surface of the silica capillaries became covered with a thick layer of samarium when the furnace was turned on. Reaction occurred between the capillary walls and samarium as shown by a myriad of lines and spots in the diffraction patterns. These patterns were so complex and of such poor quality that they could not be interpreted.

Europium

Europium was investigated by the high temperature X-ray crystallographic method primarily to determine the coefficient of expansion, since there have been no transformations observed for this metal (49, 50). Diffraction patterns were obtained up to 450°C, but the evaporation of the sample prevented exposures at higher temperatures. The metal retained its bcc structure in this temperature range as expected; accurate lattice constants were determined up to 350°C and they were plotted as a function of temperature as shown in Figure 20; the corresponding data for the atomic volume are shown in Figure 21. Since the coefficient of expansion of europium is large, the lattice constants even in this relatively short temperature range show that europium expands at a decreasing rate as temperature increases. This phenomenon

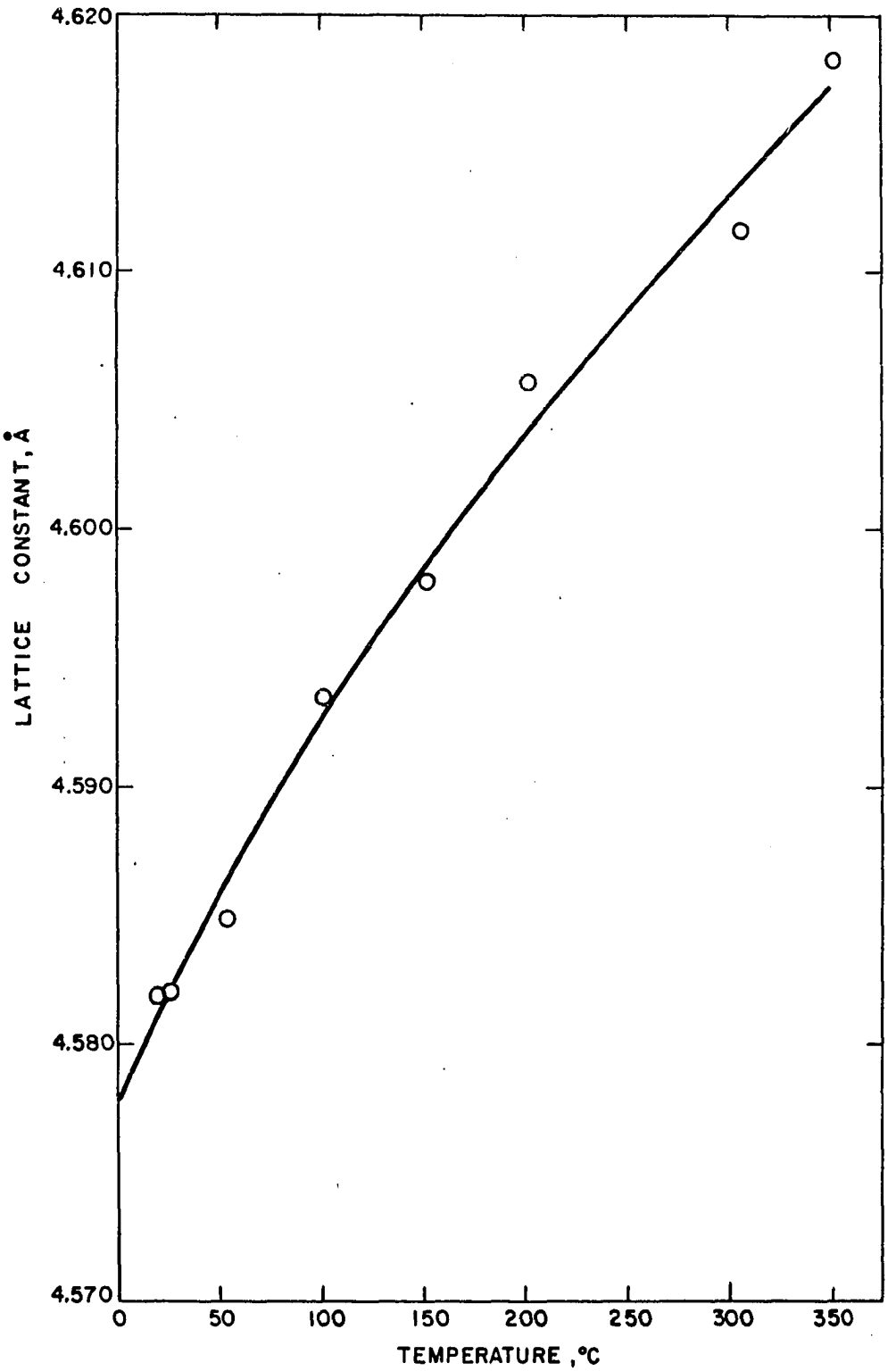

Figure 20. Lattice constant of europium, versus temperature

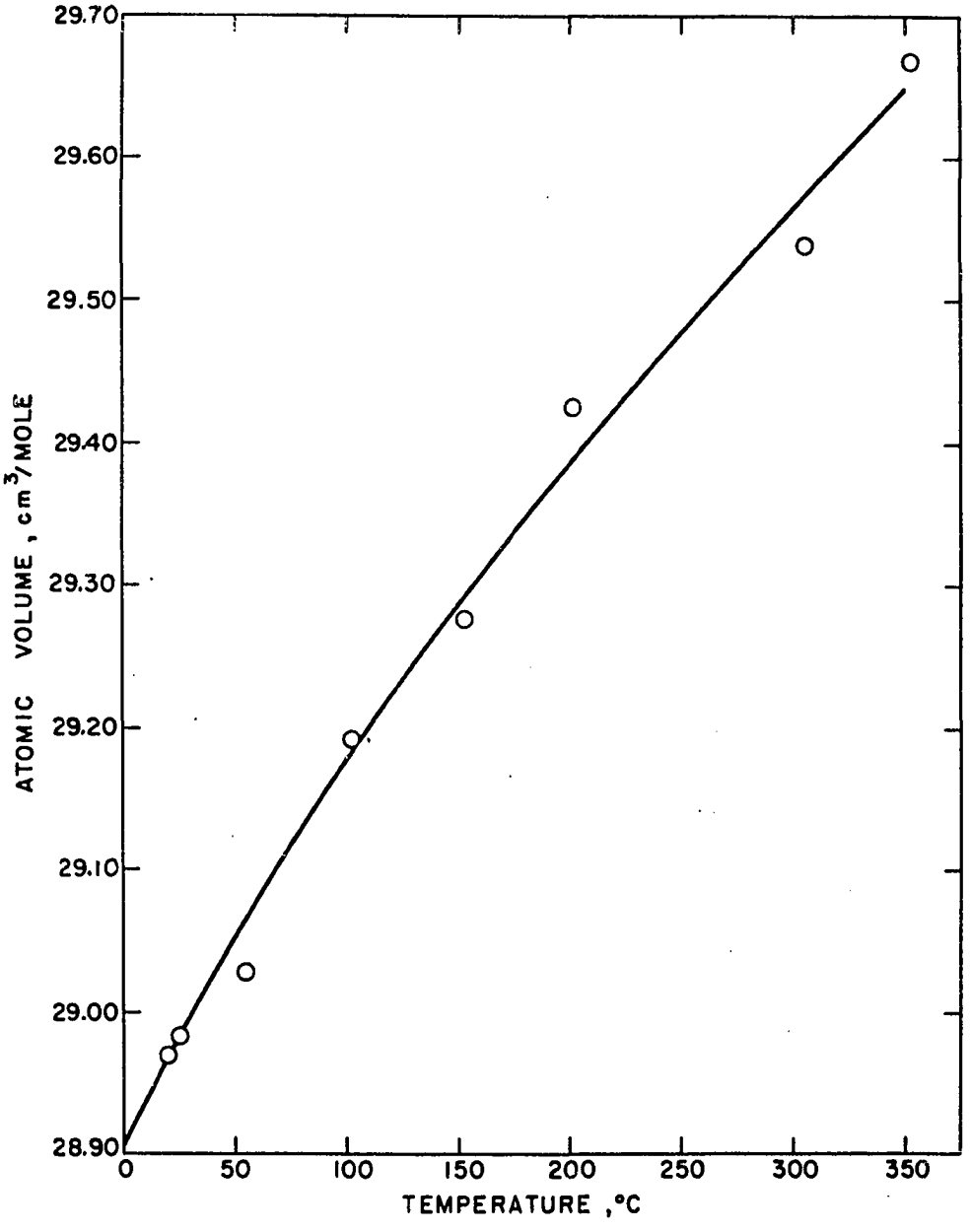

Figure 21. Atomic volume of europium versus temperature

is best illustrated by plotting the coefficient of expansion as a function of temperature as shown in Figure 10. The rate of decrease of the coefficient of expansion is too large to be attributed to experimental errors or to a poor fit of the lattice constants to an empirical cubic equation.

An impurity having a fcc structure appeared in this case also, with a lattice constant similar in magnitude to those of the fcc impurities of other rare earths considered so far. Reference to Table 4 reveals that this impurity is 29 per cent smaller by volume than the lattice of europium. The lattice constant of this impurity is almost identical with that of EuO which was reported to be 5.145 Å at room temperature (104).

Ytterbium

In the case of ytterbium, two possible crystalline transformations were sought; one in the vicinity of 300°C (51) and the other in the temperature range 730°C to 798°C (20, 21). Initial X-ray crystallographic results showed that ytterbium retained its fcc structure from room temperature to at least 600°C. A very thorough determination of the lattice constants at short temperature intervals was then made in this temperature range in order to detect whether there was a discontinuity in the lattice constant, as a function of temperature, in the vicinity of 300°C. The resulting data appear in Figure 22; they do not reveal any such discontinuity. The

Figure 22. Lattice constant of fcc ytterbium *versus* temperature

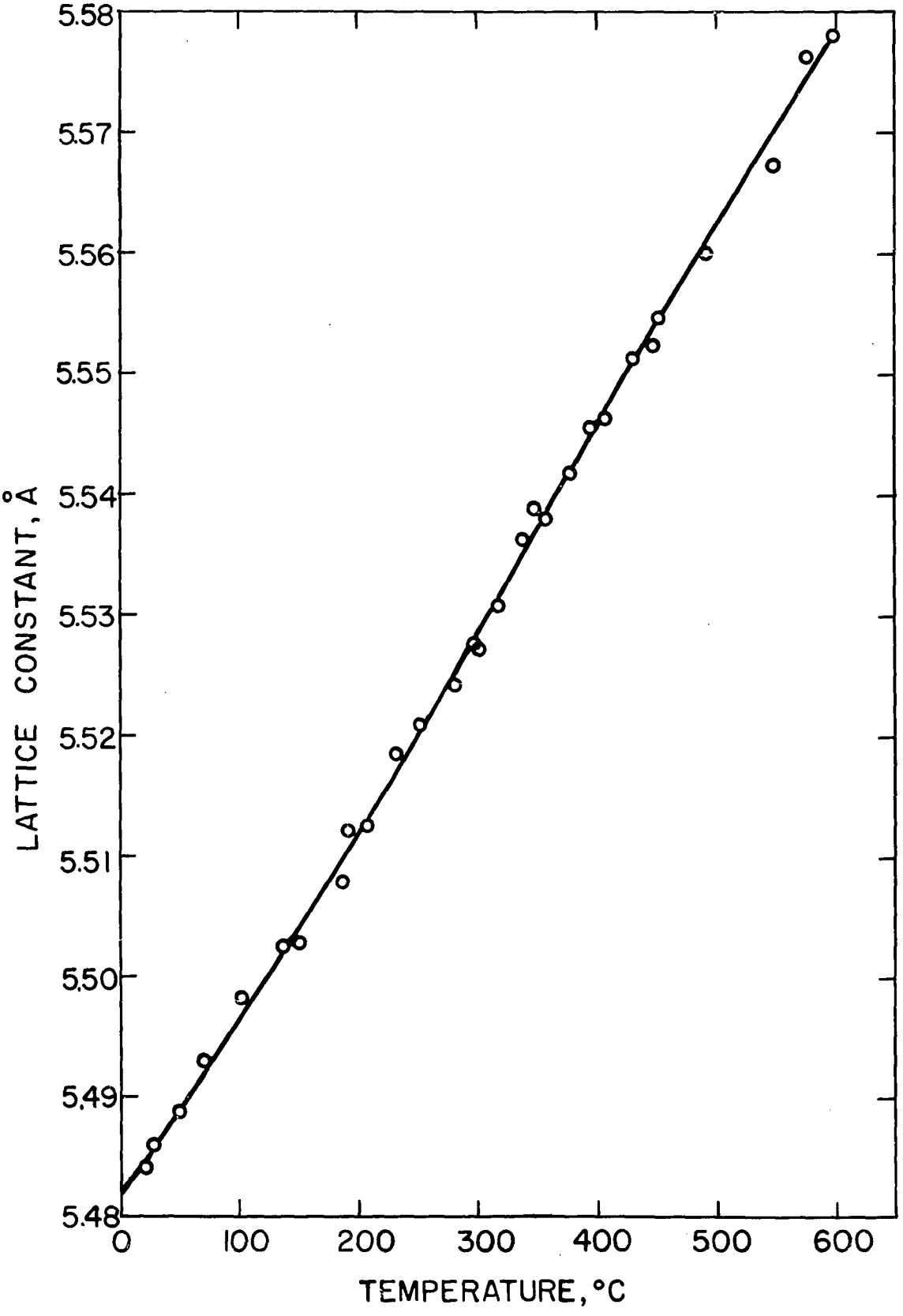
5.58
5.57
5.56
5.55
5.54
5.53
5.52
5.51
5.50
5.49
5.48
LATTICE CONSTANT, Å
0
100
200
300
400
500
600
TEMPERATURE, °C

coefficients of expansion, calculated on the basis of an empirical equation relating the lattice constants to temperature, are shown in Figure 10, and the comparison of these data with the dilatometric results appears in Table 6.

Ytterbium, being one of the most volatile rare-earth metals, vaporized completely in the X-ray capillary long before the high temperature transformation was reached. Since ytterbium is rather difficult to ignite to its oxide in air, indicating the formation of a protective oxide coating, it was reasoned that a specimen sealed in a silica capillary containing air would acquire such a coating, which would prevent it from evaporating at high temperatures.* Samples were therefore mounted in such manner and they showed no sign of evaporation even at 800°C, except when the protective coating burst; in such cases the metal evaporated rapidly leaving behind a thin, transparent shell. The surface impurity had a fcc structure with a lattice constant given in Table 4. This technique made it possible to obtain a diffraction pattern of the high temperature phase of ytterbium. The structure was found to be bcc. The average of five lattice constants computed individually from five different patterns taken in the temperature range 720°C to 807°C is 4.44 Å, the average

*Note: The volume of air contained in the silica capillary was about 2 mm^3, which is equivalent to about 2.8 x 10^{-6} gm, whereas the ytterbium specimen weighed about 0.8 x 10^{-3} gm. This is equivalent to about 1/25 of the air necessary to convert the sample to YbN or YbO.

Table 10. X-ray diffraction data for bcc ytterbium[a]

hkl	$\sin^2\theta_{obs.}$	Lattice constant Å
110	0.0604	4.438
200	0.1212	4.429
211	0.1806	4.443
220	0.2407	4.4444
310	0.3013	4.444
222	0.3620	4.438
321	0.4214	4.443
400	---	---
411, 330	0.5432	4.438
420	0.6012	4.446
	a = 4.44	
	$t_{avg.}$ = 795°C	

[a]These data are a composite of three diffraction patterns taken at 778°C, 800°C, and 807°C.

temperature being 774°C. The pertinent X-ray diffraction data for this phase appear in Table 10. The temperature of the transformation of the fcc phase to the bcc phase is apparently strongly affected by impurities, since the bcc phase was observed as low as 709°C, which is 89 degrees below

the temperature obtained by thermal analysis (21). The highest temperature at which the fcc phase was observed was 723°C.

When the temperature of a sample in the bcc phase was lowered to 650°C, the metal transformed into a hcp phase instead of the expected fcc phase. Below 260°C the hcp phase transformed into the fcc phase having a lattice constant practically identical with ytterbium metal. Since the metal was heated at high temperatures, there were large grains present in it, as indicated by the spotted lines in the diffraction patterns of the bcc, hcp and fcc structures. The pattern of the fcc impurity consisted of smooth lines. Subsequent heating and cooling of the sample above and below 260°C produced the same transformation, although in one instance both phases were found to coexist at 249°C after the sample was cooled from above 260°C to this temperature. In other cases only the single phases of the metal, namely, fcc or hcp, were observed. The lattice constants of the hexagonal phase at 283°C are 3.911 ± 0.001 Å and $c_o = 6.403 \pm 0.001$ Å with $c_o/a_o = 1.637$. The lattice constants as a function of temperature are shown in Figure 23 and the relevant X-ray diffraction data are given in Table 11.

When the same sample was heated to temperatures in the vicinity of the high temperature transformation, the hcp phase was found to persist up to 711°C although accurate lattice constants could not be obtained above 412°C; the

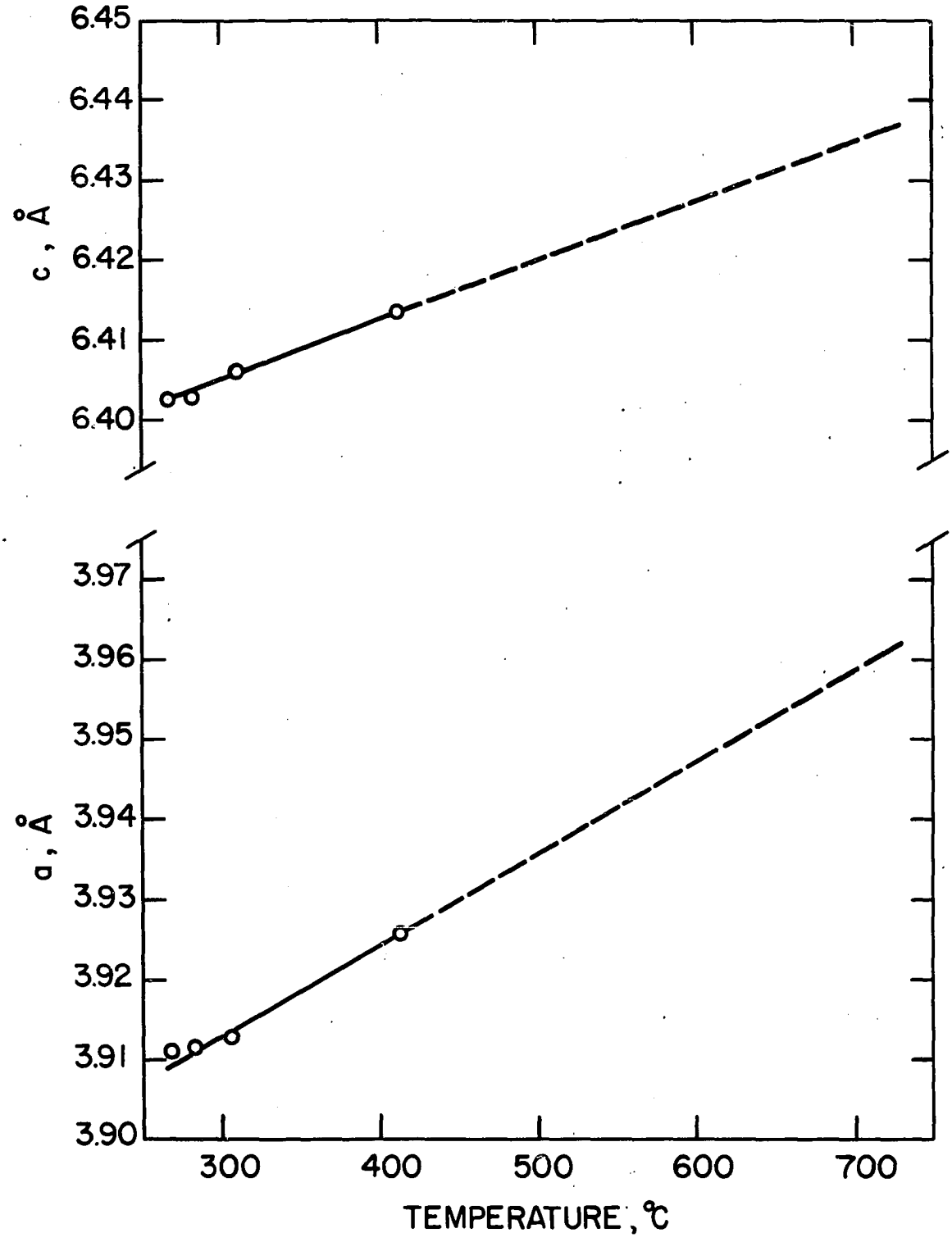

Figure 23. Lattice constants of hcp ytterbium versus temperature

Table 11. X-ray diffraction data for hcp ytterbium

hkl	$\sin^2\theta$ obs.	$\sin^2\theta$ calc.	$\sin^2\theta$ obs. $-\sin^2\theta$ calc.
001	---	0.0145	----
100	0.0513	0.0517	-0.0004
002	0.0582	0.0579	+0.0003
101	0.0662	0.0662	-0.0000
102	0.1105	0.1096	+0.0009
003	---	0.1302	----
110	---	0.1552	----
103	0.1818	0.1820	-0.0002
200	---	0.2069	----
112	---	0.2130	----
201	0.2216	0.2213	+0.0003
004	0.2304	0.2316	-0.0012
202	0.2658	0.2648	+0.0010
104	0.2836	0.2833	+0.0003
203	0.3386	0.3371	+0.0015
005	---	0.3618	----
210	0.3628	0.3620	-0.0008
211	0.3771	0.3765	+0.0006
114	0.3848	0.3867	-0.0019
105	0.4147	0.4135	+0.0012
212	0.4199	0.4199	-0.0000
204	0.4363	0.4384	-0.0021
300	---	0.4654	----
213	0.4918	0.4923	-0.0005
006	0.5206	0.5210	-0.0004
302	---	0.5242	----
205	0.5710	0.5687	+0.0023
106	0.5710	0.5727	-0.0017
214	0.5925	0.5936	-0.0011
220	---	0.6216	----
310	0.6740	0.6723	+0.0017
116	---	0.6761	----
222	---	0.6785	----
311	0.6891	0.6868	+0.0023
304	---	0.6970	----

Table 11. (Continued)

hkl	$\sin^2\theta$ obs.	$\sin^2\theta$ calc.	$\sin^2\theta$ obs. $-\sin^2\theta$ calc.
007	---	0.7091	----
215	0.7254	0.7238	+0.0016
215	0.7249	0.7238	+0.0011
206	0.7287	0.7274	+0.0013
206	0.7282	0.7274	+0.0008
312	---	0.7302	----
107	0.7629	0.7608	+0.0021
107	0.7628	0.7608	+0.0020
313	0.8038	0.8026	+0.0012
313	0.8046	0.8026	+0.0022
400	---	0.8275	----
401	---	0.8419	----
224	---	0.8521	----
216	0.8844	0.8830	+0.0014
216	0.8844	0.8830	+0.0014
402	---	0.8854	----
314	0.9047	0.9039	+0.0008
314	0.9048	0.9039	+0.0009
207	0.9169	0.9160	+0.0009
207	0.9164	0.9160	+0.0004
008	---	0.9262	----
403	---	0.9577	----
108	0.9786	0.9779	+0.0007
108	0.9777	0.9779	-0.0002

$a = 3.911 \pm 0.003$ Å

$c = 6.403 \pm 0.003$ Å $c/a = 1.637$

$t = 268^{\circ}C$

next diffraction pattern, taken at 732°C, produced the bcc structure of the metal.

The comparison of the various phases of ytterbium on the basis of the atomic volumes can be made by reference to Figure 24. One can note the increase in volume of 0.7 per cent for the transformation of the fcc to the hcp form and a decrease of 0.1 ± 0.4 per cent for the transformation of the fcc to the bcc form, or of the hcp to the bcc form.

The remaining problem was to determine why ytterbium did not transform into the hcp phase when freshly prepared samples were heated in a vacuum above 260°C. While several tentative explanations could be offered, a conclusion was reached, based on the observations which will follow, that the hcp phase was stabilized by impurities and, therefore, is not a stable phase of pure ytterbium.

One of the tentative explanations for the failure of the samples to transform at 260°C was that they were enveloped by a tightly adhering impurity coating which prevented them from expanding the necessary 0.7 per cent to form the hcp structure. Since the samples were very thin, and since the heat of transformation of the fcc to hcp structures was not expected to be large (as, for instance, in lanthanum), this explanation seemed plausible. Another tentative explanation was that the hcp phase was stabilized by impurities, which could diffuse easily into such a small sample. Since the size of the sample seemed to be an

Figure 24. Atomic volume of ytterbium *versus* temperature

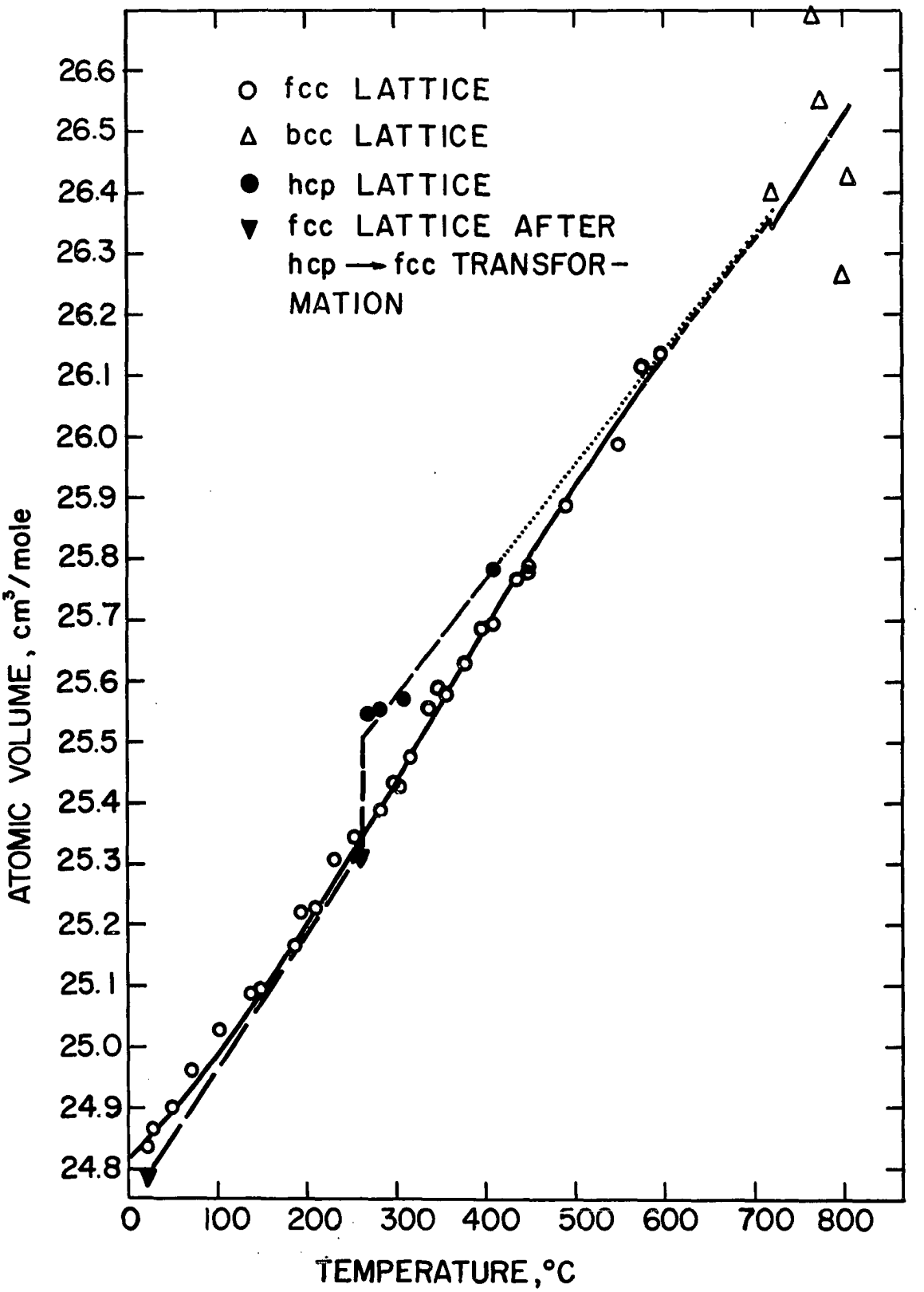
fcc LATTICE
bcc LATTICE
hcp LATTICE
fcc LATTICE AFTER hcp → fcc TRANSFORMATION
ATOMIC VOLUME, cm³/mole
TEMPERATURE, °C
26.6
26.5
26.4
26.3
26.2
26.1
26.0
25.9
25.8
25.7
25.6
25.5
25.4
25.3
25.2
25.1
25.0
24.9
24.8
0
100
200
300
400
500
600
700
800

important factor in determining the answer to the stated problem, it was decided to examine a large sample of ytterbium by means of X-rays at high temperatures. A massive sample of ytterbium of high purity was made in the shape of a rectangular prism measuring 1 x 1/2 x 3/16 inch. The sample was placed in a high temperature X-ray diffractometer (76) and diffraction patterns were recorded to temperatures as high as 450°C while the metal was kept under a vacuum. The bcc structure was found to persist. The sample was then wrapped in a thin tantalum sheet and was heated in a vacuum to 805°C (above the high temperature transformation), whereupon it was placed back into the diffractometer and diffraction patterns were taken at temperatures as high as 625°C, but again, only the fcc structure was observed. The sample was then heated in the diffractometer at 800°C for about two minutes, after which the temperature was lowered to 440°C and another diffraction pattern was taken which also showed the same fcc structure. Subsequent inspection of the sample revealed that about half of it evaporated during the experiment, indicating that at high temperatures the sample was protected by its own vapor from surface contamination, thus preventing the surface impurities, which could otherwise be formed, from diffusing into the metal. The thermal cycling of the sample through the high temperature transformation was done in order to duplicate the thermal history of the wire sample which showed the transformation to the hcp structure.

Since the hcp phase failed to appear with the massive sample after the treatments described above, it was concluded that this phase must have been stabilized in the other sample by the presence of impurities, which could diffuse with ease into the metal from the coating of impurity purposely made to adhere to the metal. The identity of the impurity could not be established because the sample was too small.

A clue to the identity of the impurity causing the appearance of the hcp structure was obtained from the investigation performed on calcium. Calcium displays a somewhat similar allotropic behavior as ytterbium. According to Smith, Carlson, and Vest (105), 99.96 per cent pure calcium exists in fcc and bcc forms only, the transformation temperature being at 464°C. Calcium samples of inferior purity show, however, the presence of a hcp phase and a complex phase, which exist in the vicinity of the transformation temperature given above. The dimensions of the hcp lattice of calcium samples of inferior purity show, however, the presence of a hcp phase and a complex phase, which exist in the vicinity of the transformation temperature given above. The dimensions of the hcp lattice of calcium and of ytterbium are strikingly similar in that the lattice constants of calcium are a_o = 3.97 Å and c_o = 6.49 Å with c/a = 1.63. The hcp phase in calcium was shown to be caused by the presence of hydrogen, as reported by Smith and Bernstein (106) who investigated the effect of added impurities on the allotropy of

calcium. Since calcium and ytterbium display similarities in many ways, it would not be surprising to find that hydrogen stabilized the hcp phase in ytterbium also.

Scandium, yttrium, gadolinium, terbium, dysprosium, holdium, erbium, thulium, and lutetium

The diffraction patterns obtained for the elements under this heading were of much better quality than those for the light rare earths, and, besides, these patterns displayed both clarity and back reflection lines to higher temperatures than the light rare earths. This improvement progressed, in general, with the increase of the atomic number and was probably due to progressively smaller amplitude of vibration of the atoms from their equilibrium positions. The improvement in quality of the diffraction patterns was also due to a large decrease in the X-ray absorption coefficients for metals following dysprosium and for scandium and yttrium.

All of the elements discussed under this heading have the same crystal structure, namely, hcp, with planes stacked in the normal, ABAB..., fashion. This structure was retained by each of these elements in the temperature range 20°C to about 1000°C; the maximum temperatures at which this structure was observed for each element are the following:

Element	Sc	Y	Gd	Tb	Dy	Ho	Er	Tm	Lu
Temperature, °C	1009	957	948	950	970	966	917	1004	1012

The lattice constants a and c and the atomic volume of these elements, except scandium, are shown as a function of temperature in Figures 25, 26, and 27, respectively. Similar data for scandium are plotted separately in Figures 28, 29, and 30, since the corresponding quantities are of much different magnitude to be plotted on the same scale.

The coefficients of expansion of the a-axes, c-axes, and the bulk coefficient of expansion appear in Figures 17, 18, and 10, respectively and the comparison of the linear coefficients of expansion with dilatometric data appears in Table 6. As in the previous cases, the coefficients of expansion were calculated on the basis of the empirical equations relating the lattice constants and atomic volume to temperature. In all cases the coefficients of expansion of the c-axis are greater by a factor of 1.6 to 4.4 than that of the a-axis. The individual values of this factor for rare-earth elements at 400°C are shown in Table 12; this temperature was chosen because the coefficients of expansion obtained here should have the most reliable value near the mid-range temperature.

In the case of gadolinium, the data obtained below 50°C do not fall on the same curves as the data obtained at higher temperatures. This phenomenon might be due to the experimental errors, or might be an actual discrepancy such as the hysteresis loop in the expansion curve observed by Trombe and Foex (65) between 100°C and 250°C. Since ferromagnetism

Figure 25. The lattice constants "a" of the hcp heavy rare-earth elements and of yttrium *versus* temperature

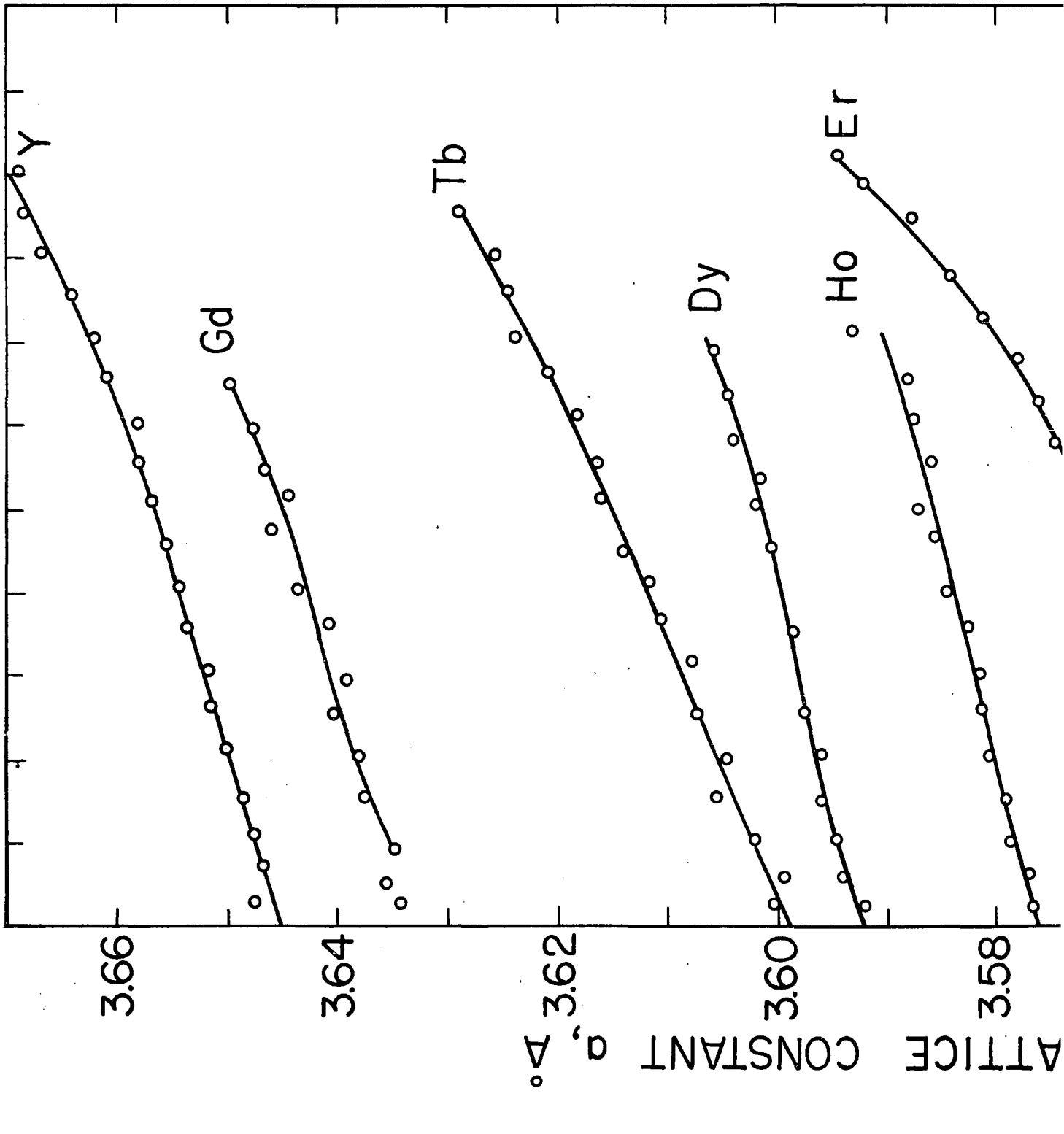
Y
Gd
Tb
Dy
Ho
Er
3.66
3.64
3.62
3.60
3.58
ATTICE CONSTANT a, Å

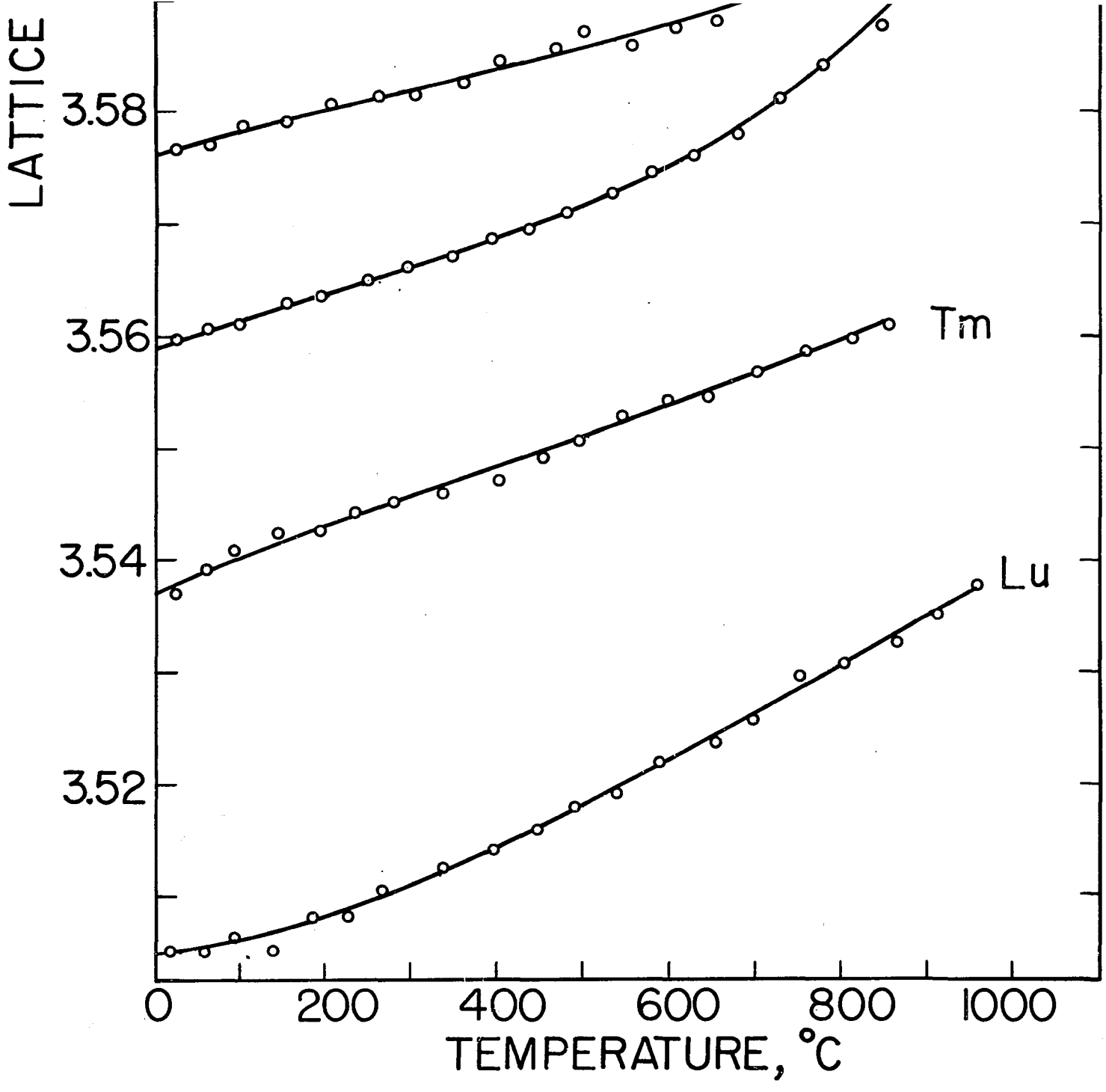
LATTICE
3.58
3.56
3.54
3.52
Tm
Lu
0
200
400
600
800
1000
TEMPERATURE, °C

Figure 26. The lattice constants "c" of the hcp heavy rare-earth elements and of yttrium *versus* temperature

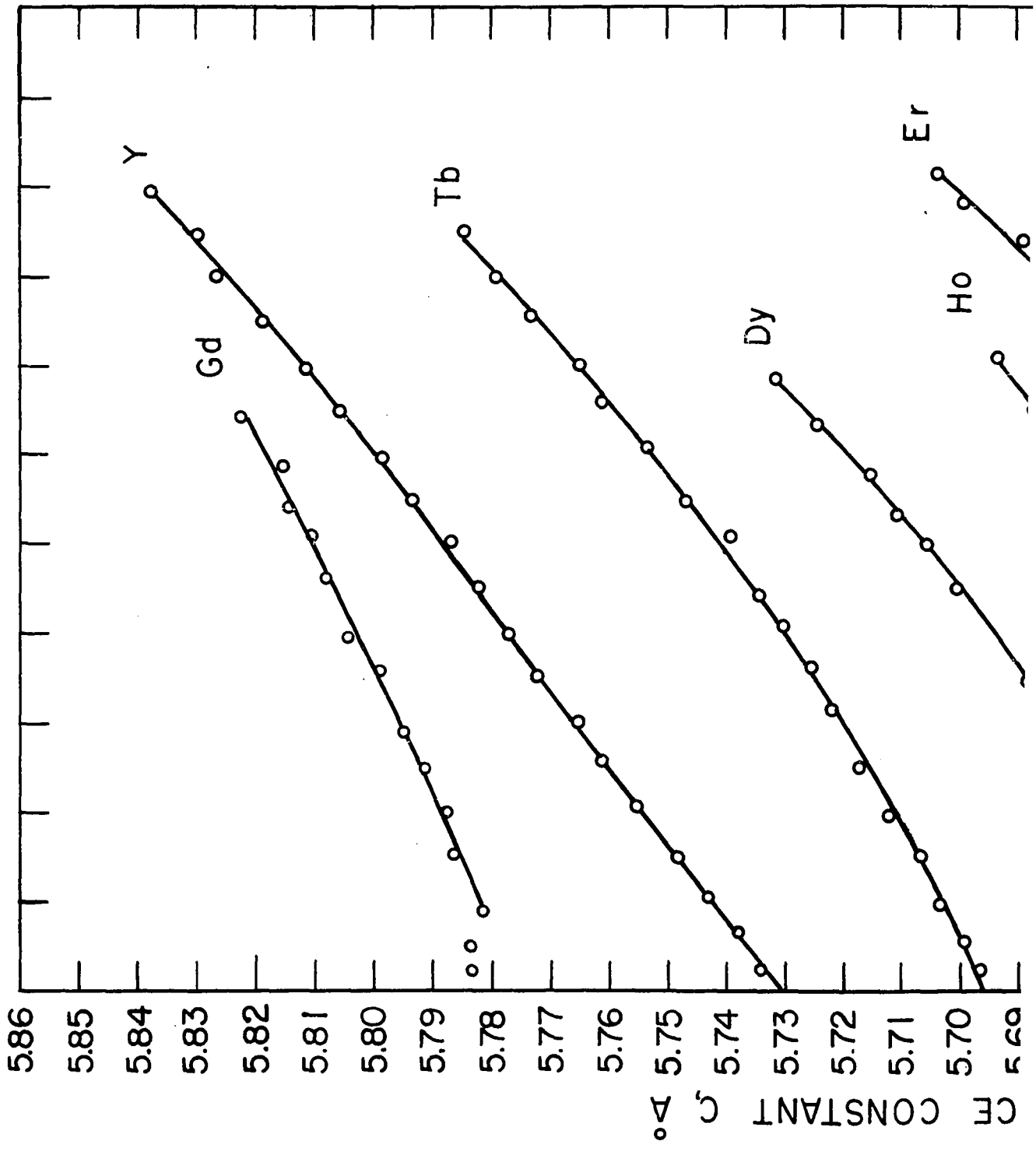
Y
Gd
Tb
Dy
Ho
Er
5.86
5.85
5.84
5.83
5.82
5.81
5.80
5.79
5.78
5.77
5.76
5.75
5.74
5.73
5.72
5.71
5.70
CE CONSTANT c, Å

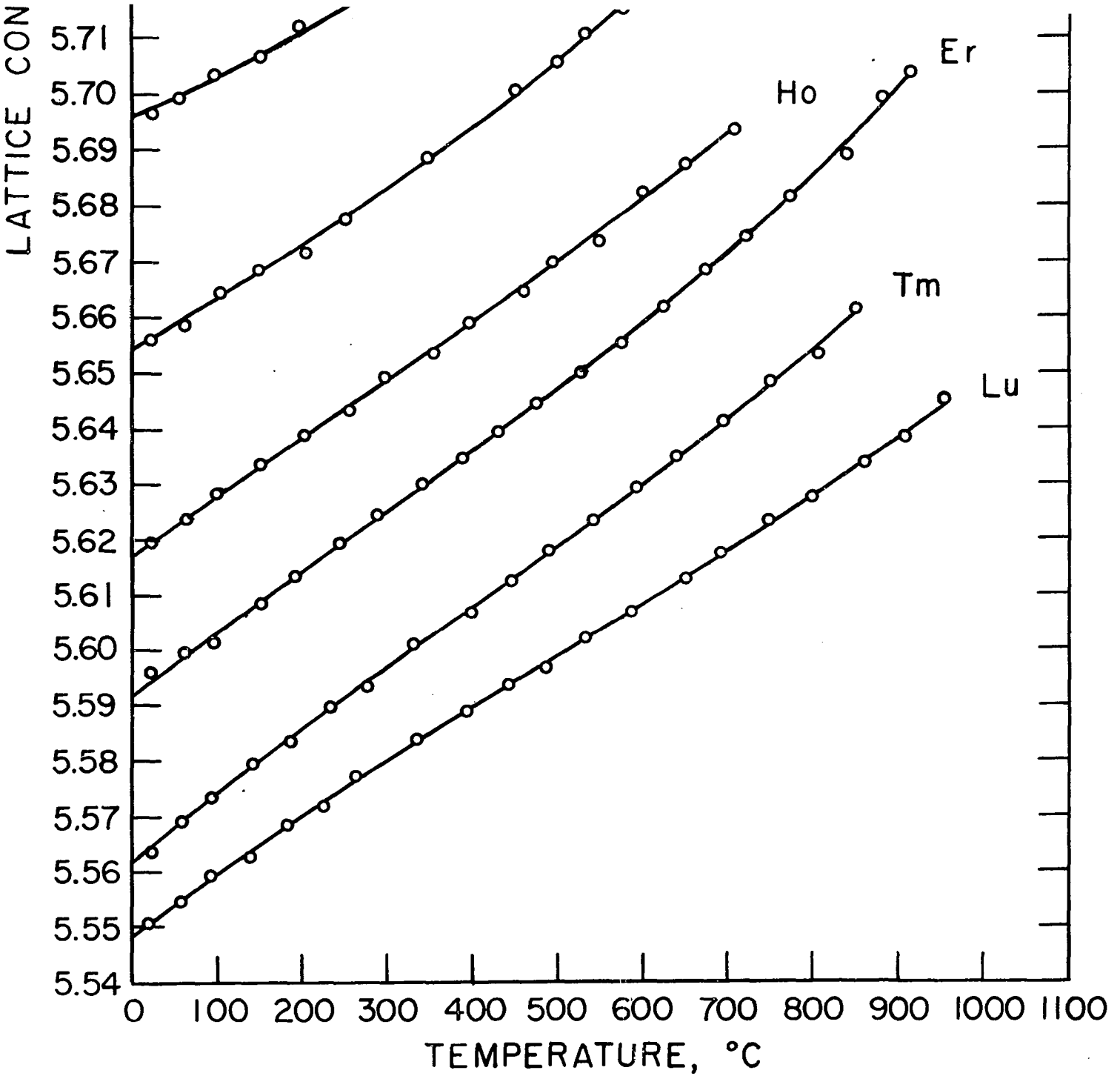
LATTICE CON
5.71
5.70
5.69
5.68
5.67
5.66
5.65
5.64
5.63
5.62
5.61
5.60
5.59
5.58
5.57
5.56
5.55
5.54
Er
Ho
Tm
Lu
0
100
200
300
400
500
600
700
800
900
1000
1100
TEMPERATURE, °C

Figure 27. The atomic volumes of the hcp heavy rare-earth elements and of yttrium *versus* temperature

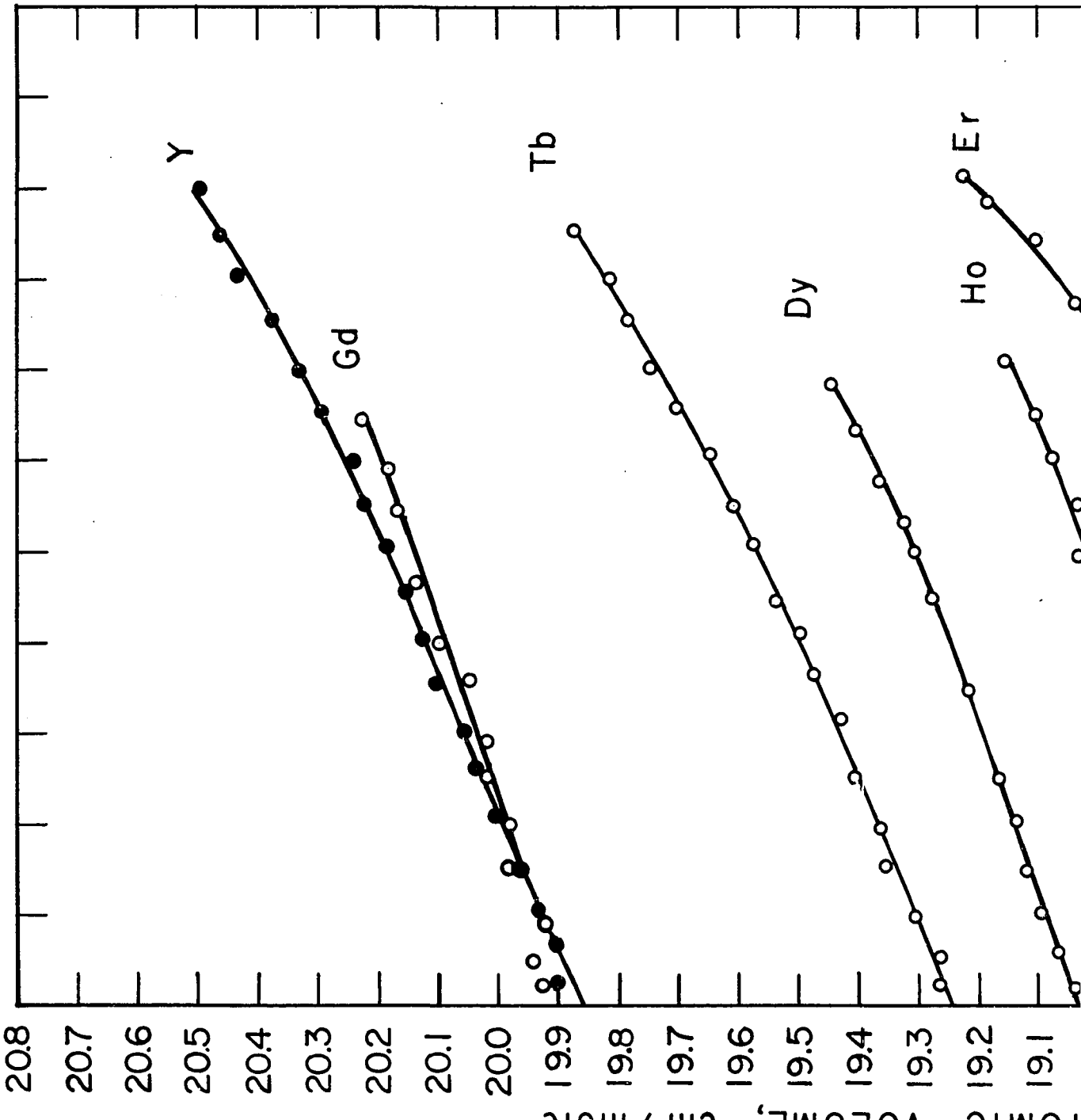
Y
Gd
Tb
Dy
Ho
Er
20.8
20.7
20.6
20.5
20.4
20.3
20.2
20.1
20.0
19.9
19.8
19.7
19.6
19.5
19.4
19.3
19.2
19.1
TOMIC VOLUME, cm³/mole

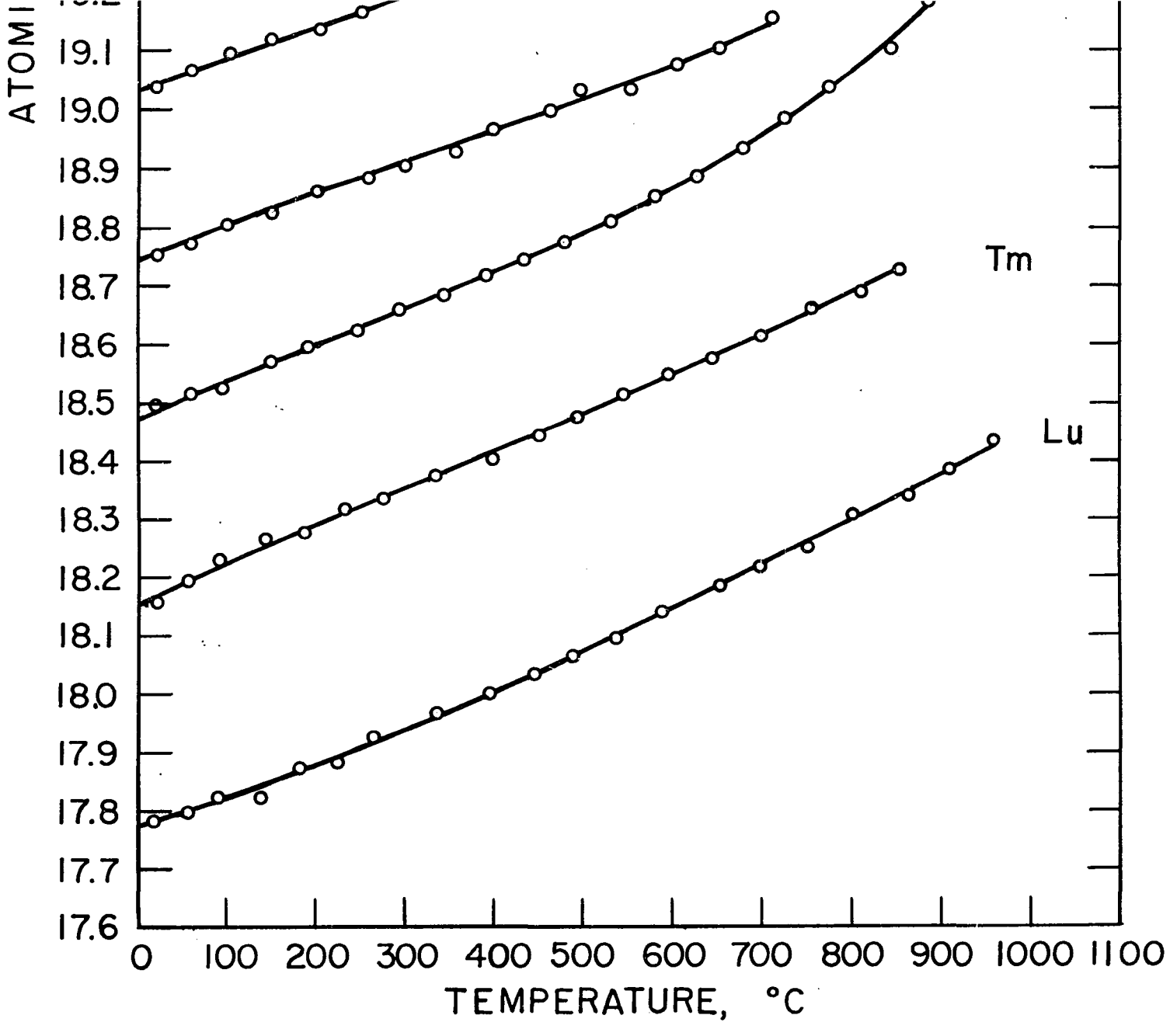
ATOMI
19.1
19.0
18.9
18.8
18.7
18.6
18.5
18.4
18.3
18.2
18.1
18.0
17.9
17.8
17.7
17.6
Tm
Lu
0
100
200
300
400
500
600
700
800
900
1000
1100
TEMPERATURE, °C

Figure 28. Lattice constant "a" of scandium *versus* temperature

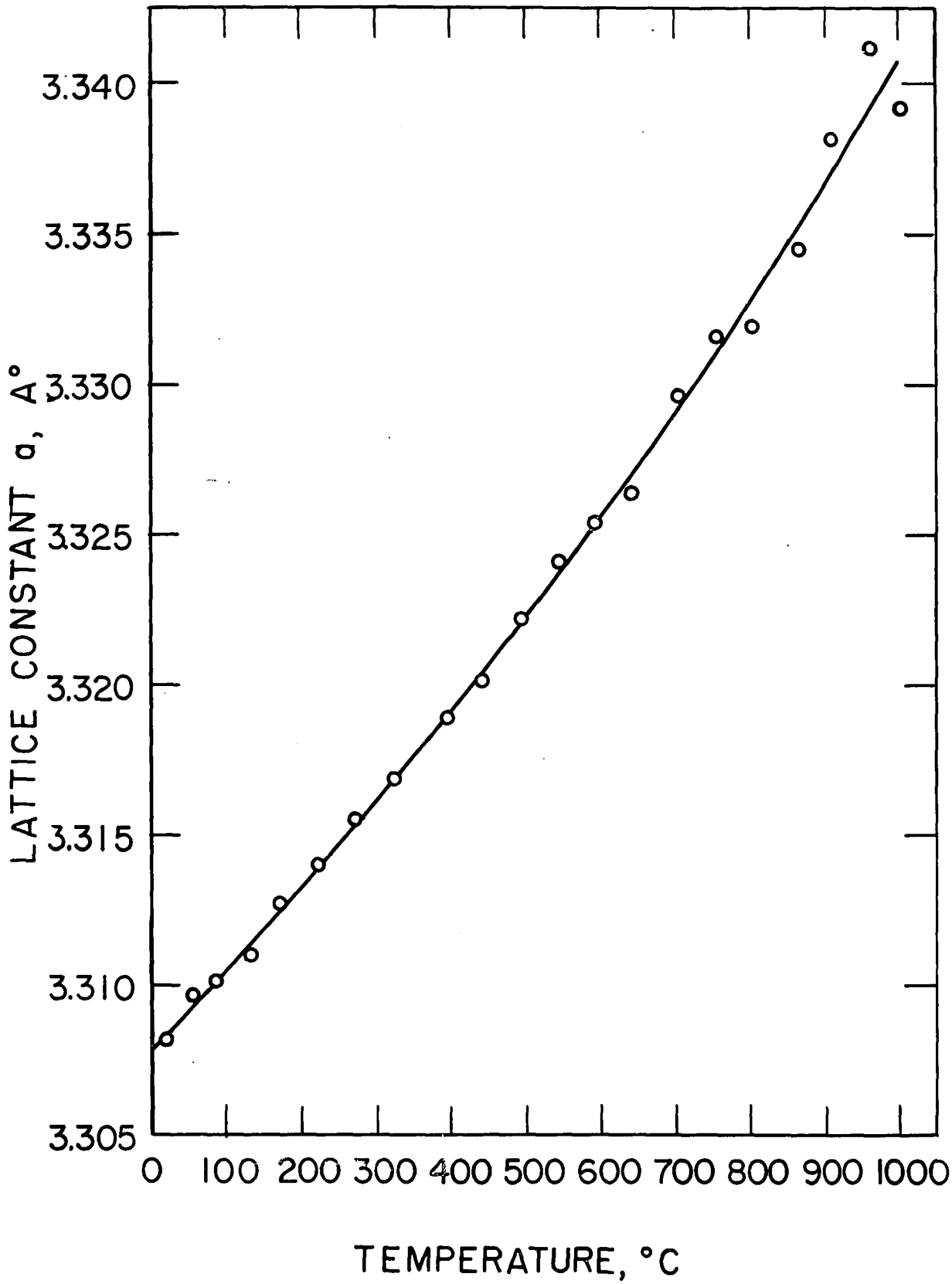
3.340
3.335
3.330
3.325
3.320
3.315
3.310
3.305
LATTICE CONSTANT a, A°
0
100
200
300
400
500
600
700
800
900
1000
TEMPERATURE, °C

Figure 29. Lattice constant "c" of scandium *versus* temperature

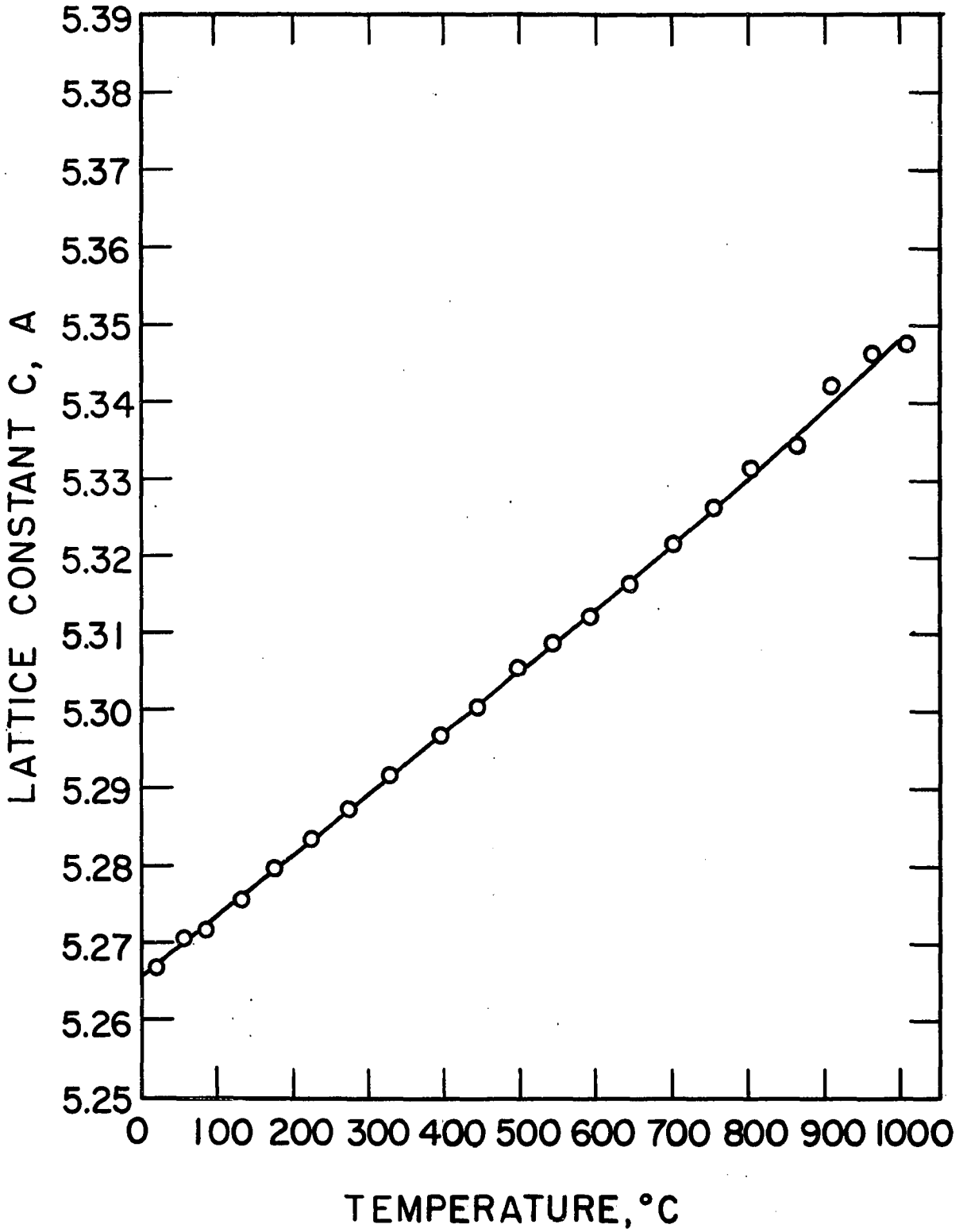
5.39
5.38
5.37
5.36
5.35
5.34
5.33
5.32
5.31
5.30
5.29
5.28
5.27
5.26
5.25
LATTICE CONSTANT C, A
0
100
200
300
400
500
600
700
800
900
1000
TEMPERATURE, °C

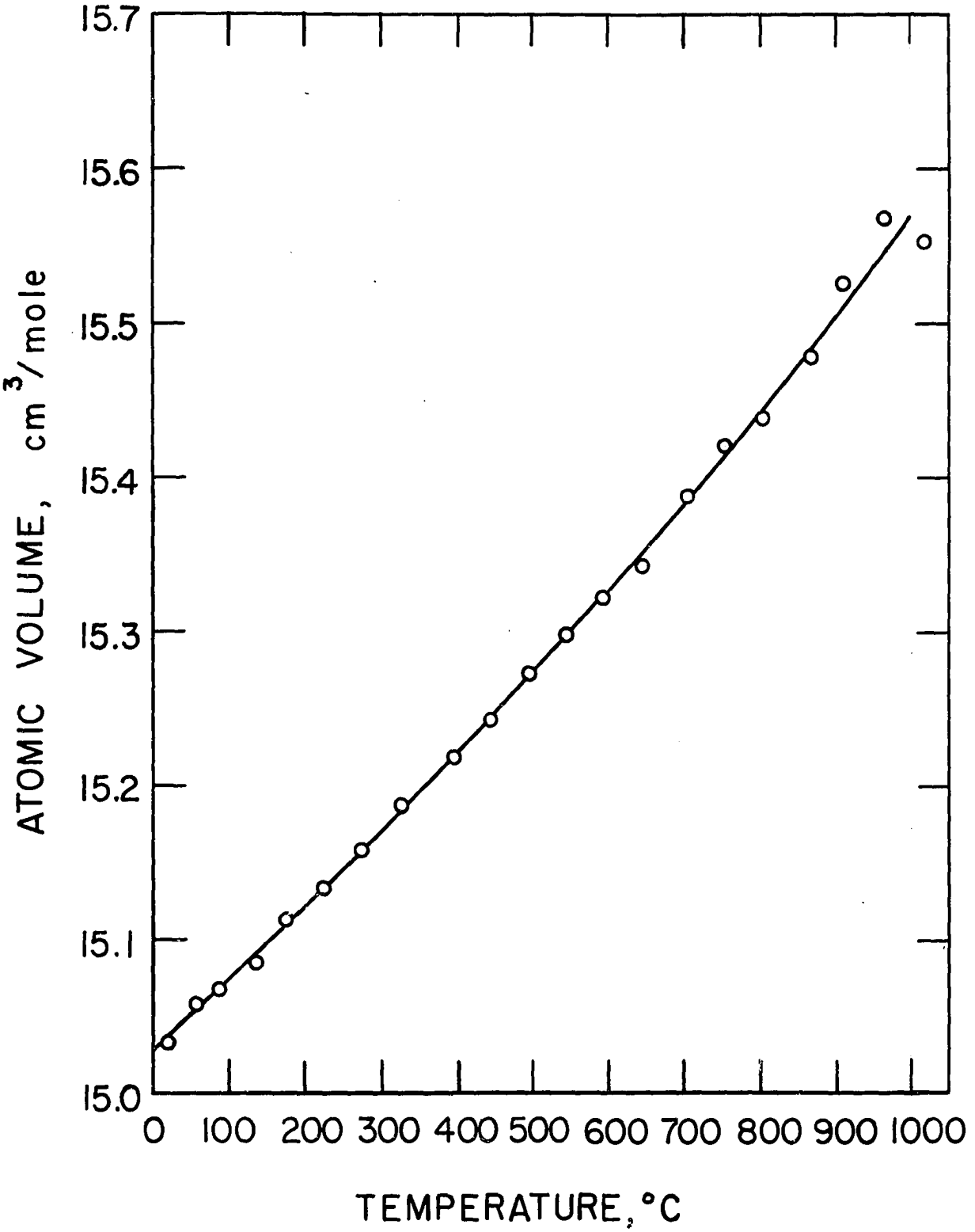

Figure 30. Atomic volume of scandium versus temperature

Table 12. Ratio a_c/a_a of the hcp rare-earth elements at 400°C

Element	a_c/a_a
Praseodymium	2.5
Neodymium	1.8
Gadolinium	2.1
Terbium	2.0
Dysprosium	4.4
Holmium	3.7
Erbium	2.6
Thulium	2.6
Lutetium	1.7
Scandium	1.6
Yttrium	3.2

occurs just below the room temperature this effect is probably due to the incipient ferromagnetism taking place in short-range order. Whatever the case may be, the data below 50°C were excluded from being fitted to an empirical equation.

There was no evidence of crystalline transformation that might correspond to the expansion anomalies reported by Barson, Legvold, and Spedding (20) for terbium in the region 700°C to 800°C and for dysprosium in the region 650°C to

900°C.

Impurities having a fcc structure with a lattice constant similar to the impurities encountered with the other rare earths were observed in most cases; their lattice constants are given in Table 4. It is interesting to note that all of these impurities have a smaller lattice than the parent metal and also that the difference is larger for the heavy rare earths. In general, the size of the impurities follows the lanthanide contraction.

Determination of High Temperature Transformations by Means of Measurements of Electrical Resistance

The measurements of electrical resistance were performed on gadolinium, terbium, dysprosium, holmium, erbium, and lutetium in the temperature range of 900°C to the respective melting points of these elements. During these measurements the samples were kept under an atmosphere of helium to prevent their evaporation at high temperatures; nevertheless, the samples of dysprosium, holmium, and erbium began evaporating. It was, therefore, necessary to envelop these three metals in a tantalum foil 0.0025 inch thick, and even to line a sight-hole, drilled in the sample to simulate black body conditions, with tantalum foil 0.0005 inch thick. It was calculated that the tantalum envelope would conduct only about 10 per cent of the total current so that the discontinuities

in the resistance, if any, should not be masked out by tantalum.

The electrical resistivity of gadolinium as a function of temperature exhibited a normal increase between 900°C and 1248°C, followed by an abrupt decrease of 0.4 per cent between 1248°C and 1275°C, and then followed by a continued increase up to the melting point. This effect can be seen in Figure 31, which also shows agreement between the heating and the cooling data. The mid-point of the discontinuity is at 1262°C and it agrees well with the transformation temperature of 1263°C determined at the Ames Laboratory by means of thermal analysis reported by Spedding and Daane (74). The large range of temperature in which the transformation occurred was apparently due to temperature gradients in the sample. These temperature gradients were large since the ends of the sample were fastened to cold copper posts.

The electrical resistivity of terbium, as a function of temperature, reveals two discontinuities as can be seen in Figure 32. One of these discontinuities was similar to that observed in gadolinium and it appeared between 1306°C and 1325°C, resulting in a 0.5 per cent decrease in resistivity. The mid-point of this discontinuity was at 1316°C, and, again, it compares reasonably well with the transformation temperature of 1310°C determined by means of thermal analysis reported by Spedding *et al.* (75).

The second discontinuity in electrical resistivity of

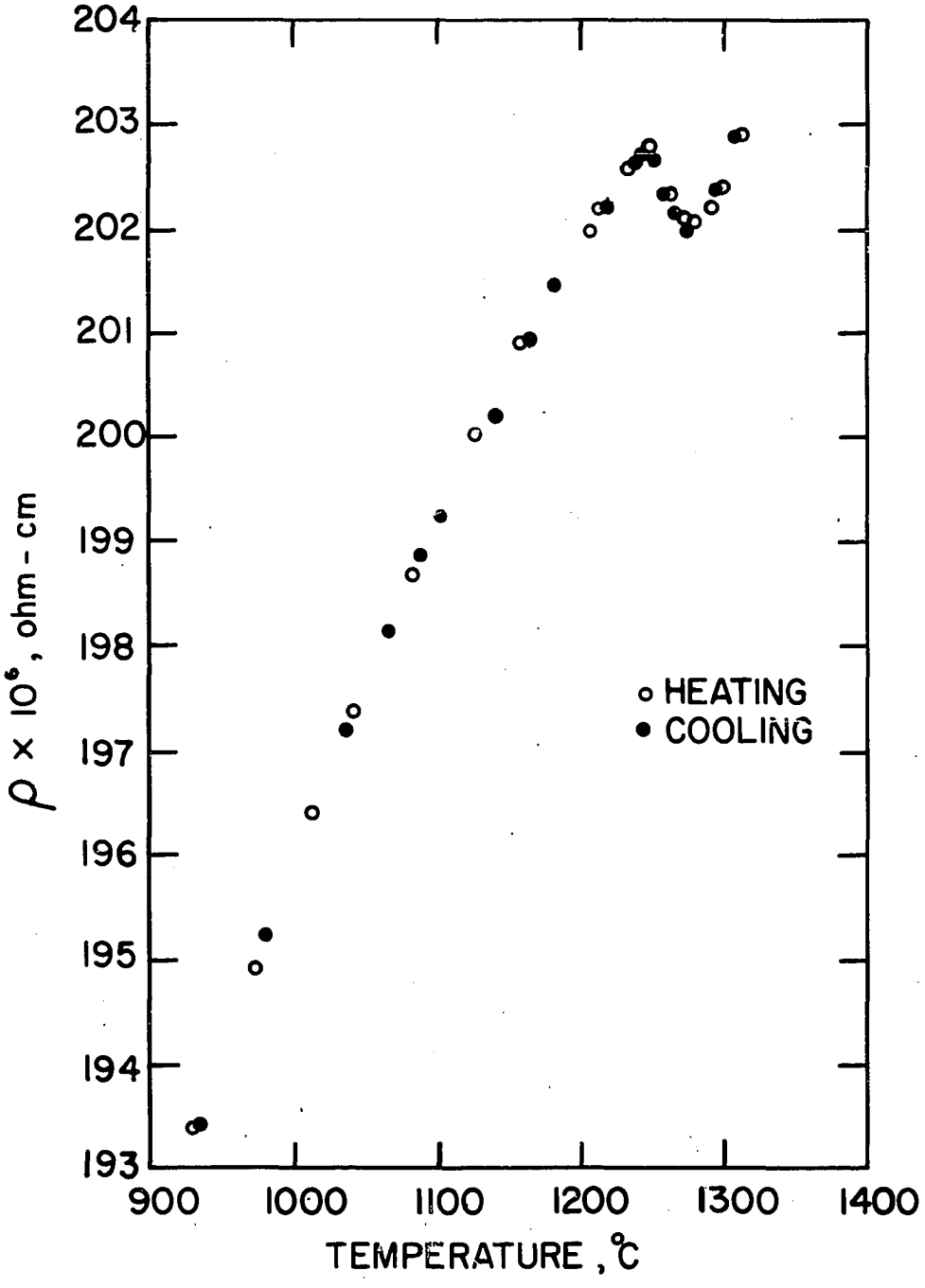

Figure 31. Electrical resistivity of gadolinium versus temperature

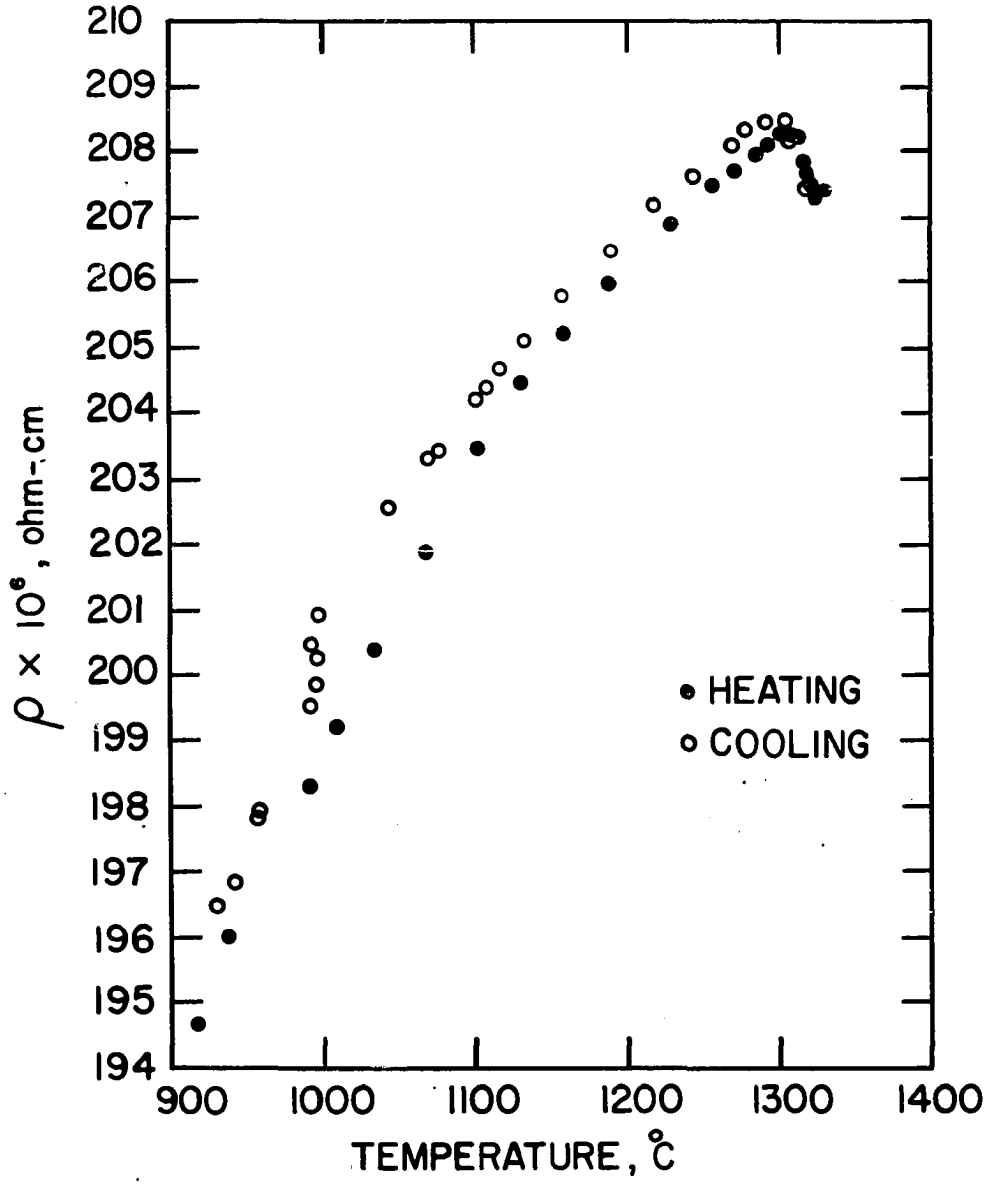

Figure 32. Electrical resistivity of terbium versus temperature

terbium was observed as a discontinuous change of slope at about 1115°C on heating, whereas on cooling, the change in resistivity occurred at 995°C, appearing both as an abrupt decrease in resistivity of about 0.8 per cent and as a change in slope. The discontinuity on heating took place instantly, whereas on cooling, the apparent isothermal break was completed in about twenty minutes. A similar thermal cycling of the sample showed that all the discontinuities were essentially reproducible, with the exception that the temperature of discontinuity mentioned last took place at 1016°C and lasted about 15 minutes. It is apparent, therefore, that if the discontinuity occurring between about 1000°C and 1115°C constitutes a phase change, the phase at the higher temperature has a tendency to supercool. Therefore, it might even be possible to quench this phase.

The results obtained for dysprosium, holmium, and erbium were not as distinct as the previous two results. For dysprosium a discontinuous increase in resistivity was observed in the temperature range of 1383°C to 1400°C in two separate thermal cycles of cooling and heating in each cycle. The sample melted at about 1410°C.

Holmium showed a slight discontinuous increase in resistivity in the temperature range of 1435°C to 1450°C, followed by melting at 1465°C.

Erbium gave no evidence of any discontinuities in this property between 900°C and its melting point.

Since the absolute values of resistivity could not be obtained for dysprosium, holmium and erbium, the data are not presented in a graphical form.

Lutetium yielded reproducible results for two thermal cycles as can be seen in Figure 33. A discontinuity constituting a hysteresis loop similar to the one observed in terbium appeared between 1407°C, on heating, and 1260°C on cooling. The discontinuity on heating appears merely as a sudden change in the slope, whereas on cooling there is a quasi-discontinuous decrease in resistivity followed by a discontinuous change in slope.

It was desired to measure the resistivity of thulium and scandium at high temperatures; however, this work had to be postponed because of the difficulties presented by the high vapor pressure of thulium and the lack of sufficient amount of scandium.

X-ray Crystallographic Results Above 1000°C

An attempt was made to determine the high temperature structures of gadolinium, terbium, and lutetium using the apparatus depicted in Figures 3, 4, and 5. These elements were selected because of their relatively low vapor pressure and the relatively large temperature intervals between their transformation temperatures and their melting points.

In the description of the X-ray method used in this work

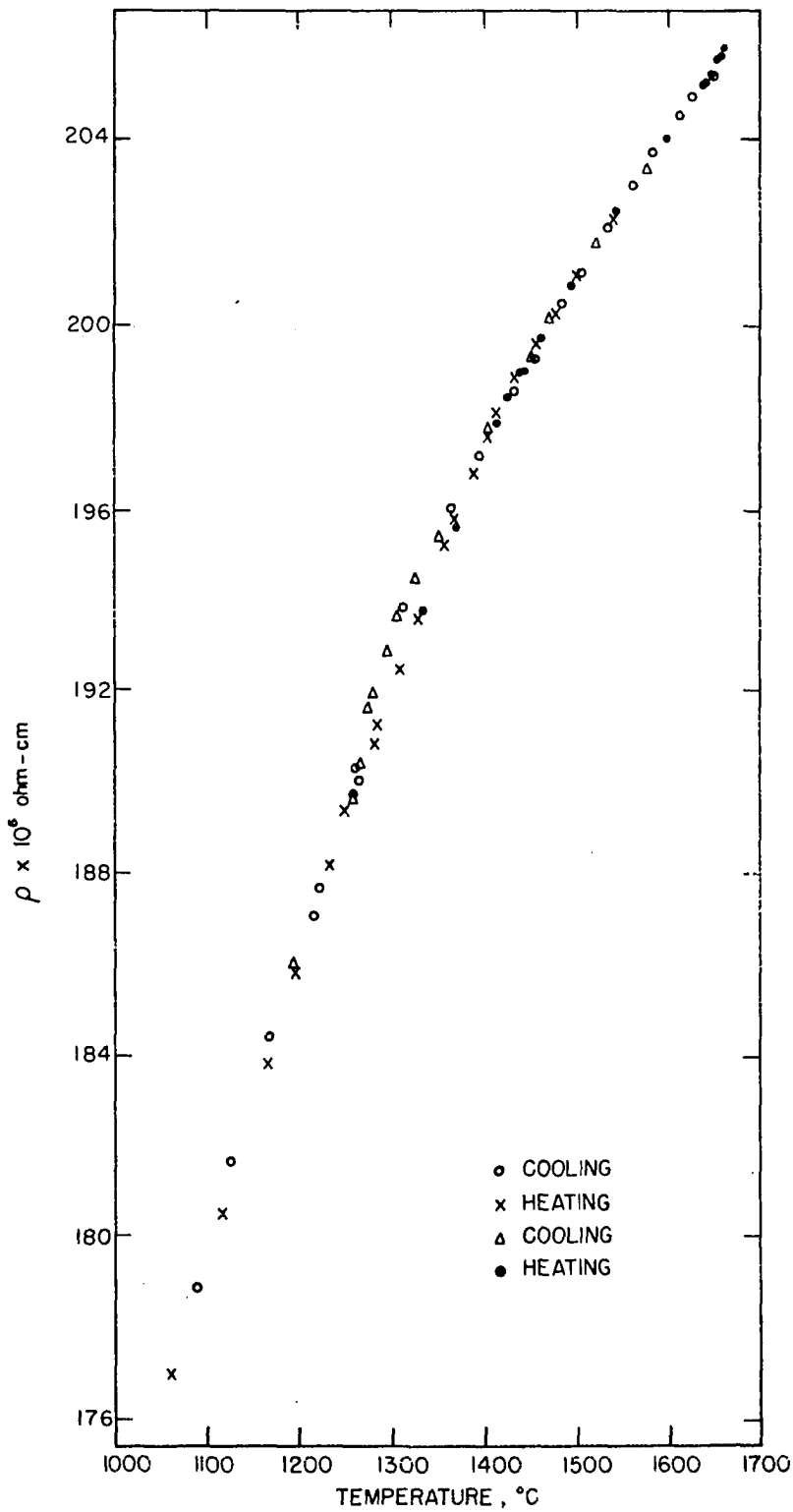

Figure 33. Electrical resistivity of lutetium versus temperature

it was mentioned that the electrical resistivity of the X-ray sample could be recorded continuously as the sample was heated. Such a record of resistivity obtained with samples of gadolinium showed small but certain discontinuities, and thus gave an indication of the occurrence of the solid state transformation. More than forty attempts were made to obtain patterns above and below the transformation temperature. The resulting patterns consisted of only a few very spotted lines, although in one case, at about 1200°C, 10 such lines were obtained which belonged to the same hcp lattice as observed at lower temperatures. Patterns obtained above the transformation temperatures yielded only two plainly visible spotted lines and two other lines which were so faint that their existence was questionable. All four lines could be indexed on the basis of a bcc lattice with a lattice constant 4.06 Å. The dilemma which the patterns presented was that the two strong lines also coincided with two lines of the hcp pattern. On the other hand, the value of the cubic lattice constant appears realistic, since it yields a value of 20.15 cm^3/mole for the atomic volume of the metal, smaller by about two per cent than the extrapolated volume of the hcp metal at 1270°C. It is also consistent with the lanthanide contraction.

Even though gadolinium is not very volatile, it volatilized somewhat at these temperatures under vacuum, thereby creating difficulties in the determination of approximate

temperatures with an optical pyrometer and causing the samples to burn out in spots where extensive evaporation took place.

Terbium, being more volatile, caused even more difficulties in estimating the temperature of the sample. The change in the slope in the resistivity curve at 1115°C, seen in Figure 32, was not large enough to be used for the temperature calibration of the terbium X-ray specimen. A few patterns taken in the vicinity of this temperature displayed but a few faint and scattered spots which proved to be insufficient for the identification of the phase assumed by the metal.

Lutetium also presented the problem of vaporization in the vicinity of 1400°C; furthermore, the anomaly in resistivity at 1407°C was apparently too nebulous to be detected. A diffraction pattern obtained in the neighborhood of this temperature showed several well-defined spotted lines which were indexed as hcp by a visual comparison with the hcp patterns of lutetium taken near 1000°C.

It is felt that the high temperature structures of these elements can be obtained by this method with a few minor modifications, one of which is the use of tantalum or tungsten wires coated with the rare-earth metal being investigated; samples prepared in this way would have a smaller tendency to burn out and to form large crystals. To improve

the detection of the discontinuities in electrical resistivity, the probes measuring the voltage across the sample should be attached to the sample in the vicinity of the X-ray beam, and not to the outer electrical conductors of the sample holder as was done in the present work. Another modification to be adopted should be the use of purified inert atmospheres instead of vacuum to surround the sample while it is heated, in order to prevent evaporation of the sample. Attempts were actually made to do this in the present investigation by passing purified argon over the hot sample, mounted in the same sample holder in the same manner. The argon was allowed to escape out of the sample holder through a tiny pinhole made in the Saran Wrap. The argon was purified by bubbling it through a sodium-potassium eutectic at 250°C, and then condensing it to liquid in a liquid nitrogen trap. Liquid argon subsequently evaporated at a slow, steady rate as the level of the liquid nitrogen decreased, and the evaporated gas was piped directly to pass over the sample. Encouraging results were obtained as indicated by only a limited surface contamination of the gadolinium samples heated to above 1200°C. Perhaps a repeated purification of the gas would produce the desired result.

DISCUSSION

Solid Phase Transformations

It was shown in this investigation, by means of high temperature X-ray studies, that lanthanum, cerium, praseodymium, neodymium, ytterbium, and, perhaps, gadolinium exhibit a bcc structure in relatively short temperature intervals just below their melting points. Similar behavior was inferred from phase diagram studies for yttrium (60, 61, 62) and for gadolinium (61). Europium was reported to be bcc in its entire solid phase region (49, 50). In all cases, excepting europium, the bcc structure, having a coordination number of eight, forms at the expense of one of three close-packed structures, having coordination numbers of 12. Upon transformation to the bcc phase, the metal atoms acquire a greater freedom of motion by decreasing their coordination number and also by assuming an environment having a center of symmetry (in the fcc structure there is a center of symmetry to start with). Greater freedom of motion results in an increase in entropy, which, in turn, becomes important in the expression for the free energy which must become negative for the transformation to take place simultaneously:

$$\Delta F_{P,\,T} = (H_{bcc} - H_{cp}) - T(S_{bcc} - S_{cp}),$$

where the subscript cp designates the close-packed structure. This argument is consistent with the theory proposed by

Zener (107), who predicted successfully the existence of close-packed structures at low temperatures for several metals having a bcc structure.

In the case of the light rare earths, a net increase in volume was observed upon the transformation to the bcc structure. In ytterbium this transformation resulted in a very small decrease in volume. In gadolinium, if its patterns at high temperature were indeed bcc, a decrease in volume took place. Both in lanthanum and in ytterbium the fcc structure was smaller in volume than the corresponding hexagonal structures at the transformation temperatures. All of these changes in volume are small in comparison to the volume change for the $\gamma - \alpha$ phase transformation in cerium involving a transfer of one electron from the 4f band to the 5d band. Therefore, it can be concluded that in the transformations mentioned above, the metals retain the same valence which they display at room temperature.

The transformation of the close packed structures to the bcc structures in the rare earths and yttrium are accompanied by abrupt changes in the electrical resistivity, as observed in this work and elsewhere (14, 60). Such transformations in zirconium and hafnium are accompanied by similar changes in electrical resistivity (108, 109). The changes in electrical resistivity of terbium at 1316°C and those of dysprosium and holmium have the characteristics of a close-packed to bcc transformation. The transformation in terbium occurring

between 1005°C and 1115°C is rather sluggish on cooling. The behavior of electrical resistivity in this transformation is similar to that observed in lanthanum at near 300°C (14). The behavior of the electrical resistivity in lutetium has similar characteristics. As stated previously, McKeown (40) reported large changes in the heat of transformation of cerium, praseodymium, and neodymium, the corresponding entropy changes being 0.70, 0.67, and 0.63 entropy units. Noting that the first of these values applies to a transformation involving the fcc and bcc phase, whereas the other two values apply to the transformation involving the hcp (double c-axis) and fcc phases, one can reason that a transformation involving the hcp (double c-axis) and the fcc phases would be accompanied by a very small change in entropy. Hence, such a transformation would be sluggish and would occur through a relatively large temperature range instead of taking place isothermally. Such is indeed the case for the hcp (double c-axis)-fcc transformation in lanthanum and cerium. Since the lower temperature transformation in terbium has similar characteristics, it might also involve the hcp and the fcc structures. The anomaly in the electrical resistivity in lutetium resembles that of the terbium at its lower temperature transformation. Since the hcp-bcc transformations in yttrium, lutetium, zirconium, and halfnium have anomalies in electrical resistivity similar to gadolinium, it is possible that the high temperature structure of lutetium might be fcc

instead of bcc.

The occurrence of the hcp allotrope in ytterbium has been shown in this work to be stabilized by an impurity. The atomic volume of this phase indicates that the metal remains divalent, that is to say, that only the $6s^2$ electrons are in the conduction band. Since in this case an almost perfect axial ratio was obtained, as in the case of calcium, it is suggested that the deficient axial ratio in the trivalent rare earths is caused by the presence of the $5d^1$ electron in the conduction band. In the trivalent rare-earth metals, including scandium and yttrium, the conduction electrons can be considered as consisting of a hybrid in which the identity of the s and d electrons is indistinguishable and in which the electrons are delocalized. In the band theory language, one would say that the ns and the (n-1)d bands overlap.

Relationships involving the axial ratio and the crystal structure of the rare earth elements

An interesting relationship was observed between the axial ratio and the crystal structure of the rare-earth elements. This relationship, to be described shortly, can be observed in Figure 34 where the axial ratios of the heavy rare-earth elements, scandium, and yttrium are plotted as a function of temperature. For the sake of clarity, the individual experimental points are not shown, but merely the results obtained from the empirical equations to which the data

Figure 34. The axial ratios of scandium, yttrium, and the heavy rare earths, as a function of temperature

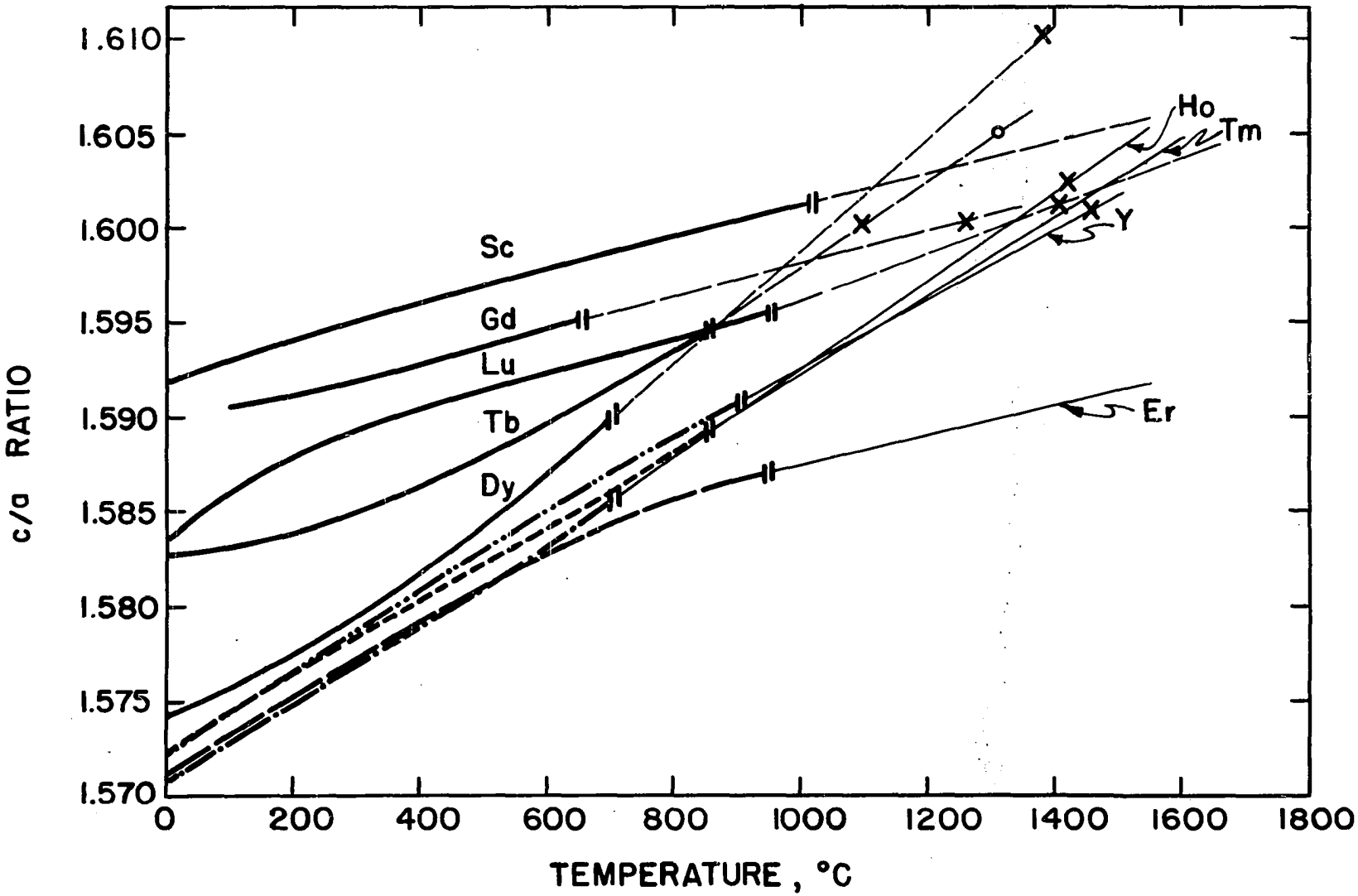
1.610
1.605
1.600
1.595
1.590
1.585
1.580
1.575
1.570
c/a RATIO
0
200
400
600
800
1000
1200
1400
1600
1800
TEMPERATURE , °C
Sc
Gd
Lu
Tb
Dy
Ho
Tm
Y
Er

were fitted. The heavy lines represent the ranges of temperature where experimental data were available and the light lines represent the linear extrapolations of the axial ratios from the ends of the heavy lines up to the melting points of the metals. Two short vertical lines on each curve represent the points from which the extrapolations were made, and the points marked as "x" are the transformation temperatures; in the case of terbium, where two transformations were observed, the second transformation is marked by "o".

The observation of interest is that the axial ratios increase with temperature and at the same time tend to converge to a limiting value, which is less than the perfect value at the melting point. Furthermore, for those elements where transformations were indicated the axial ratio attained approximately a constant value at the respective transformation temperatures. In the case of yttrium, gadolinium, terbium, holmium, and lutetium the transformations were observed between the values of 1.600 and 1.602 of the axial ratio. The values of the axial ratio not falling in this range at the transformation temperature were 1.610 for dysprosium and 1.605 for the second transformation of terbium, although the latter does not constitute a discrepancy, since the metal probably transformed from the hcp phase at the lower transformation temperature. For dysprosium, experimental values of the axial ratio were obtained only for a relatively short range of temperature, whereas the extrapolation was made for

a relatively long range, hence increasing the probability of an error in the extrapolation.

Erbium did not attain this limiting value of the axial ratio and its electrical resistance failed to give any evidence of a crystalline transformation, hence giving support to the observation that a limiting value of the axial ratio is apparently required for a solid phase transformation to take place.

Data on the existence of crystalline transformation in scandium and thulium are lacking. However, if the axial ratio criterion holds, one can expect to find transformations in these metals in the temperature ranges of 1009°C to 1140°C and 1370°C to 1480°C, respectively.

Lanthanum, cerium, praseodymium, and neodymium behave similarly in that they display a limiting value of the axial ratio upon transformation, the individual values being 1.619, 1.618, 1.619, and 1.621, respectively, as shown in Figure 35. The value for the axial ratio of cerium is that reported by McHargue et al. (33).

The axial ratio of the hcp form of ytterbium starts at a value of 1.637 at 268°C and decreases to a value of 1.634 at 412°C. Sufficient number of experimental points is lacking to make a valid extrapolation to the transformation temperature. However, it seems likely that the axial ratio attains a nearly perfect value at that temperature.

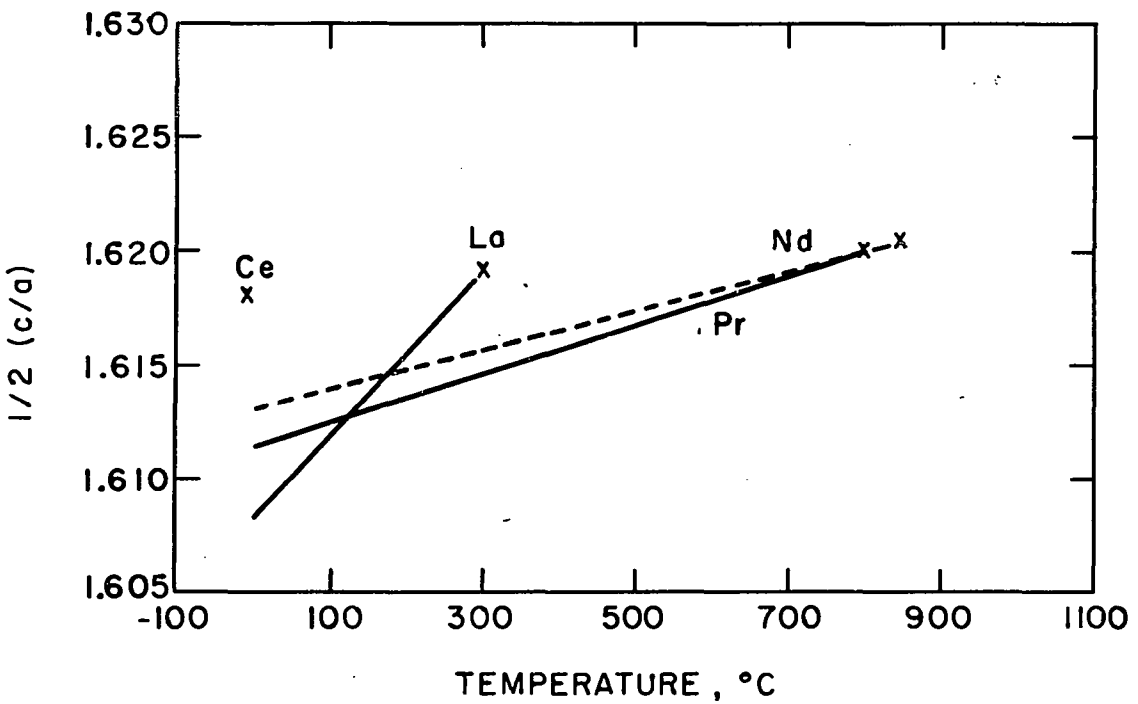

Figure 35. The axial ratios of lanthanum, cerium, praseodymium and neodymium

Thermal coefficients of expansion

The thermal expansion coefficients of the rare-earth elements shown in Figures 10, 17, and 18 represent an additional result in the determination of the structures and the lattice constants by the high temperature X-ray method. Most of the expansion curves show a parabolic curvature; this effect is a consequence of the expansion curves being derived from cubic equations relating the lattice constants or atomic volumes to temperature. The parabolic curvature may or may not be real, however, it is strongly suspected that the minima occurring in these curves are not real, except, perhaps in the case of cerium, where a minimum was observed in the coefficient of expansion determined dilatometrically (20). It was preferred to obtain the coefficients of expansion in this manner rather than obtaining them by computing the mean coefficients of expansion from consecutive lattice constants over small temperature ranges, because the coefficients of expansion obtained by the latter method were subject to large fluctuations. For example, in the case of yttrium, where relatively accurate lattice constants were obtained, the mean coefficients of expansion had an average deviation of $\pm$ 20 per cent from the best curve drawn through them. Since it would be impractical to determine the deviation in the expansion coefficients obtained from the empirical equations, a comparison of these quantities was made with the dilatometric data as shown in Table 6. The best agreement was obtained

at approximately the mid-range temperature of 400°C, where the average deviation between the two sets of results was ± 4.7 per cent and the maximum deviation was 13.3 per cent. This agreement is sufficient to enable one to compare the expansion of the two axes in the hexagonal metals and to compare, to some extent, the expansion of the individual rare-earth metals. The curves determined by empirical equations are given for the purpose of determining the magnitude of the coefficient of expansion. No great reliance should be given to the actual shape of these curves.

Three rather unusual effects were observed in the coefficients of expansion of the rare-earth metals. Two of these effects are the large coefficient of expansion of ytterbium and the rapidly increasing coefficient of expansion of erbium. Both of these effects were also observed by Barson et al. (20) previously. In ytterbium, the unusual effect is attributed to the fact that, being a divalent metal, it has fewer electrons in the conduction band than the trivalent rare earths and, hence, it exhibits a weaker bonding. Weaker bonding gives rise to larger values of atomic volume, compressibility, coefficient of expansion, etc. Explanation for the expansion behavior of erbium is not immediately apparent.

The third unusual effect was observed in europium, which exhibited a large, but decreasing coefficient expansion with increasing temperature. The magnitude of the coefficient of expansion is due to the metal's being divalent. The decrease

of the coefficiant of expansion is more unusual since the behavior of this property should be analogous to that of the specific heat, which ordinarily increases with increasing temperature. A possible explanation of this anomalous behavior is that with increasing temperature one of the 4f electrons is being promoted to the conduction band, the extent of this promotion being governed by the Boltzmann distribution. The increase of the number of electrons in the conduction band tends to enhance bonding and, hence, to shrink the lattice, thereby diminishing the expansion of the lattice due to thermal vibrations. A continued increase in the number of electrons in the conduction band could eventually result in a negative coefficient of expansion.

The promotion of the 4f electron into the conduction band is not unlikely, since the 4f band and the conduction band in europium metal must be close, judging from the fact that the element displays a variable valence in its compounds, in which trivalence is preferred.

A nearly equivalent explanation of this effect could be that proposed by Varley (110) for the occurrence of negative coefficient of expansion in metals. The criteria necessary for such an occurrence are high electronic specific heat, large increase of the density of states with energy at the Fermi energy, and a large number of overlapping bands. If the 4f electron has the tendency to go into the conduction band, it might be expected that the specific heat would be

increased and this increased would not be due to only the electronic transition, but also to the increase in electronic specific heat of the conduction band.

The heat capacity measurements of europium metal which are currently in progress at the Ames Laboratory might be helpful in resolving this phenomenon. Magnetic studies would detect a promotion of the 4f electron into the conduction band. A thorough investigation of the expansion characteristics of this metal up to its melting point is also desirable, since the observed phenomenon should be more extensive at higher temperatures if these explanations should apply.

SUMMARY

An investigation of the rare-earth metals was made by high temperature X-ray methods in order to determine their high temperature allotropy and thermal expansion characteristics. The high temperature structure of several of these metals was found to be body centered cubic (bcc). The bcc lattice constants, above the transformation temperatures reported by Spedding and his co-workers, are the following: lanthanum, 4.26 Å above 868°C; cerium, 4.12 Å above 730°C; praseodymium, 4.13 Å above 798°C; neodymium, 4.13 Å above 868°C; ytterbium 4.44 Å above 798°C. Some evidence was obtained for a bcc structure in gadolinium above 1262°C, the lattice constant being 4.06 Å.

Below their respective transformation temperatures given above, lanthanum and cerium are face centered cubic (fcc), whereas praseodymium and neodymium are hexagonal (double c-axis). At 292°C lanthanum transforms completely into the fcc phase, however, below this temperature both the fcc and the hexagonal (double c-axis) structures coexist.

Ytterbium retains its fcc structure up to the transformation temperature of the bcc phase, however, it is possible to stabilize a hcp structure above 260°C by introducing atmospheric impurities. Above 720°C this phase transforms into the bcc phase. The lattice constants for the hcp phase at 268°C, are a = 3.911 Å and c = 6.403 Å, with

c/a = 1.637. Atmospheric impurities lower the fcc-bcc transformation temperature by as much as 80°.

Gadolinium and lutetium were found to be hcp up to at least 1200°C and 1400°C, respectively. Scandium, yttrium, and the remaining trivalent heavy rare-earth metals are also hcp to at least the vicinity of 950°C.

Electrical resistivity measurements confirmed crystalline transformations in gadolinium near 1262°C and in terbium near 1316°C and gave evidence for additional transformations in terbium between 1005°C and 1115°C, in dysprosium between 1383°C and 1400°C, in holmium between 1435°C and 1450°C, and in lutetium between 1260°C and 1407°C.

The axial ratio of the hexagonal metals increases with increasing temperature and it seems to attain a nearly constant value of 1.601 ± 0.001 at the transformation temperature of the rare-earth metals having the hcp structure. For metals having the hexagonal (double c-axis), this limiting axial ratio, 1/2(c/a) is 1.619 ± 0.002.

Lattice constants were determined for scandium, yttrium and the rare-earth elements (excluding samarium) to temperatures as high as 1000°C. The data were fitted to empirical equations from which coefficients of expansion were calculated. In the case of the hcp metals, the c-axes expand more with increasing temperature than the a-axes by a factor ranging from 1.6 to 4.4.

Europium exhibits a sharply decreasing coefficient of

expansion with increasing temperature in the investigated temperature range of 20°C to 300°C. This phenomenon might be due to a gradual promotion of one of the 4f electrons into the conduction band.

The hexagonal phases of lanthanum and ytterbium are larger in volume by 0.5 and 0.7 per cent, respectively, than the fcc phases. The transformations to the bcc structure are accompanied by small increases in volume for lanthanum, cerium, praseodymium, and neodymium, and small decreases for gadolinium and ytterbium.

LITERATURE CITED

1. Klemm, W. and Bommer, H., Z. anorg. u. allgem. Chem. 231, 138 (1937).

2. McLennan, J. C. and McKay, R. W., Trans. Roy. Soc. Can. Sect. 3, 24, 33 (1930).

3. Quill, L. L., Z. anorg. u. allgem. Chem. 208, 273 (1932).

4. Zintl, E. and Neumayr, S., Z. Elektrochem. 39, 84 (1933).

5. Rossi, A., Nature (London) 133, 174 (1934).

6. Ziegler, W. T., O. N. R. Georgia Inst. Tech., State Eng. Exp. Station Tech. Report No. 1, (1949).

7. _____, Young, R. A., and Floyd, A. L., Jr., J. Am. Chem. Soc. 75, 1215 (1953).

8. Bommer, H., Z. Elektrochem. 45, 347 (1939).

9. Farr, J. D., Giorgi, A. L., and Bowman, M. G., U. S. Atomic Energy Commission Report LA-1545 [Los Alamos Scientific Laboratory]. 1953.

10. James, N. R., Legvold, S., and Spedding, F. H., Phys. Rev. 88, 1092 (1952).

11. Young, R. A. and Ziegler, W. T., J. Am. Chem. Soc. 74, 5251 (1952).

12. Spedding, F. H., Daane, A. H., and Herrman, K. W., Acta Cryst. 9, 559 (1956).

13. Jaeger, F. M., Bottema, J. A., and Rosenbohm, E., Rec. Trav. Chim. Pays-Bas 57, 1137 (1938).

14. Spedding, F. H., Daane, A. H., and Herrmann, K. W., J. Metals 9, 895 (1957).

15. Vogel, R. and Heumann, T., Z. Metallkunde 38, 1 (1947).

16. Massenhausen, W., ibid. 43, 53 (1952).

17. Vogel, R. and Klose, H., ibid. 45, 633 (1954).

18. Bridgman, P. W., Proc. Am. Acad. Arts Sci. 76, 55 (1948).

19. Trombe, F. and Foex, M., Compt. rend. 217, 501 (1943).

20. Barson, F., Legvold, S., and Spedding, F. H., Phys. Rev. 105, 418 (1957).

21. Spedding, F. H. and Daane, A. H., J. Metals 6, 504 (1954).

22. Schumacher, E. E. and Lucas, F. F., J. Am. Chem. Soc. 46, 1167 (1924).

23. Hull, A. W., Phys. Rev. 18, 88 (1921).

24. Trombe, F., Compt. rend. 198, 1591 (1934).

25. La Blanchetais, C., ibid. 220, 392 (1945)

26. Trombe, F. and Foex, M., Ann. Chim. (Paris) Ser. 11, 19, 417 (1944).

27. Foex, M., Compt. rend. 219, 117 (1944).

28. Kevane, C. J., Legvold, S., and Spedding, F. H., Phys. Rev. 91, 1372 (1953).

29. Parkinson, D. H., Simon, F. E., and Spedding, F. H., Proc. Roy. Soc. Sect. A, 207, 137 (1950).

30. Bridgman, P. W. The physics of high pressure. 2nd ed. London. G. Bell and Sons, Ltd. 1949.

31. Schuch, A. F. and Sturdivant, J. H., J. Chem. Phys. 18, 145 (1950).

32. Lawson, A. W. and Tang, T., Phys. Rev. 76, 301 (1949).

33. McHargue, C. J., Yakel, H. L., Jr., and Jetter, L. K., Acta Cryst. 10, 832 (1957).

34. McHargue, C. J., Low temperature allotropy of cerium metal. To be published in Acta Cryst. ca. 1959 .

35. Loriers, J., Compt. rend. 226, 1018 (1948).

36. Ahmann, D. H., Iowa State College J. Sci. 27, 120 (1953).

37. Gaume-Mahn, F. and Cohen, M., J. recherches centre nat. recherche sci. 29, 65 (1954).

38. _____, Compt. rend. 241, 286 (1955).

39. Bates, L. F., Leach, S. J., and Loasby, R. G., Proc. Phys. Soc. (London) Sect. B, 68, 859 (1955).

40. McKeown, J. J. The high temperature heat capacity and related thermodynamic functions of some rare earth metals. Unpublished Ph. D. Thesis. Ames, Iowa, Library, Iowa State University of Science and Technology. 1958.

41. Rossi, A., Atti accad. nazl. Lincei 15, 298 (1932).

42. Klemm, W. and Bommer, H., Z. anorg. u. allgem. Chem. 241, 264 (1939).

43. Barson, F. A low temperature dilatometric study of some rare earth metals. Unpublished M. S. Thesis. Ames, Iowa, Library, Iowa State University of Science and Technology. 1953.

44. Berg, J. R. High temperature thermodynamics of some of the rare earths. Unpublished Ph. D. Thesis. Ames, Iowa, Library, Iowa State University of Science and Technology. [ca. 1959].

45. Ellinger, F. H., J. Metals 7, 411 (1955).

46. Behrendt, D., Legvold, S., and Spedding, F. H., Phys. Rev. 106, 723 (1957).

47. Trombe, F. and Foex, M., Compt. rend. 232, 63 (1951).

48. Bates, L. F., Leach, S. J., Loasby, R. G., and Stevens, K. W. H., Proc. Phys. Soc. (London) Sect. B, 68, 181 (1955).

49. Barrett, C. S., J. Chem. Phys. 25, 1123 (1956).

50. Spedding, F. H., Hanak, J. J., and Daane, A. H., Trans. Am. Inst. Mining Met. Engrs. 212, 379 (1958).

51. Curry, M. A. Electrical resistivity of Sm, Eu, Tm, Yb, and Lu. Unpublished M. S. Thesis. Ames, Iowa, Library, Iowa State University of Science and Technology. 1958.

52. Trombe, F., Compt. rend. 206, 1380 (1938).

53. La Blanchetais, C. H. and Trombe, F., ibid. 243, 707 (1956).

54. Meisel, K., Naturwiss. 27, 230 (1939).

55. Klemm, W. Anorganische Chemie. Vol. 1. Wiesbaden, Dieterich, 1949.

56. Quill, L. L., Z. anorg. u. allgen. Chem. 208, 59 (1932).

57. McLennan, J. C. and Monkman, R. J., Trans. Roy. Soc. Can. Sect. 3, 23, 255 (1929).

58. Daane, A. H., Rundle, R. E., Smith, H. G., and Spedding, F. H., Acta Cryst. 7, 532 (1954).

59. Spedding, F. H., Daane, A. H., Wakefield, G. F., and Dennison, D. H. Preparation and properties of high purity scandium metal. To be published in Trans. Am. Inst. Mining Met. Engrs. [ca. 1959].

60. Eash, D. T. Thorium-yttrium alloy system. Unpublished Ph. D. Thesis. Ames, Iowa, Library, Iowa State University of Science and Technology. 1959.

61. Valletta, R. M. Structures and phase equilibria in intra-rare-earth alloy systems. Unpublished Ph. D. Thesis. Ames, Iowa, Library, Iowa State University of Sciency and Technology. [ca. 1959].

62. Gibson, E. D. The yttrium-magnesium alloy system. To be published in Trans. Am. Soc. Metals. [ca. 1959].

63. Fischer, R. W. and Fullhart, C. B., U. S. Atomic Energy Commission Report ISC-1039 [Iowa State College]. 1958.

64. Habermann, C. E., Daane, A. H., and Spedding, F. H. Melting points of Y, Tb, Dy, Ho, Er, Tm, and Lu. Research notebook No. 4, Ames, Iowa, Ames Laboratory of the U. S. Atomic Energy Commission, Iowa State University of Science and Technology. 1959.

65. Trombe, F. and Foex, M., Compt. rend. 235, 42 (1952).

66. Bannister, J. R., Legvold, S., and Spedding, F. H., Phys. Rev. 94, 1140 (1954).

67. Jennings, L. D., Stanton, R. M., and Spedding, F. H., J. Chem. Phys. 27, 909 (1957).

68. Thoburn, W. C., Legvold, S., and Spedding, F. H., Phys. Rev. 112, 56 (1958).

69. Trombe, F., Compt. rend. 221, 19 (1945).

70. Elliot, J. F., Legvold, S., and Spedding, F. H., Phys. Rev. 94, 1143 (1954).

71. _____, _____, and_____, ibid. 100, 1595 (1955).

72. Rhodes, B. L., Legvold, S., and Spedding, F. H., U. S. Atomic Energy Commission Report ISC-701 [Iowa State College]. 1955.

73. Jennings, L. D., Hill, E., and Spedding, F. H. The heat capacity of Tm. To be published in J. Chem. Phys. [ca. 1959].

74. Spedding, F. H. and Daane, A. H., U. S. Atomic Energy Commission Report ISC-484 [Iowa State College]. 1954.

75. _____, Legvold, S., Daane, A. H., and Jennings, L. D. Some physical properties of the rare earth metals. In Gorter, C. J., ed. Progress in low temperature physics. Vol 2, pp. 368-394. Amsterdam, North-Holland Publishing Co. 1957.

76. Chiotti, P., Rev. Sci. Instr. 25, 683 (1954).

77. Spreadborough, J. and Christian, J. W., J. Sci. Instr. 36, 116 (1959).

78. Kennedy, S. W. and Calvert, L. D., ibid. 35, 61 (1958).

79. Wansgard, A. P., Trans. Am. Soc. Metals 30, 1303 (1942).

80. Birks, L. S. and Friedman, H., Rev. Sci. Instr. 18, 576 (1947).

81. Van Valkenburg, A. and McMurdie, H. F., J. Research Natl. Bur. Stds. 38, 415 (1947).

82. Perri, J. A., Banks, E., and Post, B., J. Appl. Phys. 28, 1272 (1957).

83. Hume-Rothery, W. and Reynolds, P. W., Proc. Roy. Soc. Sect. A., 167, 25 (1938).

84. Goldschmidt, H. J. and Cunningham, J., J. Sci. Instr. 27, 177 (1950).

85. _____. Chapter IX. In Peiser, H. S., Rooksby, H. P., and Wilson, A. J. C., eds. X-ray diffraction by polycrystalline materials. London, Institute of Physics. 1955.

86. Buerger, M. J., Buerger, N. W., and Chesley, F. G., Am. Mineralogist 28, 285 (1943).

87. Basinski, Z. S. and Christian, J. W., Proc. Roy. Soc. Sect. A. 223, 554 (1954).

88. Matuyama, E., J. Sci. Instr. 32, 229 (1955).

89. Edwards, J. W., Speiser, R., and Johnson, H. L., Phys. Rev. 73, 1251 (1948).

90. Austin, A. E., Richard, N. A., and Schwartz, C. M., Rev. Sci. Instr. 27, 860 (1956).

91. Kubo, T. and Akabori, H., J. Phys. Chem. 54, 1121 (1950).

92. Aruja, E., Welch, J. H., and Gutt, W., J. Sci. Instr. 36, 16 (1959).

93. Gordon, P., J. Appl. Phys. 20, 908 (1959).

94. American Society for Metals. Metals Handbook Committee. Metals Handbook. Cleveland, Ohio, Author. 1948.

95. Chiotti, P., Rev. Sci. Instr. 25, 876 (1954).

96. Cohen, M. U., Rev. Sci. Instr. 6, 68 (1935).

97. Bradley, A. J., and Jay, A. H., Proc. Phys. Soc. (London) 44, 563 (1932).

98. Nelson, J. B. and Riley, D. P., ibid. 57, 160 (1945).

99. Jette, E. R., and Foote, F., J. Chem. Phys. 3, 605 (1935).

100. Daane, A. H., Dennison, D. H., and Spedding, F. H. J. Am. Chem. Soc. 75, 2272 (1953).

101. Klemm, W. and Winklemann, G., Z. anorg. u. allgem. Chem. 288, 87 (1956).

102. Iandelli, A. and Botti, E., Atti accad. nazl. Lincei 25, 129, 638 (1937).

103. Born, H. J. Thermal expansion of La-Y alloys. Unpublished M. S. Thesis. Ames, Iowa, Library, Iowa State University of Science and Technology. 1958.

104. Eick, H. A., Dissertation Abs. 16, 2038 (1956).

105. Smith, J. F., Carlson, O. N., and Vest, R. W., J. Electrochem. Soc., 103, 409 (1956).

106. _____ and Bernstein, B. T., J. Electrochem. Soc. 106, 448 (1959).

107. Zener, C., Phys. Rev. 71, 846 (1947).

108. Kirkpatrick, M. E., Ames, Iowa, Ames Laboratory of the U. S. Atomic Energy Commission, Iowa State University of Science and Technology. Information on the electrical resistivity of zirconium metal at high temperature. Private communication. 1959.

109. Beerntsen, D. J. Phase studies in uranium-hafnium system. Unpublished Ph. D. Thesis. Ames, Iowa, Library, Iowa State University of Science and Technology. 1958.

110. Varley, J. H. D., Proc. Roy. Soc. 237, Sect. A, 413 (1956).

ACKNOWLEDGMENTS

The author wishes to express his appreciation to Dr. A. H. Daane and Dr. F. H. Spedding for their interest and counsel during this investigation. The author is also indebted to Mr. G. Wakefield and Mr. C. Habermann for preparing most of the rare-earth metals and to the analytical groups of the Ames Laboratory for performing analyses on these metals. Acknowledgment is due to Dr. P. Chiotti and Dr. D. Eash for their kind assistance in conducting the electrical resistivity measurements and to the members of the Statistical Laboratory for their assistance with the IBM-650 computer.

APPENDIX

Detailed results of the high temperature X-ray investigation of scandium, yttrium, and the rare-earth metals appear in the Appendix in Tables 13 to 34, inclusive. For the sake of convenience in listing the data, the results for the hexagonal metals appear first, in Tables 13 to 25, inclusive, followed by the results for the cubic metals given in Tables 26 to 34, inclusive. The data for the high temperature bcc structures are grouped together in Tables 30 to 34, inclusive. In Tables 13 to 34, inclusive, T designates the temperature in ^{o}C, A and C, the lattice constants "a" and "c" in Angstrom units, C/A, the axial ratio, and V the atomic volume in cm^3/mole.

Most of the data given in Tables 13 to 29, inclusive, were fitted to empirical equations of the type

$$R = A + Bt + Ct^2 + Dt^3 \text{ or of the type } R = A + Bt.$$

The coefficients A, B, C, and D of t^n ($t = {}^{o}C$) are given in Table 35. In this table M designates the metal investigated, R, a given physical property, S, the crystal structure, T the upper temperature limit for the equation, σ , the standard deviation of the experimental points from the fitted curves, "a" and "c", the lattice constants, V, the atomic volume, and d, the density.

The lower temperature limit for the equations is

approximately 20°C, except in the case of gadolinium, where the lower temperature limit is 88°C.

TABLE 13. LANTHANUM, HCP DOUBLE C AXIS

T	A	C	C/A	V
20	3.771	12.13	1.609	22.50
50	3.774	12.12	1.607	22.52
93	3.772	12.17	1.613	22.57
148	3.772	12.21	1.618	22.65
189	3.771	12.20	1.617	22.62
231	3.774	12.21	1.618	22.68
284	3.775	12.20	1.615	22.67

TABLE 14. PRASEODYMIUM, HCP DOUBLE C AXIS

T	A	C	C/A	V
22	3.670	11.830	1.6115	20.78
22	3.670	11.833	1.6120	20.79
42	3.672	11.828	1.6106	20.80
49	3.671	11.833	1.6119	20.79
107	3.673	11.844	1.6124	20.84
131	3.673	11.847	1.6129	20.84
155	3.673	11.850	1.6132	20.85
190	3.673	11.849	1.6130	20.85
236	3.673	11.860	1.6143	20.87
252	3.674	11.867	1.6150	20.89
292	3.675	11.869	1.6149	20.90
355	3.675	11.880	1.6164	20.92
409	3.677	11.879	1.6156	20.94
449	3.679	11.883	1.6148	20.98

TABLE 15. NEODYMIUM, HCP DOUBLE C AXIS

T	A	C	C/A	V
20	3.660	11.807	1.6131	20.62
58	3.660	11.811	1.6136	20.63
101	3.660	11.815	1.6139	20.65
158	3.663	11.826	1.6144	20.69
201	3.663	11.827	1.6145	20.69
256	3.665	11.842	1.6157	20.74
304	3.666	11.846	1.6156	20.76
348	3.666	11.855	1.6167	20.78
397	3.670	11.852	1.6149	20.81
451	3.668	11.867	1.6178	20.82
486	3.669	11.867	1.6170	20.84
549	3.672	11.875	1.6169	20.88
639	3.675	11.906	1.6199	20.97
696	3.678	11.905	1.6184	21.00

TABLE 16. GADOLINIUM, HCP

T	A	C	C/A	V
22	3.634	5.784	1.5914	19.93
47	3.636	5.784	1.5908	19.94
88	3.635	5.782	1.5908	19.92
151	3.638	5.786	1.5907	19.97
199	3.638	5.788	1.5908	19.98
249	3.640	5.792	1.5909	20.02
290	3.639	5.795	1.5923	20.02
359	3.641	5.799	1.5928	20.05
397	3.644	5.804	1.5930	20.10
465	3.646	5.808	1.5930	20.14
511	3.644	5.812	1.5944	20.13
542	3.647	5.815	1.5945	20.17
589	3.648	5.815	1.5942	20.18
644	3.650	5.822	1.5953	20.23

TABLE 17. TERBIUM, HCP

T	A	C	C/A	V
24	3.600	5.697	1.5823	19.26
55	3.600	5.700	1.5835	19.26
99	3.602	5.704	1.5834	19.30
152	3.606	5.707	1.5827	19.35
196	3.605	5.712	1.5846	19.36
251	3.608	5.717	1.5849	19.41
314	3.608	5.722	1.5859	19.43
364	3.611	5.726	1.5857	19.47
409	3.612	5.730	1.5866	19.50
444	3.614	5.734	1.5866	19.54
508	3.616	5.739	1.5870	19.58
549	3.616	5.747	1.5892	19.61
607	3.618	5.754	1.5901	19.65
659	3.621	5.762	1.5912	19.70
700	3.624	5.765	1.5908	19.75
754	3.625	5.774	1.5929	19.78
799	3.626	5.779	1.5940	19.81
852	3.629	5.785	1.5939	19.87

TABLE 18. DYSPROSIUM, HCP

T	A	C	C/A	V
20	3.592	5.656	1.5745	19.04
60	3.594	5.659	1.5744	19.07
102	3.595	5.665	1.5758	19.10
150	3.596	5.669	1.5763	19.12
204	3.596	5.672	1.5771	19.13
252	3.598	5.678	1.5782	19.17
347	3.599	5.689	1.5808	19.22
449	3.601	5.700	1.5831	19.28
500	3.602	5.705	1.5839	19.31
533	3.602	5.711	1.5856	19.32
578	3.604	5.715	1.5857	19.36
633	3.605	5.725	1.5881	19.40
685	3.606	5.732	1.5895	19.44

TABLE 19. HOLMIUM, HCP

T	A	C	C/A	V
22	3.577	5.620	1.5713	18.75
61	3.577	5.624	1.5722	18.77
99	3.579	5.628	1.5726	18.80
151	3.579	5.634	1.5740	18.83
200	3.581	5.639	1.5747	18.86
258	3.581	5.643	1.5757	18.88
298	3.582	5.649	1.5773	18.90
355	3.583	5.654	1.5780	18.93
397	3.584	5.659	1.5787	18.96
461	3.586	5.664	1.5796	19.00
495	3.587	5.670	1.5806	19.03
552	3.586	5.674	1.5822	19.03
602	3.588	5.682	1.5839	19.08
651	3.588	5.687	1.5849	19.10
708	3.591	5.693	1.5853	19.15

TABLE 20. ERBIUM, HCP

T	A	C	C/A	V
20	3.560	5.596	1.5719	18.50
59	3.561	5.599	1.5724	18.52
94	3.561	5.601	1.5729	18.53
150	3.563	5.608	1.5741	18.57
190	3.564	5.613	1.5752	18.59
245	3.565	5.619	1.5763	18.63
292	3.566	5.625	1.5772	18.66

TABLE 20. CONTINUED

T	A	C	C/A	V
342	3.567	5.630	1.5783	18.68
389	3.569	5.635	1.5789	18.72
432	3.570	5.639	1.5798	18.74
477	3.571	5.644	1.5806	18.77
529	3.573	5.650	1.5814	18.81
577	3.575	5.655	1.5820	18.85
626	3.576	5.662	1.5833	18.89
676	3.578	5.669	1.5841	18.93
723	3.581	5.675	1.5845	18.98
774	3.584	5.682	1.5853	19.04
843	3.588	5.689	1.5856	19.10
883	3.592	5.700	1.5866	19.18
917	3.595	5.704	1.5868	19.22

TABLE 21. THULIUM, HCP

T	A	C	C/A	V
20	3.537	5.564	1.5730	18.16
58	3.539	5.569	1.5737	18.20
93	3.541	5.573	1.5740	18.23
141	3.543	5.579	1.5750	18.26
186	3.543	5.583	1.5761	18.28
232	3.544	5.590	1.5770	18.32
275	3.545	5.593	1.5776	18.34
333	3.546	5.601	1.5795	18.37
398	3.547	5.607	1.5807	18.40
448	3.549	5.613	1.5814	18.44
492	3.551	5.618	1.5821	18.47
543	3.553	5.624	1.5828	18.51
593	3.554	5.630	1.5839	18.55
641	3.555	5.635	1.5852	18.57
696	3.557	5.641	1.5860	18.61
753	3.559	5.648	1.5871	18.66
808	3.560	5.653	1.5880	18.69
853	3.561	5.661	1.5897	18.73

TABLE 22. YTTERBIUM, HCP

T	A	C	C/A	V
268	3.911	6.403	1637	25.54
283	3.911	6.403	1637	25.55
310	3.912	6.406	1638	25.57
412	3.926	6.413	1634	25.78

TABLE 23. LUTETIUM, HCP

T	A	C	C/A	V
18	3.505	5.551	1.5836	17.79
57	3.505	5.555	1.5848	17.80
92	3.507	5.559	1.5854	17.83
137	3.505	5.563	1.5870	17.82
181	3.508	5.568	1.5873	17.87
225	3.508	5.572	1.5882	17.89
264	3.511	5.577	1.5886	17.93
335	3.513	5.584	1.5897	17.97
393	3.514	5.589	1.5903	18.00
443	3.516	5.594	1.5909	18.04
487	3.518	5.597	1.5908	18.07
536	3.519	5.602	1.5918	18.10
587	3.522	5.607	1.5919	18.14
651	3.524	5.613	1.5927	18.18
695	3.526	5.617	1.5932	18.21
748	3.530	5.624	1.5933	18.27
800	3.531	5.627	1.5937	18.30
863	3.533	5.634	1.5947	18.34
908	3.535	5.638	1.5949	18.38
956	3.538	5.645	1.5957	18.43

TABLE 24. SCANDIUM, HCP

T	A	C	C/A	V
20	3.308	5.267	1.5921	15.03
58	3.310	5.270	1.5924	15.06
87	3.310	5.272	1.5926	15.07
135	3.311	5.276	1.5934	15.09
174	3.313	5.280	1.5938	15.11
222	3.314	5.283	1.5942	15.13
271	3.315	5.287	1.5947	15.16
329	3.317	5.292	1.5953	15.19
398	3.319	5.297	1.5960	15.22
442	3.320	5.301	1.5965	15.24
498	3.322	5.306	1.5970	15.27
543	3.324	5.308	1.5969	15.30
592	3.325	5.312	1.5974	15.32
644	3.326	5.317	1.5983	15.34
702	3.330	5.322	1.5984	15.39
756	3.332	5.326	1.5987	15.42
804	3.332	5.332	1.6003	15.44
868	3.334	5.335	1.5999	15.47
910	3.338	5.342	1.6004	15.53
963	3.341	5.347	1.6002	15.57
1009	3.339	5.348	1.6014	15.55

TABLE 25. YTTRIUM, HCP

T	A	C	C/A	V
23	3.648	5.735	1.5721	19.90
67	3.647	5.738	1.5735	19.90
105	3.648	5.743	1.5744	19.93
148	3.649	5.749	1.5756	19.96
207	3.650	5.755	1.5767	20.00
259	3.652	5.761	1.5776	20.04
300	3.652	5.766	1.5788	20.06
352	3.654	5.772	1.5798	20.10
400	3.655	5.778	1.5809	20.13
452	3.656	5.782	1.5817	20.15
501	3.657	5.787	1.5825	20.18
548	3.658	5.794	1.5838	20.22
597	3.658	5.798	1.5850	20.24
649	3.661	5.806	1.5858	20.30
696	3.662	5.812	1.5869	20.33
750	3.664	5.819	1.5881	20.38
800	3.667	5.827	1.5889	20.44
847	3.669	5.830	1.5891	20.46
897	3.669	5.837	1.5908	20.50

TABLE 26. LANTHANUM, FCC

T	A	V
21	5.305	22.48
68	5.305	22.49
114	5.305	22.49
250	5.310	22.55
279	5.317	22.63
307	5.314	22.60
313	5.317	22.63
338	5.315	22.61
369	5.317	22.63
388	5.318	22.65
396	5.316	22.62
346	5.317	22.63
461	5.320	22.68
510	5.324	22.72
552	5.323	22.72
598	5.328	22.78

TABLE 27. CERIUM, FCC

T	A	V
13	5.160	20.69
16	5.161	20.70
25	5.161	20.71
55	5.162	20.72
97	5.164	20.74
99	5.164	20.73
150	5.165	20.75
200	5.167	20.77
213	5.167	20.77
248	5.168	20.79
297	5.171	20.82
302	5.171	20.82
304	5.170	20.81
355	5.171	20.82
397	5.173	20.85
451	5.176	20.88
500	5.177	20.89
546	5.179	20.92
619	5.182	20.95

TABLE 28. EUROPIUM, BCC

T	A	V
20	4.582	28.97
20	4.582	28.97
25	4.582	28.98
54	4.585	29.03
102	4.594	29.19
152	4.598	29.28
202	4.606	29.43
305	4.612	29.54
352	4.618	29.67

TABLE 29. YTTERBIUM, FCC

T	A	V
23	5.484	24.84
28	5.486	24.86
50	5.489	24.90
71	5.493	24.96
103	5.498	25.03
139	5.502	25.09
151	5.503	25.09

TABLE 29. CONTINUED

T	A	V
187	5.508	25.16
193	5.512	25.22
208	5.513	25.23
233	5.518	25.31
254	5.521	25.34
283	5.524	25.39
297	5.528	25.43
302	5.527	25.43
317	5.531	25.48
338	5.536	25.55
348	5.539	25.59
358	5.538	25.58
378	5.542	25.63
395	5.546	25.68
397	5.546	25.68
408	5.546	25.69
437	5.551	25.76
449	5.552	25.78
452	5.554	25.81
492	5.560	25.88
549	5.567	25.98
576	5.576	26.11
598	5.578	26.14

TABLE 30. LANTHANUM, BCC

T	A	V
878	4.26	23.3
881	4.25	23.1
902	4.26	23.2

TABLE 31. CERIUM, BCC

T	A	V
742	4.11	21.0
748	4.12	21.0
749	4.13	21.2
756	4.12	21.0
759	4.11	20.9
761	4.10	20.8
763	4.13	21.2
779	4.12	21.0

TABLE 32. PRASEODYMIUM, BCC

T	A	V
814	4.13	21.2
815	4.15	21.5
818	4.13	21.2
824	4.12	21.1
825	4.11	20.9
832	4.14	21.4

TABLE 33. NEODYMIUM, BCC

T	A	V
850	4.12	21.1
890	4.12	21.1
895	4.14	21.4
895	4.14	21.4

TABLE 34. YTTERBIUM, BCC

T	A	V
720	4.44	26.4
763	4.46	26.7
778	4.45	26.5
800	4.43	26.3
807	4.44	26.4

Table 35. Coefficients of empirical equations relating the rare-earth metal properties determined by X-ray studies to temperature

M	R	S	T	σ	Equation coefficients A	B x 10^5	C x 10^8	D x 10^{11}
La	a	hcp	292	0.002	3.770	1.7	--	--
La	c	hcp	292	0.02	12.13	33.0	--	--
La	v	hcp	292	0.03	22.50	70.	--	--
La	d	hcp	292	0.008	6.174	-19.1	--	--
La	a	fcc	598	0.002	5.303	3.4	1.0	0.0
La	v	fcc	598	0.02	22.46	44.	13.	0.
La	d	fcc	598	0.005	6.186	-12.0	- 3.8	.8
Ce	a	fcc	619	0.0005	5.1604	3.28	- 0.59	1.37
Ce	v	fcc	619	0.006	20.695	38.3	- 3.2	13.4
Ce	d	fcc	619	0.001	6.771	-12.6	1.5	- 4.5
Pr	a	hcp	449	0.0008	3.6702	1.66	--	--
Pr	c	hcp	449	0.004	11.828	13.3	--	--
Pr	v	hcp	449	0.008	20.778	42.4	--	--
Pr	d	hcp	449	0.003	6.782	-13.7	--	--
Nd	a	hcp	696	0.0008	3.6582	3.18	- 3.96	4.92
Nd	c	hcp	696	0.004	11.802	16.6	-14.1	17.8
Nd	v	hcp	696	0.01	20.60	65.	-70.	88.
Nd	d	hcp	696	0.003	7.004	-21.9	23.2	-28.7
Eu	a	bcc	352	0.001	4.578	17.4	-28.2	31.0
Eu	v	bcc	352	0.02	28.91	309.	-439.	457.
Eu	d	bcc	352	0.004	5.259	-56.6	84.5	-86.8
Gd	a	hcp	644	0.0009	3.6315	4.26	- 5.49	5.05
Gd	c	hcp	644	0.001	5.777	4.8	5.4	- 3.5
Gd	c/a	hcp	644	0.0004	1.5906	- 0.27	3.02	- 2.36
Gd	v	hcp	644	0.01	19.88	49.	3.	3.
Gd	d	hcp	644	0.005	7.895	-25.0	17.0	-17.5
Tb	a	hcp	852	0.0009	3.5990	3.37	- .72	1.03
Tb	c	hcp	852	0.001	5.696	6.9	3.8	.6
Tb	c/a	hcp	852	0.0006	1.5827	.43	1.38	- 0.31
Tb	v	hcp	852	0.009	19.245	59.2	5.5	13.7
Tb	d	hcp	852	0.004	8.272	-25.4	- 1.8	- 5.3
Dy	a	hcp	685	0.0004	3.5923	2.73	- 3.53	3.69
Dy	c	hcp	685	0.0009	5.6545	8.74	1.43	3.34
Dy	c/a	hcp	685	0.0004	1.5741	1.24	1.93	- 0.68
Dy	v	hcp	685	0.005	19.032	58.7	-33.0	51.1

Table 35. (Continued)

M	R	S	T	σ	Equation coefficients A	B x 10^5	C x 10^8	D x 10^{11}
Dy	d	hcp	685	0.002	8.536	-26.3	15.0	-22.1
Ho	a	hcp	708	0.0007	3.5761	2.64	- 2.55	2.42
Ho	c	hcp	708	0.0008	5.6174	11.13	- 3.78	4.71
Ho	c/a	hcp	708	0.0004	1.5708	1.95	0.05	0.25
Ho	v	hcp	708	0.008	18.742	61.6	-32.4	37.0
Ho	d	hcp	708	0.003	8.803	-30.4	18.7	-18.9
Er	a	hcp	917	0.0003	3.5590	2.95	- 2.99	4.37
Er	c	hcp	917	0.001	5.592	11.9	- 4.1	4.9
Er	c/a	hcp	917	0.0002	1.5711	2.06	0.13	- 0.56
Er	v	hcp	917	0.006	18.473	70.2	-45.8	63.5
Er	d	hcp	917	0.003	9.051	-33.8	20.9	-28.3
Tm	a	hcp	853	0.0006	3.5372	3.19	- 1.41	1.19
Tm	c	hcp	853	0.0007	5.5619	12.51	- 3.89	3.27
Tm	c/a	hcp	853	0.0003	1.5723	2.15	- .55	0.43
Tm	v	hcp	853	0.007	18.151	73.7	-26.7	23.1
Tm	d	hcp	853	0.004	9.332	-37.4	14.0	-11.2
Yb	a	fcc	598	0.001	5.481	14.1	7.0	- 6.2
Yb	v	fcc	598	0.02	24.80	191.	103.	-85.
Yb	d	fcc	598	0.004	6.977	-54.1	-23.0	23.4
Lu	a	hcp	956	0.0007	3.5050	.77	4.83	- 2.17
Lu	c	hcp	956	0.0006	5.5486	11.50	- 4.55	3.16
Lu	c/a	hcp	956	0.0002	1.5831	2.90	- 3.44	1.86
Lu	v	hcp	956	0.008	17.779	45.0	34.1	-11.1
Lu	d	hcp	956	0.005	9.842	-24.7	-18.4	6.9
Sc	a	hcp	1009	0.0008	3.3080	2.46	0.78	0.01
Sc	c	hcp	1009	0.0009	5.2653	8.06	- 0.52	0.79
Sc	c/a	hcp	1009	0.0003	1.5917	1.23	- 0.51	0.22
Sc	v	hcp	1009	0.009	15.028	45.5	5.7	2.7
Sc	d	hcp	1009	0.002	- 2.992	- 9.1	- 0.9	- 0.4
Y	a	hcp	897	0.0007	3.6451	2.76	- 1.92	2.16
Y	c	hcp	897	0.0009	5.7305	12.40	- 3.13	2.92
Y	c/a	hcp	897	0.0002	1.5722	2.21	- 0.09	- 0.09
Y	v	hcp	897	0.01	19.86	73.	-32.	34.
Y	d	hcp	897	0.002	4.478	-16.8	8.1	- 7.9